

Shear viscosity of nucleonic matter

Xian-Gai Deng^{a,b}, De-Qing Fang^{a,b}, Yu-Gang Ma^{a,b,*}

^a*Key Laboratory of Nuclear Physics and Ion-beam Application (MOE), Institute of Modern Physics, Fudan University, Shanghai 200433, China*

^b*Shanghai Research Center for Theoretical Nuclear Physics, NSFC and Fudan University, Shanghai 200438, China*

Abstract

The research status of the shear viscosity of nucleonic matter is reviewed. Some methods to calculate the shear viscosity of nucleonic matter are introduced, including mean free path, Green-Kubo, shear strain rate, Chapman-Enskog and relaxation time approximation. Based on these methods, results for infinite and finite nucleonic matter are discussed, which are attempts to investigate the universality of the ratio of shear viscosity over entropy density and transport characteristics like the liquid-gas phase transition in nucleonic matter. In addition, shear viscosity is also briefly discussed for the quantum chromodynamical matter produced in relativistic heavy-ion collisions.

Keywords: shear viscosity, ratio of shear viscosity to entropy density, nucleonic matter, KSS bound, Green-Kubo, Chapman-Enskog, relaxation time approximation

arXiv:2401.02293v1 [nucl-th] 4 Jan 2024

*Corresponding author

Email address: mayugang@fudan.edu.cn (Yu-Gang Ma)

Contents

1	Introduction	3
2	Analysis methods of shear viscosity	7
2.1	The definition of shear viscosity	7
2.2	Green-Kubo method	9
2.3	Shear strain rate method	14
2.4	Chapman-Enskog method	16
2.5	Relaxation time method	19
3	Theoretical aspects of shear viscosity in nucleonic matter	21
3.1	Infinite nuclear matter	21
3.2	Finite nuclear matter	36
4	Experimental aspects of shear viscosity in nucleonic matter	48
4.1	Analysis method by experiment	48
4.2	Shear viscosities of finite nuclei in experiment	51
4.3	Others	56
5	η/s in relativistic heavy-ion collision	58
5.1	Ratio of shear viscosity to entropy density across the QCD phase diagram	58
5.2	The dependence of ratio of shear viscosity to entropy density on collision centrality	58
5.3	Magnetic field effect on ratio of shear viscosity to entropy density	61
5.4	Bayesian estimation of ratio of shear viscosity to entropy density	63
6	Summary and outlook	66
A	Appendices, if necessary	100

1. Introduction

In a non-perfect fluid, viscosity represents internal friction, which causes an irreversible energy dissipation process, and it is a measure of the flow resistance to the liquid, which means the higher value, and the more resistance, and thus the fluid flows more slowly. Shear viscosity, which describes momentum transfer ability in a flowing fluid, is one of the important transport properties for lots of substances, such as macroscopic matter as well as microscopic and quantum matter, e.g. hot dense quark matter, etc. [1, 2]. Viscosity, which affects solute dynamics and reaction rates in a solvent, is crucial for understanding biological processes and chemical reactions [3–5]. In astrophysics, properties of transport coefficients (bulk viscosity, shear viscosity, and thermal conductivity) have been studied in different layers of neutron stars (NS), e.g. in the crust and in the core [6–8]. The transport coefficients were described in the framework of Brueckner-Hartree-Fock (BHF) theory [9, 10], and comparisons were made using several equations of states (EoSs) [8]. For viscosity, one of the most important features is the damping of oscillations. So it plays an important role for r -modes in rotating pulsars [11] and affects the emission and propagation of gravitational waves, which is important for the planning of advanced gravitational wave experiments [12, 13]. The study on transport coefficients could improve our understanding of the dynamical behaviour of the merging of binary neutron stars through the signal of gravitational waves, which was observed by LIGO and Virgo on August 17, 2017 (GW170817) [14]. The most common astrophysical manifestation of the NSs is the radio pulsars, which are driven by the strong magnetic field [15] as high as 10^{12} - 10^{13} G [16]. With such high magnetic fields, it could impact the EoS and have strong effects on the NS matter. How the magnetic field affects the transport coefficients of the magnetized NS should be considered [12].

Viscous liquids like honey, syrup, and oil flow slowly, and less viscous liquids like water and gasoline flow quickly. The Navier-Stokes (NS) equation can be used to describe the motion of non-perfect fluid in fluid mechanics, where the shear viscosity coefficient and the bulk viscosity coefficient are included [17, 18]. At the microscopic level, viscosity is caused by the potential and collisions of particles (or molecules). While macroscopically or hydrodynamically, it is determined by a constitutive relationship as the ratio of the shear stress to the shear rate [19, 20]. In equilibrium molecular dynamics (EMD), the viscosity η is given as an integral of the shear-stress autocorrelation function determined during the simulation [21], which is called Green-Kubo (GK) formula derived from linear response theory [22] or given by Einstein relation [23]. In the framework of EMD methods, for the convergence of shear-stress autocorrelation function, it would take a long simulation time due to relatively large fluctuations in the shear tensor. In molecular simulations for calculating viscosity, a nonequilibrium molecular dynamics

(NEMD) method with a planar Couette flow field at strain rate $\dot{\gamma} = \partial u_x / \partial y$ becomes increasingly popular and has been used extensively to predict the rheological properties of real fluids [21].

In 2005, Kovtun, Son, and Starinets (KSS) [24] studied the shear viscosity with certain supersymmetric gauge theories with gravity duals and gave a lower limit value for the ratio of shear viscosity to entropy density, $\eta/s \geq \hbar/(4\pi k_B)$ (\hbar is the Planck's constant divided by 4π and k_B is the Boltzmann constant), which is called the KSS bound. It has been conjectured that this ratio is the lowest limit for a large class of quantum field theories [24]. A new state of matter, the quark gluon plasma (QGP), is created in ultra-relativistic heavy-ion collisions, which is manifested by the results from the Relativistic Heavy Ion Collider (RHIC) at Brookhaven [25–32] and the Large Hadron Collider (LHC) at CERN [33–38]. Based on heavy-ion data from these two colliders and theoretical modeling, lots of efforts are paid to uncover the fundamental properties of the quark gluon plasma [39–43]. The analysis of the elliptic flow v_2 in the ultra-relativistic heavy-ion collisions shows that QGP behaves like a near perfect liquid with a lower limit of η/s [44]. How perfect is the fluid in relativistic heavy-ion collisions [45]? In explaining the data from RHIC, the results [46, 47] from the viscous hydrodynamics model suggest that the ratio of shear viscosity to entropy density has a very small value. It indicates that the quark-gluon plasma (QGP) is nearly an ideal fluid. Moreover, in the analysis by Csernai *et al.* [48], it shows that the transition from hadrons to quarks and gluons has behavior similar to helium, nitrogen, and water at and near their phase transitions in the ratio η/s .

Near and below a critical temperature, T_c , the condensates of bosons or fermion pairs behave like superfluids, which are frictionless [49]. The behavior of shear viscosity versus temperature for bosonic and fermionic system is different below T_c [49]. For instance, like the bosonic ^4He , viscosity increases as the temperature approaches zero below T_c [50] and in the Fermionic ^3He , the shear viscosity decreases to zero with decreasing of temperature below T_c [51–53]. The shear viscosity for ^3He at the transition temperature $T_A = 2.6$ mK appears a rapid decrease [52]. The research on shear viscosity and its ratio over entropy density as well as for a Fermions system with the unitary Fermi gas has attracted lots of attention over the past few years [49, 54–60]. The unitary Fermi gas where particles interact at infinite scattering length is experimentally investigated with ultracold atoms in a balanced mixture of, e.g., the two lowest hyperfine levels of ^6Li at a Feshbach resonance [56, 58, 59]. It is found that the viscosity of a unitary Fermi gas is closer to that of fermionic ^3He than to that of bosonic ^4He [49, 60]. And both the viscosity and the ratio (η/s) of the unitary gas are predicted to exhibit a minimum, somewhat below T_c [60]. One found that a minimum value of $\eta/s \simeq 0.44$ (in units of \hbar/k_B) at the temperature $T/T_F \simeq 0.27$, with T_F the Fermi temperature [59].

And it is also very interesting to see the ratio of shear viscosity to entropy density for nuclear matter,

which is composed of protons and neutrons. Experimentally, some nuclear experimental facilities, such as FAIR (the International Accelerator Facility for Antiproton and Ion Research) [61], GANIL (Grand Accélérateur National d'Ions Lourds-National Large Heavy Ion Accelerator) [62] in Europe, and High Intensity Accelerator Facility (HIAF) in China [63–65] offer chances to explore phase diagram of nuclear matter in the region of high baryon density as well as transport properties [66–72]. Theoretically, transport coefficients such as shear viscosity have been studied for a few decades in nuclear physics and attracted lots of attentions [24, 44, 73–81]. The equation of state and transport coefficients are important quantities for the hot and dense hadron gases in nuclear physics [76]. The behaviors of shear viscosity depend on the nucleon-nucleon cross sections as well as the nuclear equation of state, etc. For infinite nuclear matter, the effects of Pauli blocking, nucleon-nucleon cross section, temperature, density, isospin asymmetry, etc. on shear viscosity are discussed [74, 75, 82–84]. With the help of transport models like Boltzmann-Uehling-Uhlenbeck model (BUU) and quantum molecular dynamics model (QMD) [85–90], the relation between shear viscosity and the liquid-gas (LG) phase transitions, or collective flow, or giant dipole resonance (GDR) has been investigated [78, 79, 91, 92].

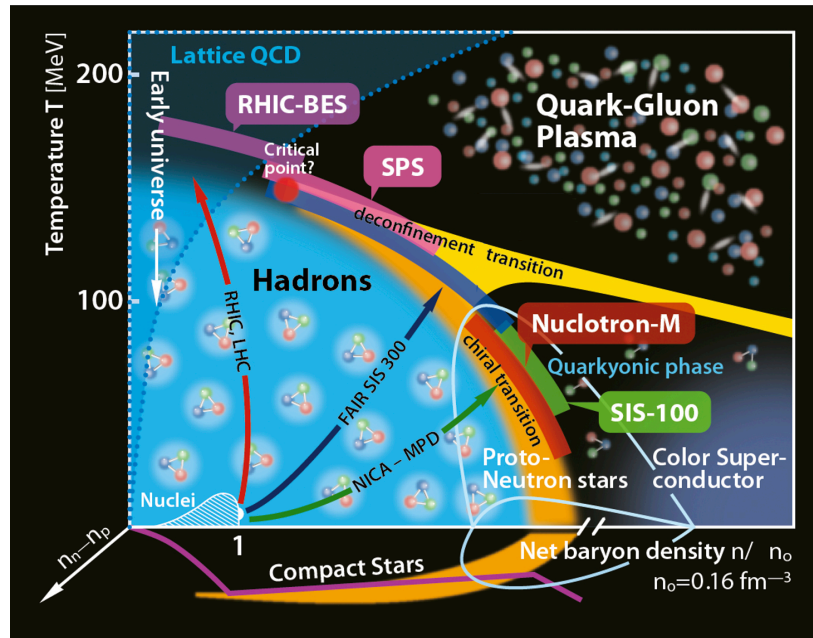


Figure 1.1: (Color online) The QCD diagram. Picture taken from this (CSQCD 2017) conference poster.

The nuclear matter driven by the strong interaction acting like the Van der Waals potential for water can undergo the liquid-gas phase transitions in lower energy heavy-ion collisions [93–100]. The QCD diagram in Fig. 1.1, which presents the relationship among temperature, baryon density (or baryon chemical potential), and nuclear asymmetry ($n_n - n_p$), was explored by the experimental facilities of LHC, RHIC, FAIR, and NICA, etc. The understanding of the properties of the strong interaction phase transition is still rather limited. The exploration of nuclear matter properties and QCD phase

diagram would need both new experimental data with extended detection capabilities and theoretical calculations [29, 101–105]. As seen from the QCD diagram, the phase transition is not only for nuclear matter but also for the QGP matter. Compilation of data for different substances [48] demonstrates a drop of the shear viscosity in the region of a phase transition, when the entropy density is employed as a universal reference. Furthermore, from the calculations of shear viscosity of QCD matter in the hadronic phase by the coupled Boltzmann equations of pions and nucleons in low temperatures and low baryon-number densities, one found that η/s shows a discontinuity in the bottom of the valley for a first-order phase transition which is similar to water [106, 107]. The studies on the specific shear viscosity near the liquid–gas phase transition may shed new light on the nature of this transition in nucleonic matter [78, 83].

2. Analysis methods of shear viscosity

Shear viscosity is a common property of substances, and there are some methods to calculate it, such as the mean free path, Green-Kubo formula, shear strain rate method, Chapman-Enskog method, and relaxation time method. In this chapter, the details of these methods will be introduced.

2.1. The definition of shear viscosity

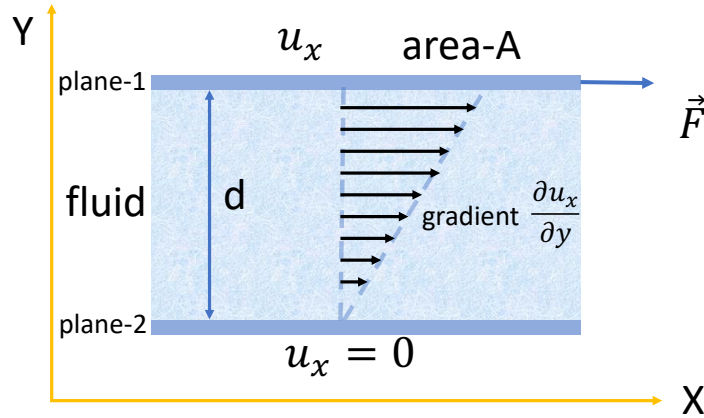


Figure 2.1: (Color online) The illustration of shear stress.

Considering two planes ‘1’ and ‘2’ with area A as in Fig. 2.1, a fluid with thickness d is between them. When the plane ‘2’ is fixed, one drags plane ‘1’ with a force \vec{F} . Sometime later, the fluid velocity will decrease from the value u_x at plane ‘1’ to zero at the stationary plane ‘2’. The velocity gradient of the fluid is determined by the shear force between flow layers. The shear stress F/A is proportional to u_x/d which is called Newton’s equation and is written as follows:

$$\frac{F}{A} = -\eta \frac{u_x}{d}, \quad (2.1)$$

where η is called the friction coefficient or the coefficient of shear viscosity. Rewritten Eq. (2.1) in a differential form, one has

$$\frac{F}{A} = -\eta \frac{\partial u_x}{\partial y}. \quad (2.2)$$

It is seen that the shear viscosity as internal friction causes the irreversible transfer of momentum from points with large velocity to small ones [18]. So the physical meaning of shear viscosity is the ability to transfer momentum over a distance of the mean free path, which measures the average distance traveled

by a particle between collisions. Hence, a system with lower values of η indicates that the constituents of the system interact strongly to transfer momentum easily. On the contrary, a system with a large η means that the constituents of the system interact weakly, and it becomes strenuous for the momentum transfer between the constituents [108].

Recalling the fluid mechanics [18], for the ideal fluid, we have,

$$\frac{\partial p_\alpha}{\partial t} = \frac{\partial \hat{\rho} u_\alpha}{\partial t} = -\frac{\partial T_{\alpha\beta}}{\partial r_\beta}, \quad \alpha, \beta = x, y, z, \quad (2.3)$$

where p , $\hat{\rho}$, and u are the local momentum density, particle mass density and local fluid velocity, respectively. The tensor $T_{\alpha\beta}$ is called momentum flux density tensor which is defined as (for ideal fluid),

$$T_{\alpha\beta} = P\delta_{\alpha\beta} + \hat{\rho}u_\alpha u_\beta, \quad (2.4)$$

where P is the pressure and $\delta_{\alpha\beta}$ is equal to 1 (or 0) when $\alpha = \beta$ ($\alpha \neq \beta$). For viscous fluid, an irreversible viscous term- $\Pi_{\alpha\beta}$ is added in momentum flux density tensor,

$$T_{\alpha\beta} = \hat{P}\delta_{\alpha\beta} + \hat{\rho}u_\alpha u_\beta + \Pi_{\alpha\beta}. \quad (2.5)$$

The form of the tensor $\Pi_{\alpha\beta}$ which is called viscous stress tensor, can be written as follows,

$$\Pi_{\alpha\beta} = -\eta\left(\frac{\partial u_\alpha}{\partial r_\beta} + \frac{\partial u_\beta}{\partial r_\alpha} - \frac{2}{3}\delta_{\alpha\beta}\frac{\partial u_\gamma}{\partial r_\gamma}\right) - \xi\delta_{\alpha\beta}\frac{\partial u_\gamma}{\partial r_\gamma}, \quad \alpha, \beta, \gamma = x, y, z, \quad (2.6)$$

where η and ξ are shear viscosity and bulk viscosity, respectively. In a flat-parallel flow of uniform fluid $u = u_x$, the x, y component of $T_{\alpha\beta}$ can be obtained,

$$T_{xy} = \Pi_{xy} = -\eta\frac{\partial u_x}{\partial y}. \quad (2.7)$$

In this case, the momentum flux density tensor is equal to the viscous stress tensor. And here the Eq. (2.7) corresponds to the Eq. (2.2).

Above, shear viscosity is given by a direct definition or from fluid mechanics. In thermodynamics, a simple estimate of the shear viscosity for a dilute gas can be obtained by the mean free path of particles, which reads as [44, 109],

$$\eta = \frac{1}{3}\rho m \bar{v} \lambda, \quad (2.8)$$

where ρ is the density, \bar{v} is the average velocity of particles, and λ is the mean free path, which can be written as $\lambda = 1/(\rho\sigma)$. Here σ is the transport cross section.

2.2. Green-Kubo method

It is a very traditional way [110] to obtain shear viscosity (or other transport coefficients) for a liquid from pressure or momentum fluctuations with the Green-Kubo relation at equilibrium [111], which is related to the linear response theory [22]. It can be found that the shear viscosity of a gas or liquid system arises from the instantaneous fluctuations due to the thermal motion in the stress tensor. In the classical limit [112], the standard Green-Kubo formula for the calculation of the shear viscosity coefficient η can be expressed by [22, 113–115]:

$$\eta = \frac{V}{T} \int_{t_0}^{\infty} \langle T_{\alpha\beta}(t)T_{\alpha\beta}(t_0) \rangle dt; \quad \alpha, \beta = x, y, z, \alpha \neq \beta, \quad (2.9)$$

where V and t_0 are system volume and equilibrium time, respectively. And the integral kernel $\langle T_{\alpha\beta}(t)T_{\alpha\beta}(t_0) \rangle$ is called the correlation function $C(t)$. The bracket $\langle \dots \rangle$ denotes average over an equilibrium ensemble of events. In the Green-Kubo method, the convergence of the correlation function $C(t)$ is important. For the nuclear matter, $C(t)$ was checked in the Improved Quantum Molecular Dynamics (ImQMD) model with mean field [115] as shown in Fig. 2.2. One can see that $C(t)$ of nucleonic matter is convergent.

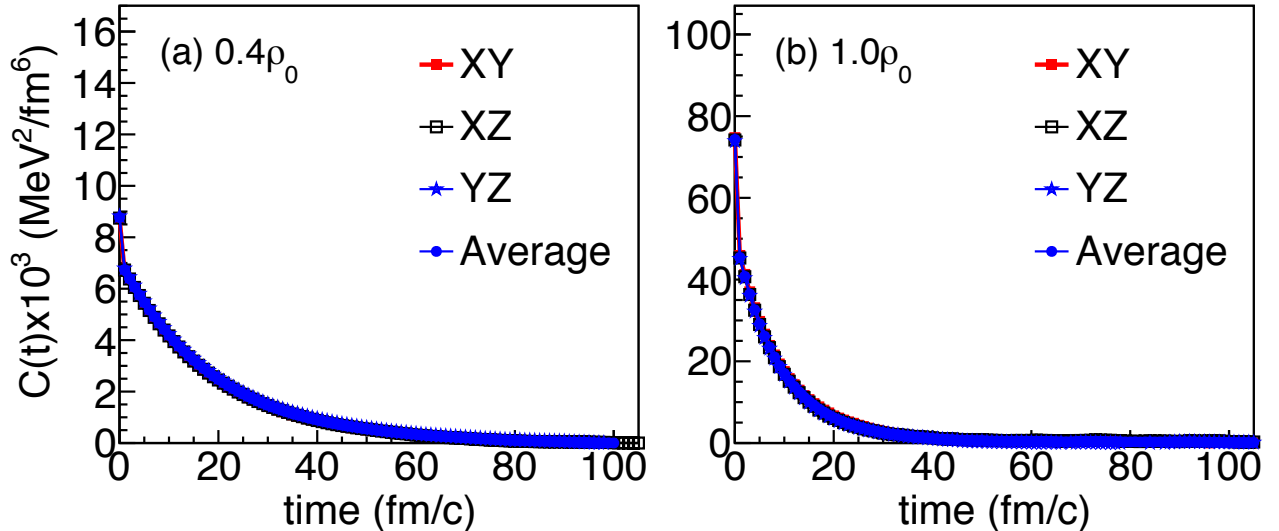


Figure 2.2: (Color online) The evolution of autocorrelation function for different components at $T_0 = 30$ MeV and different densities of $0.4\rho_0$ (a) or $1.0\rho_0$ (b) (here $\rho_0 = 0.16 \text{ fm}^{-3}$ is the saturation density for nuclear matter). It is worth to mention that the calculations for this figure is without mean field [115]

At densities of $0.4\rho_0$, the correlation function $C(t)$ tends to zero in a period of time ~ 60 fm/c, and it

decreases faster at a higher density of $1.0\rho_0$. Since it is symmetric in the simulation box, correlation functions for different components are almost the same.

In Eq. (2.9), $T_{\alpha\beta}(t)$ is an off-diagonal element of the stress tensor, which can be given by,

$$T_{\alpha\beta}(t) = \frac{1}{V} \int d^3r T_{\alpha\beta}(\vec{r}, t), \quad (2.10)$$

where $T_{\alpha\beta}(\vec{r}, t)$ is local tensor which is regarded as the momentum flux density tensor. Let us start from the momentum conservation law [17, 116, 117]:

$$\frac{\partial \mathbf{p}(\vec{r}, t)}{\partial t} + \nabla_r \cdot \mathbf{T}(\vec{r}, t) = 0, \quad (2.11)$$

where $\mathbf{p}(\vec{r}, t)$ and $\mathbf{T}(\vec{r}, t)$ are momentum density and momentum flux density, respectively. One can rewrite Eq. (2.11) as tensor form:

$$\frac{\partial p_\alpha}{\partial t} + \frac{\partial}{\partial r_\beta} T_{\alpha\beta} = 0. \quad (2.12)$$

With a distribution function $f(\vec{r}, \vec{p}, t)$, the local momentum density can be defined as [118]:

$$\mathbf{p}(\vec{r}, t) = \int \vec{p} f(\vec{r}, \vec{p}, t) d^3p. \quad (2.13)$$

In statistical mechanics, a system is no longer considered as a continuous fluid, but rather treated an ensemble consisted of particles with the number A . In a many-particle system, the distribution function $f(\vec{r}, \vec{p}, t)$ could have Dirac's form [85]:

$$f(\vec{r}, \vec{p}, t) = \sum_i^A \delta(\vec{r} - \vec{R}_i(t)) \delta(\vec{p} - \vec{P}_i(t)), \quad (2.14)$$

where $\vec{R}_i(t)$ and $\vec{P}_i(t)$ are the time-dependent coordinate and momentum of particle- i , or Gauss form [86]:

$$f(\vec{r}, \vec{p}, t) = \frac{1}{(\pi\hbar)^3} \sum_i^A \exp\left[-\frac{(\vec{r} - \vec{R}_i(t))^2}{2L}\right] \exp\left[-\frac{2L(\vec{p} - \vec{P}_i(t))^2}{\hbar^2}\right], \quad (2.15)$$

where L is square of width of Gauss wave packet in unit of fm^2 . With distribution function $f(\vec{r}, \vec{p}, t)$,

one can have following integral relations:

$$\int f(\vec{r}, \vec{p}, t) d^3p = \rho(\vec{r}), \quad (2.16)$$

$$\int f(\vec{r}, \vec{p}, t) d^3r = g(\vec{p}). \quad (2.17)$$

where $\rho(\vec{r})$ and $g(\vec{p})$ are the densities in coordinate and momentum spaces, respectively. Substituted $f(\vec{r}, \vec{p}, t)$ into Eq.(2.13), one can get:

$$\mathbf{p}(\vec{r}, t) = \sum_i^A \vec{P}_i \rho_i, \quad (2.18)$$

where the ρ_i is density of particle i which can be expressed as:

$$\rho_i(\vec{r}) = \delta(\vec{r} - \vec{R}_i), \quad (2.19)$$

or

$$\rho_i(\vec{r}) = \frac{1}{(2\pi L)^{3/2}} \exp \left[-\frac{(\vec{r} - \vec{R}_i)^2}{2L} \right]. \quad (2.20)$$

Taking derivative of Eq. (2.18) with respect to time:

$$\frac{\partial \mathbf{p}}{\partial t} = \sum_i^A \frac{\partial \vec{P}_i}{\partial t} \rho_i + \sum_i^A \vec{P}_i \frac{\partial \rho_i}{\partial t}. \quad (2.21)$$

For the derivative of ρ_i with respect to time:

$$\frac{\partial \rho_i}{\partial t} = \frac{\partial \rho_i}{\partial \vec{R}_i} \frac{\partial \vec{R}_i}{\partial t} = -\frac{\partial \rho_i}{\partial \vec{r}} \frac{\partial \vec{R}_i}{\partial t}. \quad (2.22)$$

Thus the second term of right hand side of Eq. (2.21) can reach:

$$\sum_i^A \frac{\partial \rho_i}{\partial t} P_{i\alpha} = -\frac{\partial}{\partial r_\beta} \sum_i^A \left(\frac{P_{i\alpha} P_{i\beta}}{m} \right) \rho_i. \quad (2.23)$$

And for the first term of right hand side of Eq. (2.21):

$$\sum_i^A \frac{\partial \vec{P}_i}{\partial t} \rho_i = \sum_i^A \vec{F}_i \rho_i. \quad (2.24)$$

If the interaction is only two-body, we have

$$\vec{F}_i = \sum_{i \neq j} \vec{F}_{ij}. \quad (2.25)$$

Thus,

$$\sum_i^A \vec{F}_i \rho_i = \frac{1}{2} \left(\sum_i^A \vec{F}_i \rho_i + \sum_j^A \vec{F}_j \rho_j \right) = \frac{1}{2} \left(\sum_i \sum_{i \neq j} \vec{F}_{ij} \rho_i + \sum_j \sum_{j \neq i} \vec{F}_{ji} \rho_j \right), \quad (2.26)$$

where \vec{F}_{ij} is force exerted on particle- i by particle- j . And $\vec{F}_{ij} = -\vec{F}_{ji}$, then

$$\sum_i^A \vec{F}_i \rho_i = \frac{1}{2} \left[\sum_i \sum_{i \neq j} \vec{F}_{ij} (\rho_i - \rho_j) \right]. \quad (2.27)$$

With Taylor series (due to $R_{ij\beta} = R_{i\beta} - R_{j\beta}$ which is relative position of particle i and j is finite):

$$\begin{aligned} \rho_i(r_\beta - R_{i\beta}) &= \rho_i[r_\beta - R_{j\beta} + (R_{j\beta} - R_{i\beta})] \\ &= \rho_i[r_\beta - R_{j\beta} + R_{ji\beta}] \\ &= \sum_{n=0}^N \frac{(R_{ij\beta})^n}{n!} \rho_j^{(n)}(r_\beta - R_{j\beta}) \\ &\approx \rho_j(r_\beta - R_{j\beta}) + R_{ji\beta} \frac{\partial}{\partial r_\beta} \rho_j(r_\beta - R_{j\beta}). \end{aligned} \quad (2.28)$$

Then $R_{ij\beta} = -R_{ji\beta}$,

$$\rho_i(r_\beta - R_{i\beta}) - \rho_j(r_\beta - R_{j\beta}) = -R_{ij\beta} \frac{\partial}{\partial r_\beta} \rho_j(r_\beta - R_{j\beta}). \quad (2.29)$$

According to Eq. (2.24), Eq. (2.27), and Eq. (2.29),

$$\sum_i^A \frac{\partial \vec{P}_i}{\partial t} \rho_i = -\frac{1}{2} \sum_i \sum_{i \neq j} F_{ij\alpha} R_{ij\beta} \frac{\partial}{\partial r_\beta} \rho_j(r_\beta - R_{j\beta}) = \frac{\partial}{\partial r_\beta} \left(-\frac{1}{2} \sum_i \sum_{i \neq j} F_{ij\alpha} R_{ij\beta} \rho_j \right). \quad (2.30)$$

If interaction includes three-body component, in the same way, one can get

$$\frac{1}{2} \sum_i \sum_{i \neq j} \sum_{i \neq j \neq k} F_{ijk\alpha} \rho_i = \frac{1}{6} \sum_i \sum_{i \neq j} \sum_{i \neq j \neq k} (F_{ijk\alpha} \rho_i + F_{jki\alpha} \rho_j + F_{kij\alpha} \rho_k). \quad (2.31)$$

With the condition,

$$F_{ijk\alpha} + F_{jki\alpha} + F_{kij\alpha} = 0. \quad (2.32)$$

Then we obtain,

$$\frac{1}{2} \sum_i \sum_{i \neq j} \sum_{i \neq j \neq k} F_{ijk\alpha} \rho_i \approx \frac{\partial}{\partial r_\beta} \left[-\frac{1}{6} \sum_i \sum_{i \neq j} \sum_{i \neq j \neq k} (F_{ijk\alpha} R_{ik\beta} + F_{jki\alpha} R_{jk\beta}) \rho_k \right]. \quad (2.33)$$

Finally, according to Eqs.(2.12), (2.23), (2.24), (2.31), and (2.33), the momentum flux density tensor can be given,

$$\begin{aligned} T_{\alpha\beta}(\vec{r}, t) &= \sum_i^A \frac{P_{i\alpha} P_{i\beta}}{m_i} \rho_i(\vec{r}, t) \\ &+ \frac{1}{2} \sum_i^A \sum_{i \neq j}^A F_{ij\alpha} R_{ij\beta} \rho_j(\vec{r}, t) \\ &+ \frac{1}{6} \sum_i^A \sum_{i \neq j}^A \sum_{i \neq j \neq k}^A (F_{ijk\alpha} R_{ik\beta} + F_{jki\alpha} R_{jk\beta}) \rho_k(\vec{r}, t) \\ &+ \dots, \end{aligned} \quad (2.34)$$

The first term on the right-hand side is the momentum term, the second is the two-body interaction term, and the third is the three-body interaction term.

The η in Eq. (2.9) is a normal (or traditional) form of the Green-Kubo formula. In the last few decades, it has been extensively used in molecular dynamics simulations. In Ref. [115], a more general form of the Green-Kubo formula is given for the calculation of the shear viscosity for both Fermi-Dirac and Boltzmann distribution systems, which is read as,

$$\eta_{new} = \frac{mVA}{\langle \frac{1}{3} \sum_i^A p_i^2 \rangle} \int_{t_0}^{\infty} \langle T_{\alpha\beta}(t) T_{\alpha\beta}(t_0) \rangle dt, \quad (2.35)$$

where m is the particle mass. The derivation can be found in the Ref. [115]. It is obvious, of course, in

the classic limit, one has,

$$\left\langle \frac{1}{3} \sum_i^A p_i^2 \right\rangle = Amk_B T, \quad (2.36)$$

where k_B is the Boltzmann constant (here k_B set to 1). Substituting Eq. (2.36) into Eq. (2.35), we can get Eq. (2.9). To calculate shear viscosity directly from the Green-Kubo relation, one simply performs an equilibrium simulation of an A -particle system.

2.3. Shear strain rate method

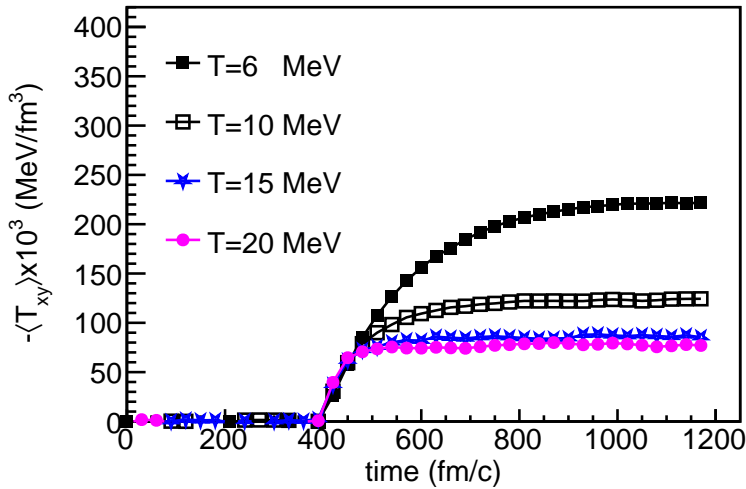


Figure 2.3: (Color online) Stress tensor as a function of time at different temperatures and density of $0.4\rho_0$ ($\rho_0 = 0.16 \text{ fm}^{-3}$ called saturation density of nuclear matter) without the mean field [115].

Instead of measuring the intrinsic fluctuations of the system, the viscosity can also be obtained using the non-equilibrium molecular dynamics (NEMD) calculation by imposing a Couette flow. This method was proposed by Evans and Morriss [21] and named the SLLOD algorithm, which has been extensively applied to predict the rheological properties of real fluids [21]. The SLLOD algorithm is related to the dynamics with strain rate $\dot{\gamma}$ associated with the Lees-Edwards periodic boundary conditions [119] and it is for shear viscosity with a planar Couette flow field at shear rate $\dot{\gamma} = \partial v_x / \partial y$ which is the change in streaming velocity v_x in the x -direction with vertical position y . We can obtain shear viscosity by

$$\eta = -\frac{\langle T_{xy} \rangle}{\dot{\gamma}}. \quad (2.37)$$

In Ref. [115], the strain rate was implanted in the framework of an improved quantum molecular dynamic (ImQMD) model without mean field, which is the cascade mode. As in Fig. 2.3 [115], it shows the stress

tensor as a function of time at different temperatures, which increases when the shear rate is $\dot{\gamma}$ at 400 fm/c and reaches a constant value after a time equals to the calculated shear viscosity.

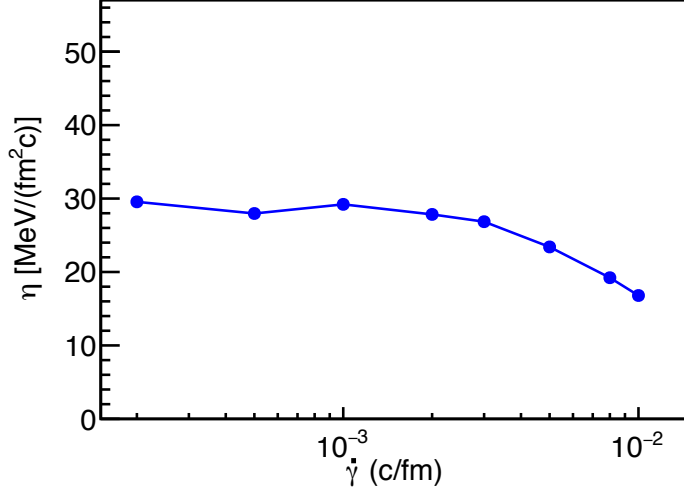


Figure 2.4: (Color online) Deduced shear viscosity as a function of the shear rate $\dot{\gamma}$ applied within the SLLOD algorithm, in the system at the density of $0.2\rho_0$ and temperature $T = 10$ MeV, when no mean field is employed.

The effect of the shear rate on the shear viscosity has been checked. As in Fig. 2.4, one can only notice in some ranges the shear viscosity keeps constant. So in the simulations, the shear rate cannot be too large or small. If it is small, flow fields cannot be implanted in the system. On the other hand, when shear rate is too large, energy can not be kept conservative when the dynamical equations of motion are solved with a finite time step.

By adding the shear rate, the dynamical equations of motion for the system can be rewritten as

$$\frac{d\vec{r}_i}{dt} = \frac{\vec{p}_i}{m_i} + \dot{\gamma}y_i\hat{x} \quad (2.38)$$

$$\frac{d\vec{p}_i}{dt} = \vec{F}_i - \dot{\gamma}p_{yi}\hat{x} - a\vec{p}_i. \quad (2.39)$$

Eq. (2.38) and Eq. (2.39) are called the SLLOD equations. In order to keep the kinetic energy conservation, one needs a ‘thermostat’. Thus a multiplier is applied to motion equations. Considering conservation of kinetic energy, one can get

$$a = \frac{\sum_i(\vec{F}_i \cdot \vec{p}_i/m_i - \dot{\gamma}p_{xi}p_{yi}/m_i)}{\sum_i p_i^2/m_i}. \quad (2.40)$$

2.4. Chapman-Enskog method

Chapman and Enskog (CE) have extracted the shear viscosity η in a gas of nonrelativistic particles by using the Boltzmann kinetic equation for the phase-space distribution function [120]. One should notice that originally the CE method was for Maxwell-Boltzmann statistics, but here it is for the Fermi system with the same strategy [75]. In the CE method, one can solve the Boltzmann equation by applying a series expansion to the distribution function [121]. In Ref. [74], one considered Boltzmann-Uehling-Uhlenbeck equation without potential U [85],

$$\frac{\partial}{\partial t} f_1(\vec{r}, \vec{p}, t) + \frac{\vec{p}}{m} \cdot \nabla_{\vec{r}} f_1(\vec{r}, \vec{p}, t) = I_{coll}. \quad (2.41)$$

The right-hand side (rhs) of Eq.(2.41) is the collision term ($I_{coll.}$), which denotes collision process of $1+2 \rightarrow 3+4$, and it can be read as [87]:

$$I_{coll.} = \left(\frac{\partial f_1}{\partial t} \right)_{coll.} = \frac{g}{(2\pi\hbar)^3} \int d^3 p_2 d\Omega \frac{d\sigma_{NN}}{d\Omega} |\vec{v}_1 - \vec{v}_2| \times \mathcal{P} \times \delta^3(\vec{p}_1 + \vec{p}_2 - \vec{p}_3 - \vec{p}_4). \quad (2.42)$$

where $g = 4$ is the spin and isospin degeneracy factor, and σ_{NN} is the nucleon-nucleon cross section. And the $\delta^3(\vec{p}_1 + \vec{p}_2 - \vec{p}_3 - \vec{p}_4)$ term is for keeping momentum conservation in the collisions. In Eq.(2.42), \mathcal{P} denotes the Pauli blocking factor, which reads,

$$\mathcal{P} = f_3 f_4 (1 - f_1)(1 - f_2) - f_1 f_2 (1 - f_3)(1 - f_4) \quad (2.43)$$

where the first term of the right-hand side is the gain term ($3+4 \rightarrow 1+2$) and the second term of the right-hand side is the loss term ($1+2 \rightarrow 3+4$).

Allowing the system to be slightly out of equilibrium, the first order of f can be written as [74, 122, 123],

$$f = f_{eq} + \delta f = f^0 + f^0(1 - f^0)\Phi, \quad (2.44)$$

where $f_{eq} = f^0$. Substituting Eq.(2.44) into the collision integral Eq.(2.42) and neglecting terms of quadratic and higher order in Φ [74, 123], one can obtain

$$\begin{aligned} \frac{\partial}{\partial t} f_1^0 + \frac{\vec{p}}{m} \cdot \nabla_{\vec{r}} f_1^0 &= \frac{g}{(2\pi\hbar)^3} \int d^3 p_2 d\Omega \frac{d\sigma_{NN}}{d\Omega} |\vec{v}_1 - \vec{v}_2| \times f_1^0 f_2^0 (1 - f_3^0)(1 - f_4^0) \\ &\times (\Phi_3 + \Phi_4 - \Phi_1 - \Phi_2) \times \delta^3(\vec{p}_1 + \vec{p}_2 - \vec{p}_3 - \vec{p}_4). \end{aligned} \quad (2.45)$$

In the first-order approximation, the contribution of δf on the left side can be neglected, and f_1 is replaced by f_1^0 . Considering the existence of a motion with a slightly inhomogeneous velocity \vec{u} in the liquid [116], we can write the distribution function f^0 as,

$$f^0 = \frac{1}{e^{(E - \vec{p} \cdot \vec{u} - \mu)/T} + 1}, \quad (2.46)$$

where μ is chemical potential. By substituting (2.46) to the left-hand side of (2.41), expanding in terms of gradients of temperature and fluid velocity and assuming $\nabla \cdot \vec{u} = 0$ for an incompressible fluid that drives bulk viscosity and is neglected here [74, 116, 124], we have

$$\begin{aligned} \frac{\partial f^0}{\partial t} + \frac{\vec{p}}{m} \cdot \nabla_{\vec{r}} f^0 &= \frac{1}{2mT} f^0 f^0 \left[(p_\alpha p_\beta - \frac{1}{3} \delta_{\alpha\beta} p^2) \left(\frac{\partial u_\alpha}{\partial r_\beta} + \frac{\partial u_\beta}{\partial r_\alpha} - \frac{2}{3} \delta_{\alpha\beta} \nabla \cdot \mathbf{u} \right) + \frac{1}{mT} (p^2 - \frac{5}{3} \langle p^2 \rangle) p_\alpha \frac{\partial T}{\partial r_\alpha} \right] \\ &= \frac{1}{2mT} f^0 f^0 \left[(p_\alpha p_\beta - \frac{1}{3} \delta_{\alpha\beta} p^2) \left(\frac{\partial u_\alpha}{\partial r_\beta} + \frac{\partial u_\beta}{\partial r_\alpha} \right) + \frac{1}{mT} (p^2 - \frac{5}{3} \langle p^2 \rangle) p_\alpha \frac{\partial T}{\partial r_\alpha} \right]. \end{aligned} \quad (2.47)$$

where $\langle p^2 \rangle$ is an average over distribution. In Eq.(2.47), we only pick up the terms which are relevant to shear viscosity and heat conduction coefficient. For symmetry consideration between the right-hand side of Eq.(2.45) and the right-hand side of Eq.(2.47), it can be found that Φ has the form

$$\Phi = q^{(1)} (p_\alpha p_\beta - \frac{1}{3} \delta_{\alpha\beta} p^2) \left(\frac{\partial u_\alpha}{\partial r_\beta} + \frac{\partial u_\beta}{\partial r_\alpha} \right) + q^{(2)} (p^2 - \frac{5}{3} \langle p^2 \rangle) p_\alpha \frac{\partial T}{\partial r_\alpha}, \quad (2.48)$$

where the $q^{(1)}$ and $q^{(2)}$ are constant factors [74, 116]. And by multiplying both sides of Eq.(2.45) by Φ_1 and integrating over the momenta $d^3 p_1$, one can obtain the constants.

Shear viscosity (η) as the coefficient proportional to the shear momentum flux tensor (one also can see from Eq. 2.6) without bulk viscosity,

$$\begin{aligned} \Pi_{\alpha\beta} &= -\eta \left(\frac{\partial u_\alpha}{\partial r_\beta} + \frac{\partial u_\beta}{\partial r_\alpha} - \frac{2}{3} \delta_{\alpha\beta} \nabla \cdot \vec{u} \right) \\ &= -\eta \left(\frac{\partial u_\alpha}{\partial r_\beta} + \frac{\partial u_\beta}{\partial r_\alpha} \right) \end{aligned} \quad (2.49)$$

where the $\nabla \cdot \vec{u}$ is assumed to be zero. A slight out of equilibrium produces a change in the dissipative

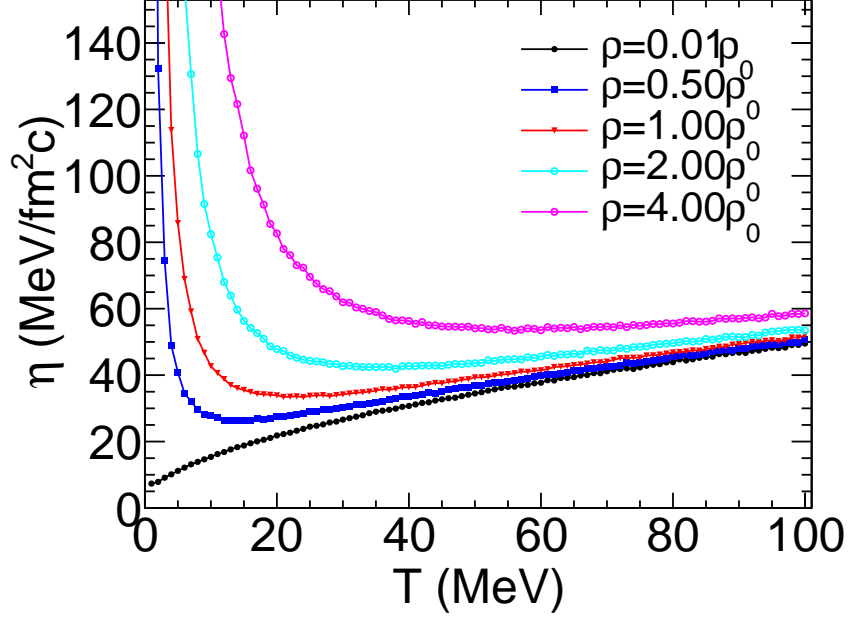


Figure 2.5: (Color online) Shear viscosity as a function of temperature at different nuclear matter densities.

stress tensor; at the lowest order in δf , we can obtain,

$$\begin{aligned}
\Pi_{\alpha\beta} &= \frac{g}{(2\pi\hbar)^3} \int d^3p \frac{p_\alpha p_\beta}{m} f = \frac{g}{(2\pi\hbar)^3} \int d^3p \frac{p_\alpha p_\beta}{m} f_0 + \frac{g}{(2\pi\hbar)^3} \int d^3p \frac{p_\alpha p_\beta}{m} \delta f \\
&= \frac{g}{(2\pi\hbar)^3} \int d^3p \frac{p_\alpha p_\beta}{m} \delta f \\
&= \frac{g}{(2\pi\hbar)^3} \int d^3p \frac{p_\alpha p_\beta}{m} f^0 (1 - f^0) \Phi.
\end{aligned} \tag{2.50}$$

The equilibrium term with f_0 in $\Pi_{\alpha\beta}$ is zero. Substituting (2.48) into (2.50), one can get the expression for shear viscosity [74, 125]:

$$\eta = \frac{5T}{9} \frac{\left(\int d^3p_1 p_1^2 f_1 \right)^2}{\int d^3p_1 d^3p_2 d\Omega v_{12} q_{12}^4 \sin^2\theta \frac{d\sigma_{NN}}{d\Omega} f_1 f_2 \tilde{f}_3 \tilde{f}_4}, \tag{2.51}$$

where $v_{12} = |\vec{v}_1 - \vec{v}_2|$, $q_{12} = |\vec{p}_1 - \vec{p}_2|/2$ and θ are relative velocity, relative momentum, and scattering angle between the total momentum $\vec{p}_t = \vec{p}_1 + \vec{p}_2 = \vec{p}_3 + \vec{p}_4$ and the relative momentum of the final state $\vec{p}_r = \vec{p}_3 - \vec{p}_4$, respectively. σ_{NN} is the total nucleon-nucleon cross section, and $\tilde{f}_3 \tilde{f}_4 = [1 - f(p_3)][1 - f(p_4)]$ is the Pauli blocking term. In Eq.(2.51), the conservations of momentum and energy between p_1, p_2 and p_3, p_4 are needed to be taken into account in the collisions.

By solving Eq.(2.51) with the Monte-Carlo approach, one obtains the shear viscosity as shown in

Fig.2.5. Here the $\frac{d\sigma_{NN}}{d\Omega}$ is set to 40 mb/4 π . It is seen that the shear viscosity increases as temperature increases for very low density ($0.01\rho_0$) which can be treated as Fermion gas. For the Fermion gas, the Pauli blocking effect is weak, and so the behavior for shear viscosity acts like that of classic gas. For higher densities, however, shear viscosity decreases with increasing of temperature in low-temperature region since Pauli blocking effect is strong. As temperature increases again, particle velocity becomes dominative leading to the increasing of shear viscosity.

2.5. Relaxation time method

In the relaxation time approximation method, one assumes that the effect of collisions is always to bring the perturbed distribution function close to the equilibrium distribution function [126, 127], $f = f_{eq} + \delta f$ which is as Eq.(2.44). Then one writes the collision term exponentially with a relaxation time of τ ,

$$\mathcal{D}f = -\frac{f - f_{eq}}{\tau} = -\frac{\delta f}{\tau} \quad (2.52)$$

where $\mathcal{D} = \frac{\partial}{\partial t} + \vec{v} \cdot \nabla_{\vec{r}} - \nabla_{\vec{r}}U \cdot \nabla_{\vec{p}}$. In the relaxation time approximation, one starts from shear force between flow layers per unit area and obtains the shear viscosity [82]

$$\eta = -\sum_{\tau} \frac{g}{(2\pi)^3} \int \tau_{\tau}(p) \frac{p_z^2 p_x^2}{p m_{\tau}^*} \frac{df_{\tau}^0}{dp} d^3p, \quad (2.53)$$

where the subscript τ is the isospin factor, which is set to 1/2 (-1/2) for neutrons (protons). So here the degeneracy factor $g=2$. And m_{τ}^* is the effective mass, which reads as,

$$\frac{1}{m_{\tau}^*} = \frac{1}{m} + \frac{1}{p} \frac{dU_{\tau}}{dp}, \quad (2.54)$$

where U_{τ} is the single-particle potential for a nucleon with momentum \vec{p} and isospin τ in a nuclear matter medium, which can be found in Ref. [82]. In Eq. (2.53), f_{τ} is the local momentum distribution, which is written as,

$$f_{\tau} = \frac{1}{\exp\left[\frac{p^2}{2m} - U_{\tau}(\vec{p}) - \mu_{\tau}\right]/T + 1}. \quad (2.55)$$

And in Eq. (2.53), $\tau_{\tau}(p)$ is the relaxation time which can be expressed as,

$$\frac{1}{\tau_{\tau}(p_1)} = \frac{1}{\tau_{\tau}^{\text{same}}(p_1)} + \frac{1}{\tau_{\tau}^{\text{diff}}(p_1)} \quad (2.56)$$

where $\tau_\tau^{\text{same(diff)}}(p_1)$ is the average collision time for a nucleon with isospin τ and momentum p_1 when colliding with other nucleons of same (different) isospin, and they can be calculated from [82],

$$\begin{aligned} \frac{1}{\tau_\tau^{\text{same}}(p_1)} &= \left(g - \frac{1}{2}\right) \frac{1}{2\pi} \int p_2^2 dp_2 d\cos\theta_{12} d\cos\theta \frac{d\sigma_{\tau,\tau}}{d\Omega} \left| \frac{\vec{p}_1}{m_\tau^*} - \frac{\vec{p}_2}{m_\tau^*} \right| \\ &\times [f_\tau^0(p_2) - f_\tau^0(p_2)f_\tau^0(p_3) - f_\tau^0(p_2)f_\tau^0(p_4) + f_\tau^0(p_3)f_\tau^0(p_4)], \end{aligned} \quad (2.57)$$

$$\begin{aligned} \frac{1}{\tau_\tau^{\text{diff}}(p_1)} &= \frac{g}{2\pi} \int p_2^2 dp_2 d\cos\theta_{12} d\cos\theta \frac{d\sigma_{\tau,\tau}}{d\Omega} \left| \frac{\vec{p}_1}{m_\tau^*} - \frac{\vec{p}_2}{m_{-\tau}^*} \right| \\ &\times [f_{-\tau}^0(p_2) - f_{-\tau}^0(p_2)f_\tau^0(p_3) - f_{-\tau}^0(p_2)f_{-\tau}^0(p_4) + f_\tau^0(p_3)f_{-\tau}^0(p_4)], \end{aligned} \quad (2.58)$$

where θ_{12} is the angel between \vec{p}_1 and \vec{p}_2 .

In this chapter, the definition of shear viscosity is given from two planes, and some methods to estimate shear viscosity are given. There are more methods for calculating shear viscosity as in Refs. [127–129].

3. Theoretical aspects of shear viscosity in nucleonic matter

3.1. Infinite nuclear matter

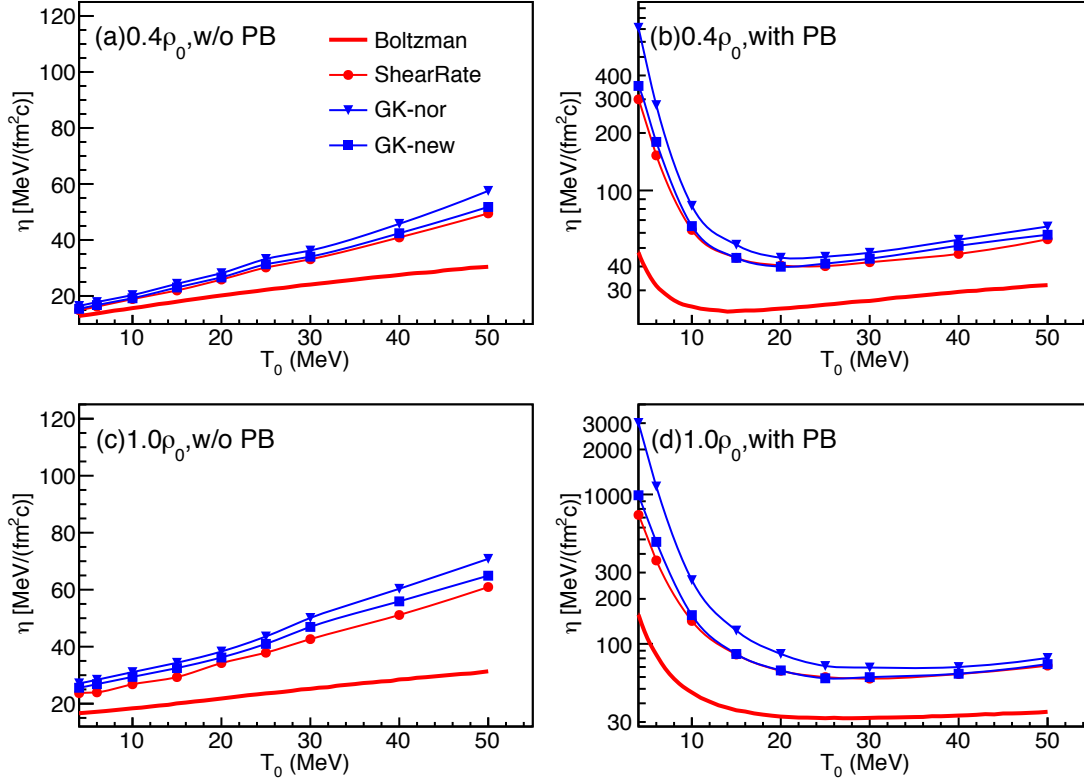


Figure 3.1: (Color online) Different calculations of shear viscosity as a function of temperature in cases of w/ or w/o Pauli blocking (PB) at $0.4 \rho_0$ and $1.0 \rho_0$ and the nucleon-nucleon cross section is fixed at 40 mb [115].

In the last section, some approaches to extracting the shear viscosity of nuclear matter or a Fermi system are introduced. In the previous work [115], comparisons have been done among methods of Chapman-Enskog (for the Fermi system), shear strain rate, and Greek-Kubo in a periodic box by using an improved quantum molecular dynamic (ImQMD) model without mean field as displayed in Fig. 3.1. It should be mentioned that ‘Boltzman’ denotes the Chapman-Enskog method as the Eq. (2.51). The GK-nor and GK-new are the normal Green-Kubo formula as Eq. (2.9) and new form of the Green-Kubo formula as Eq. (2.35), respectively. As shown in Fig. 3.1, the Pauli blocking effect is studied in the calculation. It is worth to mention that for a Fermi system Pauli blocking should be taken into account. It can be seen that in Fig. 3.1(a) and Fig. 3.1(c) without the Pauli blocking, shear viscosity increases with temperature at both densities of $0.4\rho_0$ and $1.0\rho_0$. Seeing from Fig. 3.1 (b) and Fig. 3.1(d) with the Pauli blocking, unlike Fig. 3.1(a) and Fig. 3.1(c) in the low-temperature region, shear viscosity increases with the decreasing of temperature. It is due to a stronger Pauli blocking effect in the low temperature region. At lower temperature and with stronger Pauli blocking effect, it indicates that

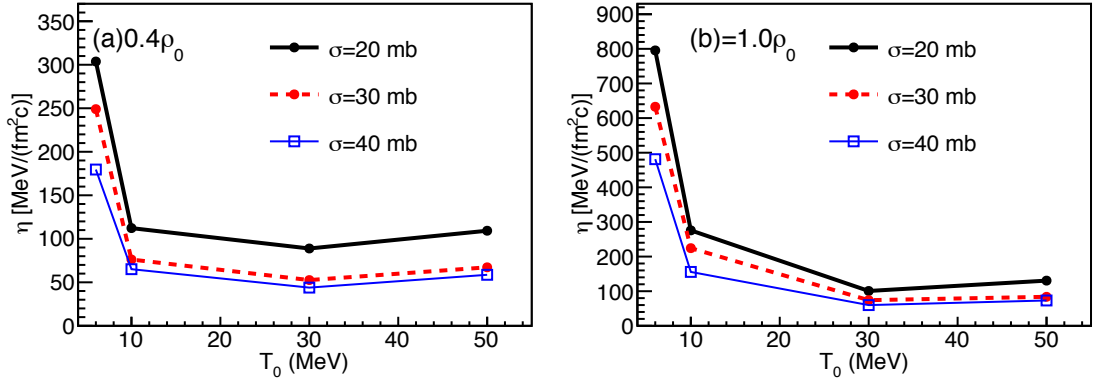


Figure 3.2: (Color online) Shear viscosity as a function of temperature (T_0) at densities $0.4\rho_0$ (a) and $1.0\rho_0$ (b) for different cross sections with Green-Kubo formula as Eq. (2.35) in ImQMD model.

a good Fermi sphere is formed and thus the elastic scattering rate is greatly suppressed due to the Pauli blocking. Hence, the system in lower temperature region has larger shear viscosity. However, an uncertainty in extracting the value of the shear viscosity at $T = 0$ is given here for the small or finite values of shear viscosity being given in the Refs. [130–134], such an uncertainty is explained by different dissipation mechanisms [134]. As temperature increases, the Pauli blocking effect becomes weaker and collision increases which makes the momentum transfer easier and shear viscosity decreasing. As the temperature increases again, even though the collision rate increases, velocity becomes dominant. Thus, shear viscosity increases with temperature. It is concluded that the naive kinetic approach is not valid for the description of the unitary Fermi gas at low temperature, where the system becomes strongly correlated [135]. For the dilute gas case as black dot-line in Fig. 2.5, it increases with temperature since it is dominated by the term of temperature (or particle velocity).

Besides, one can find that, among these three approaches, shear viscosity determined by the Boltzmann type equation of Eq. (2.51) is lower than that calculated by the shear rate and the Green-Kubo method. At very low densities such as $0.05\rho_0$, however, we found that the result by the Boltzmann type equation (Eq. 2.51) is consistent with other methods, which indicates that a low density approximation for Eq. 2.51 could be valid. Then one would expect that shear viscosities determined by the shear rate and the Green-Kubo approaches are the same. In Ref. [115], we re-derived and gave a new form of the Green-Kubo formula for the calculation of shear viscosity as Eq. (2.35). In the Boltzmann statistical analysis without Pauli blocking, we found that shear viscosities from the shear rate method, the normal form of the Green-Kubo formula, and new form of the Green-Kubo formula are close. As the Pauli blocking is taken into account as shown in Fig. 3.1 (b) and Fig. 3.1 (d), however, one sees that in the low temperature region, the shear viscosity from the normal form of the Green-Kubo formula (2.9) is higher than those from both the shear strain rate method and the new form of the Green-Kubo formula.

However, shear viscosities from the shear rate method and the new form of the Green-Kubo formula are almost the same. At high temperatures, shear viscosities from the shear rate method, the normal form of the Green-Kubo formula, and the new form of the Green-Kubo formula are to be the same since particle collisions become dominant and Pauli blocking can be ignored as temperature increases. So one should be careful when applying the normal form of the Green-Kubo formula to extract shear viscosity of Fermi system at low-temperature region.

From both the Chapman-Enskog method and relaxation time approximation method, we can see that the collision has an important role for the shear viscosity. For the results in Fig. 3.1, the nucleon-nucleon cross section is fixed at 40 mb. When one increases the cross section, the shear viscosity would reduce, as shown in Fig. 3.2. It is obvious that as the cross-section increases, momentum transfer becomes quite easier, which would lead to lower shear viscosity. It can be seen that the shear viscosity is sensitive to the nucleon-nucleon cross section. Thus, one adjusts the in-medium nucleon-nucleon (NN) cross section in a transport model which is named pBUU [136–139] to reproduce the nuclear stopping data and use the fitted cross sections to calculate the shear viscosity self-consistently [125]. The NN cross-section should also be affected by the surrounding medium. The authors discussed three kinds of media cross-sections with nuclear stopping. One is

$$\sigma_{NN}^{\text{med}} = \sigma_0 \tanh\left(\frac{\sigma_{NN}^{\text{free}}}{\sigma_0}\right), \quad (3.1)$$

where $\sigma_0 = \nu\rho^{-2/3}$, ν and ρ are a parameter in order of 1 and medium of number density, respectively. And $\sigma_{NN}^{\text{free}}$ is free NN cross section. A in-medium cross section carried out at the University of Rostock [140] within a thermodynamic T-matrix approach is given by a parametrization of the cross-section reduction [125],

$$\sigma_{NN}^{\text{med}} = \sigma_{NN}^{\text{free}} \exp\left(-0.6 \frac{\rho/\rho_0}{1 + [T_{c.m.}/150 \text{ MeV}]^2}\right), \quad (3.2)$$

where $T_{c.m.}$ is the total kinetic energy of the two interacting particles in the frame where the local medium is at rest. The last one is derived by Fuchs et al. [141] which is parameterized with,

$$\sigma_{nn}^{\text{med}} = \sigma_{nn}^{\text{free}} \exp\left(-1.7 \frac{\rho/\rho_0}{1 + [T_{c.m.}/12 \text{ MeV}]^{3/2}}\right), \quad (3.3)$$

$$\sigma_{np}^{\text{med}} = \sigma_{np}^{\text{free}} \exp\left(-1.4 \frac{\rho/\rho_0}{1 + [T_{c.m.}/33 \text{ MeV}]}\right). \quad (3.4)$$

With the help of the different cross-section reductions above, the authors can compare predictions from

pBUU to stopping data, as shown in Fig. 3.3. The stopping observable $varxz$ is defined as [142],

$$varxz = \frac{\Delta y_x}{\Delta y_z}, \quad (3.5)$$

where Δy_x is the variance of particle rapidity along a randomly chosen direction that is transverse to the beam and Δy_z is the variance of the standard particle longitudinal rapidity. From Fig. 3.3, it is seen that around the peak region in $varxz$ versus energy with the Rostock cross section or the tempered cross section with $\nu = 0.8$, the results from pBUU can describe the data well. Then, by combining the constrained in-media cross-sections σ_{NN}^{med} and the Eq. (2.51), one can obtain shear viscosity as shown in Fig. 3.4. In such a way, the shear viscosity is hopefully of greater generality than even the transport model itself [125]. Shear viscosity versus temperature is sensitive to different kinds of in-media cross-sections σ_{NN}^{med} . But it can be seen that a uniform factor could not describe the data for the whole energy region, which indicates that the factor for in-media cross-sections should be energy dependence. Here, the behavior of shear viscosity versus temperature is no more different from that in Fig. 2.5. In Ref. [125], it only considers the elastic collision cross section. Like comments in Ref. [125], however, as collision energy or temperature increases to a high value, meson effects and modifications of inelastic processes need to be explored in the simulations.

In a more general sense, Shi and Danielewicz [75] solved the set of Boltzmann equations for a binary system of fermions to find thermodynamic fluxes driven by specific thermodynamic forces and to find general expressions for the shear viscosity and other transport coefficients. The transport coefficients are calculated numerically for nuclear matter using experimental nucleon-nucleon cross sections. The numerical results for the coefficients have been obtained,

$$\eta = (1 + 0.10\delta^2) \left[\frac{856}{T^{1.10}} \left(\frac{\rho}{\rho_0} \right)^{1.81} - \frac{240.9}{T^{0.95}} \left(\frac{\rho}{\rho_0} \right)^{2.12} + 2.154T^{0.75} \right], \quad (3.6)$$

$$D_I = (1 - 0.19\delta^2) \left[\frac{11.34}{T^{2.38}} \left(\frac{\rho}{\rho_0} \right)^{1.54} + \frac{1.746}{T} \left(\frac{\rho}{\rho_0} \right)^{0.56} + 0.00585T^{0.913} \left(\frac{\rho}{\rho_0} \right) \right], \quad (3.7)$$

$$\kappa = (1 + 0.10\delta^2) \left[\frac{0.235}{T^{0.755}} \left(\frac{\rho}{\rho_0} \right)^{0.951} - 0.0582 \left(\frac{\rho}{\rho_0} \right)^{0.0816} + 0.0238T^{0.5627} \left(\frac{\rho}{\rho_0} \right)^{0.0171} \right]. \quad (3.8)$$

where T is temperature in MeV, η is shear viscosity in MeV/(fm²c), D_I is isospin diffusivity in fm²c, heat conductivity κ is in c/fm²; and $\delta = \frac{\rho_n - \rho_p}{\rho}$ is isospin asymmetry. From these Eqs. (3.6)–(3.8), it is found that the shear viscosity diffusion coefficient and heat-conduction coefficient weakly depend on isospin asymmetry. One can also see from Fig. 3.5 in which shear viscosity as a function of temperature at different isospin asymmetries is displayed.

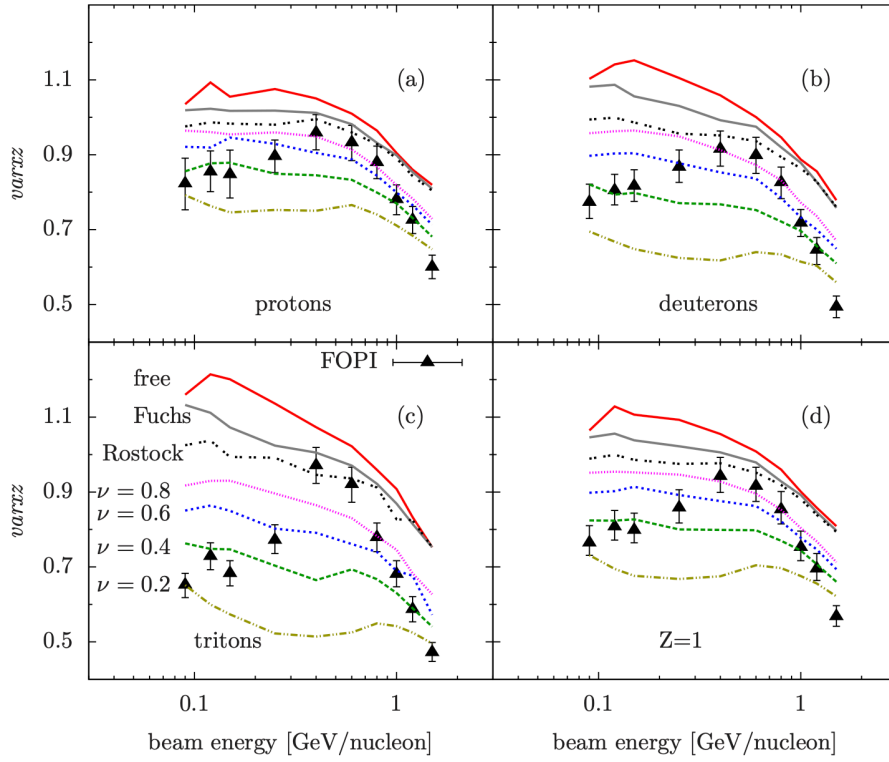


Figure 3.3: (Color online) Stopping observable $varxz$ for protons (a), deuterons (b), tritons (c), and particles with $Z=1$ (d) in Au + Au collisions at different beam energies at $bred < 0.15$. Lines show the effects of different in-medium reductions of the NN cross section [125]. The “tempered” cross-section reductions are marked with their tunable parameter ν . Symbols are experimental data from the FOPI Collaboration [143].

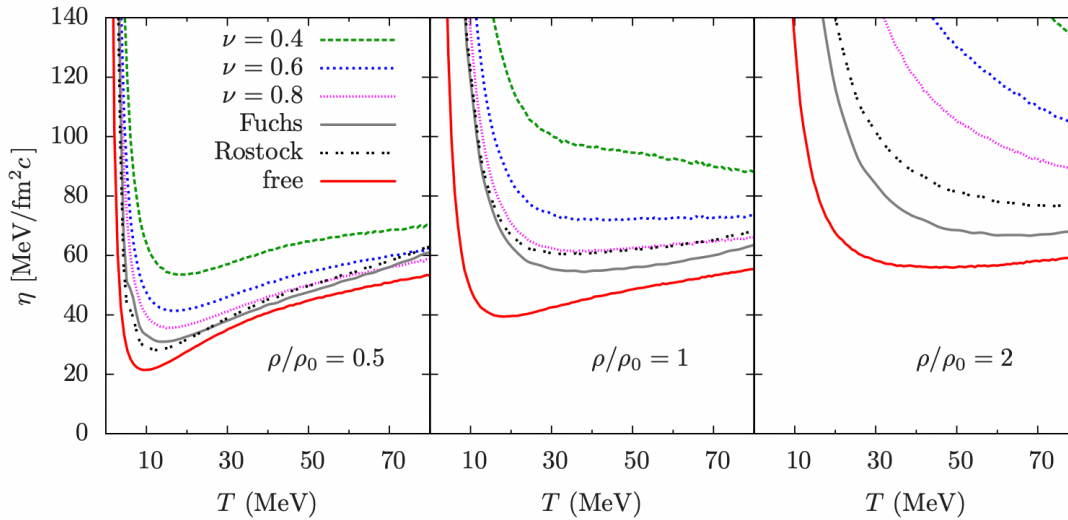


Figure 3.4: (Color online) Shear viscosity for symmetric nuclear matter at different densities and temperatures, deduced from Boltzmann equation with in-medium cross sections [125].

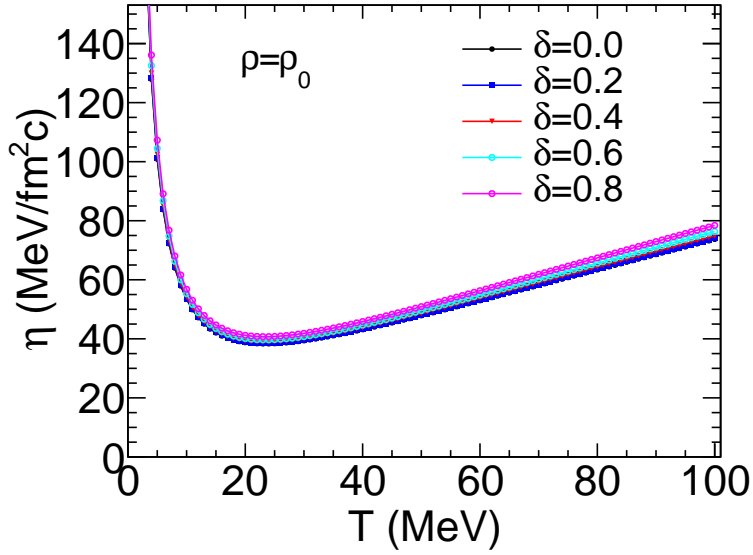


Figure 3.5: (Color online) Shear viscosity as a function of temperature at different isospin asymmetries.

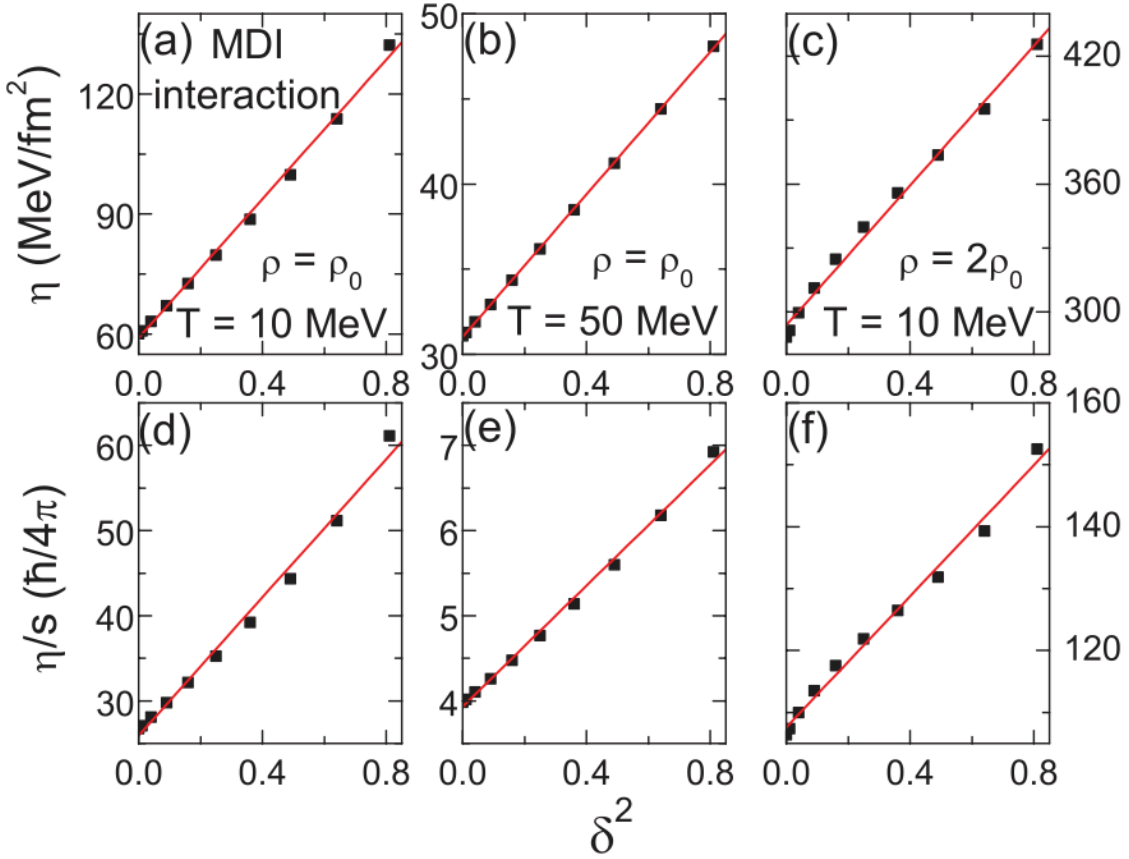


Figure 3.6: (Color online) Shear viscosity η and specific viscosity η/s (s is entropy density) as functions of isospin asymmetry δ^2 for different densities and temperatures. The solid lines are from the linear fit [82].

On the other hand, one derives the shear viscosity of neutron-rich nuclear matter from the relaxation time approximation approach using an isospin- and momentum-dependent interaction and the nucleon-nucleon cross sections taken as those from the experimental data modified by the in-medium effective masses as used in the isospin-dependent Boltzmann-Uehling-Uhlenbeck (IBUU) transport model calculations [82]. The expression for shear viscosity is shown by Eq. (2.53).

As shown in Fig. 3.6, shear viscosity η and specific viscosity η/s (s is entropy density) as functions of isospin asymmetry δ^2 for different densities and temperatures are displayed. Here, the entropy density s can be obtained by [82],

$$s = - \sum_{\tau} \frac{g}{(2\pi\hbar)^3} \int \left[f_{\tau} \ln f_{\tau} + (1 - f_{\tau}) \ln(1 - f_{\tau}) \right] d^3p. \quad (3.9)$$

With $\delta^2 = 0$ for the symmetry nuclear matter in Fig. 3.6 (a), a simple comparison is shown for shear viscosity from the Boltzmann type equation of Eq. (2.51), shear rate, and the Green-Kubo methods. We can see that the shear viscosity by relaxation time approximation approach is close to the one by Boltzmann type equation. However, it is less than those from the shear rate and the Green-Kubo methods. And η shows parabolic approximation relation to isospin asymmetry δ^2 . It presents that isospin asymmetry has a large effect on shear viscosity, which could be different from the results obtained by solving the set of Boltzmann equations as mentioned above. The reason here could be due to the isospin interaction used in the calculations. The specific viscosity η/s which is a hot agenda and relates to a bound value of $\hbar/4\pi$ is shown in Fig. 3.6. It can be seen that specific viscosity η/s also shows parabolic approximation relation to isospin asymmetry δ^2 . From Fig. 3.6 (d), (e), and (f), we can see that at $T = 10$ MeV and $\rho = \rho_0$, η/s is larger than 25 times of $\hbar/4\pi$. When $T = 50$ MeV, the specific viscosity is about $4 \sim 5 \hbar/4\pi$, which is already close to KSS bound. At a higher density at $\rho = 2\rho_0$, specific viscosity becomes larger with the increase in shear viscosity.

For common matter like water, as shown in Fig. 3.7, it can be seen that below the critical pressure of 22.06 MPa, η/s shows a discontinuity at the minimum. Above the critical pressure, η/s becomes smooth [106]. In Ref. [106], from the results computed for the shear viscosity of QCD in the hadronic phase by the coupled Boltzmann equations of pions and nucleons in low temperatures and low baryon-number densities and combined common matter such as Ar, CO, CO₂, H, He, H₂S, Kr, N, NH₃, Ne, O, and Xe, the authors suspect that the general feature for a first-order phase transition is that η/s has a discontinuity in the bottom of the η/s valley. And the valley gradually disappears when the phase transition turns into a crossover. Near the critical point, there is a smooth valley in the crossover, which is similar to the confinement-deconfinement crossover of QCD at $\mu = 0$. And as the pressure

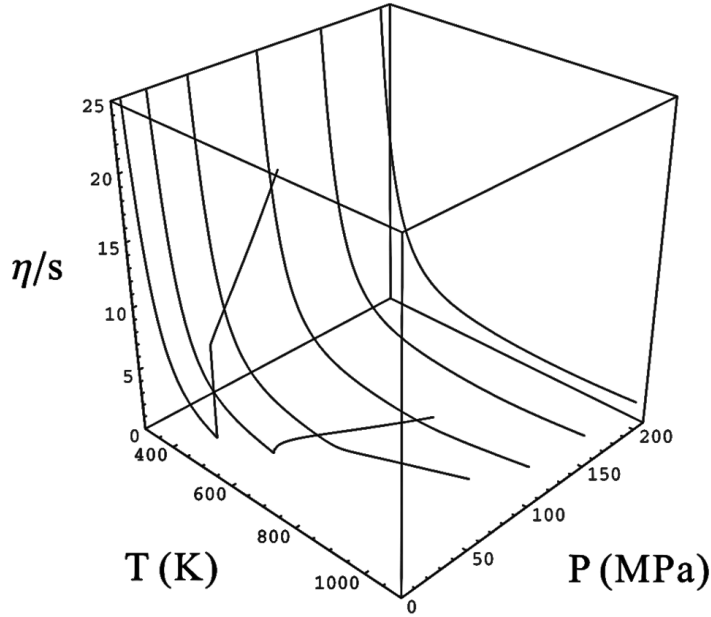


Figure 3.7: (Color online) Specific shear viscosity η/s of water as a function of temperature in different pressures [106].

is far away from the critical point, the valley shape will disappear. The authors argue that these are general features of first-order phase transitions which indicates that specific viscosity η/s may be used as a probe to study the phenomenon of liquid–gas phase transition. Also, in Fig. 3.7, the η/s of water shows a positive jump across the phase transition line from the gas to liquid phase. The sign of the η/s jump of water for first-order phase transitions is similar to the materials including Ar, CO₂, H, He, H₂S, Kr, N, NH₃, Ne, O, and Xe. But it might not be universal, as the jump for QCD in the limit of a large number of colors is negative from the low to high temperature phases [48] and the behavior of nucleonic matter [83].

The specific viscosity (η/s) of neutron-rich nucleonic matter near its liquid–gas phase transition was studied with the relaxation time approximation approach [83]. In this framework, one treats the phase coexistence region with a volume fraction ξ , and the average number and entropy densities are given by,

$$\rho = \xi\rho_l + (1 - \xi)\rho_g, \quad (3.10)$$

$$s = \xi s_l + (1 - \xi)s_g. \quad (3.11)$$

where $\rho_{l(g)}$ and $s_{l(g)}$ are the number and entropy densities of the liquid (gas) phase, respectively. To construct a phase coexistence state for nuclear matter, the Gibbs conditions are used. For phase coexistence, it is governed by the Gibbs conditions. For asymmetric nuclear matter, two-phase coexistence

equations are [144],

$$\mu_i^l(T, \rho_i^l) = \mu_i^g(T, \rho_i^g) \quad (i = n \text{ and } p), \quad (3.12)$$

$$P_i^l(T, \rho_i^l) = P_i^g(T, \rho_i^g) \quad (i = n \text{ or } p), \quad (3.13)$$

where P is the pressure. To determine shear viscosity, one considers a stationary flow field in the z direction and the shear force on the particles for a single phase of gas or liquid [82, 83],

$$F_i = \sum \langle (p_z - m_\tau u_z) \rho_\tau v_x \rangle_i, \quad (3.14)$$

where τ refers to a neutron or proton, $i = l$ is for the liquid phase and g is for the gas phase, and m_τ is the nucleon mass. And $\langle \dots \rangle$ denotes the thermal average of the product of the flux $\rho_\tau v_x$ in the x direction and the momentum transfer $p_z - m_\tau u_z$ in the z direction. The shear viscosity is determined by,

$$F_{l(g)} = -\eta_{l(g)} \frac{\partial u_z}{\partial x}. \quad (3.15)$$

In the phase coexistence region, one can imagine gas bubbles in a liquid or liquid droplets in a gas. Thus, finally, the average shear viscosity of the mixed phase can be expressed as,

$$\eta = \xi \eta_l + (1 - \xi) \eta_g. \quad (3.16)$$

Here, η_l and η_g can be separately calculated owing to the density is uniform in each phase. And the strategy is as in Ref.[82].

In Fig.3.8, density (top panels), shear viscosity (middle panels), and specific shear viscosity (bottom panels) as functions of temperature at the fixed pressure of $P = 0.1 \text{ MeV}/\text{fm}^3$ for different isospin symmetries with the stiffer symmetry energy $x=0$ are shown. For a given pressure, the shear viscosity of the liquid phase is greater than that of the gas phase. And with $\delta = 0$, there is a sudden jump for density, shear viscosity, and specific shear viscosity at a temperature $T \sim 12 \text{ MeV}$, which is due to liquid–gas phase transition of first-order of symmetric nucleonic matter [83]. The behavior here for shear viscosity versus temperature is similar to that of ${}^3\text{He}$ [52]. From Fig.3.8, it can be seen that the minimum of the specific shear viscosity is exactly located at the critical temperature when a first-order phase transition happens, while it is located at the boundary of the gas phase if the phase transition is a second-order [83]. In a Fermi system, as we know, there is competition between the Pauli blocking

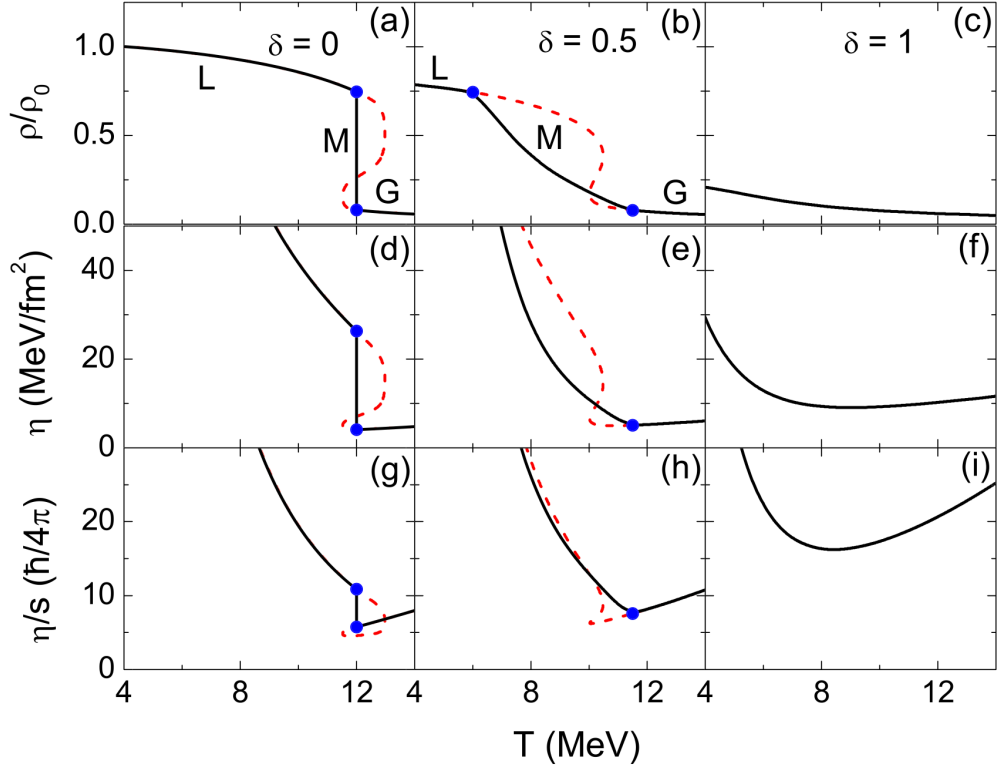


Figure 3.8: (Color online) Density (top panels), shear viscosity (middle panels), and specific shear viscosity (bottom panels) as functions of temperature at the fixed pressure of $P = 0.1 \text{ MeV}/\text{fm}^3$ for isospin symmetric matter ($\delta = 0$) (left column), neutron-rich matter ($\delta = 0.5$) (middle column), and pure neutron matter ($\delta = 1$) (right column) with the stiffer symmetry energy $x = 0$. Solid lines are results including the liquid-gas phase transition with ‘L’, ‘M’, and ‘G’ denoting the liquid phase, the mixed phase, and the gas phase, respectively. Dashed lines are results obtained by assuming the liquid–gas phase transition does not happen inside the binodal surface [83].

and collision among particles with changes of temperature. So even for pure neutron matter without a liquid-gas phase transition, it is also seen that there is still a valley-shape around phase transition region. In Fig.3.8 (a), (b), (c), the jumps show a negative sign and differ from water as in Fig. 3.7.

Furthermore, one can get more results for specific shear viscosity as functions of temperature and density from Ref. [83], as shown in Fig.3.9. The results show that the specific shear viscosity of nucleonic matter is about 4–5 $\hbar/4\pi$ for isospin-symmetric nucleonic matter and is generally smaller than that in neutron-rich nucleonic matter. It is obvious that there are valley shapes for symmetric nuclear matter and pure neutron matter. The symmetry energy effect is investigated as the solid and dashed lines display. In the phase coexistence region, the softer ($x = 1$) symmetry energy would give a larger specific shear viscosity than that with the stiffer ($x = 0$) symmetry energy for the liquid-like region, as in Fig.3.9 (b) and Fig.3.9 (e). And for pure neutron matter without the liquid-gas phase transition under a fixed pressure, specific shear viscosity for $x = 1$ is similar to that for $x = 0$, as in Fig.3.9(c). At fixed temperature, specific shear viscosities from different symmetry energies are the same for pure neutron matter, as shown in Fig.3.9 (f).

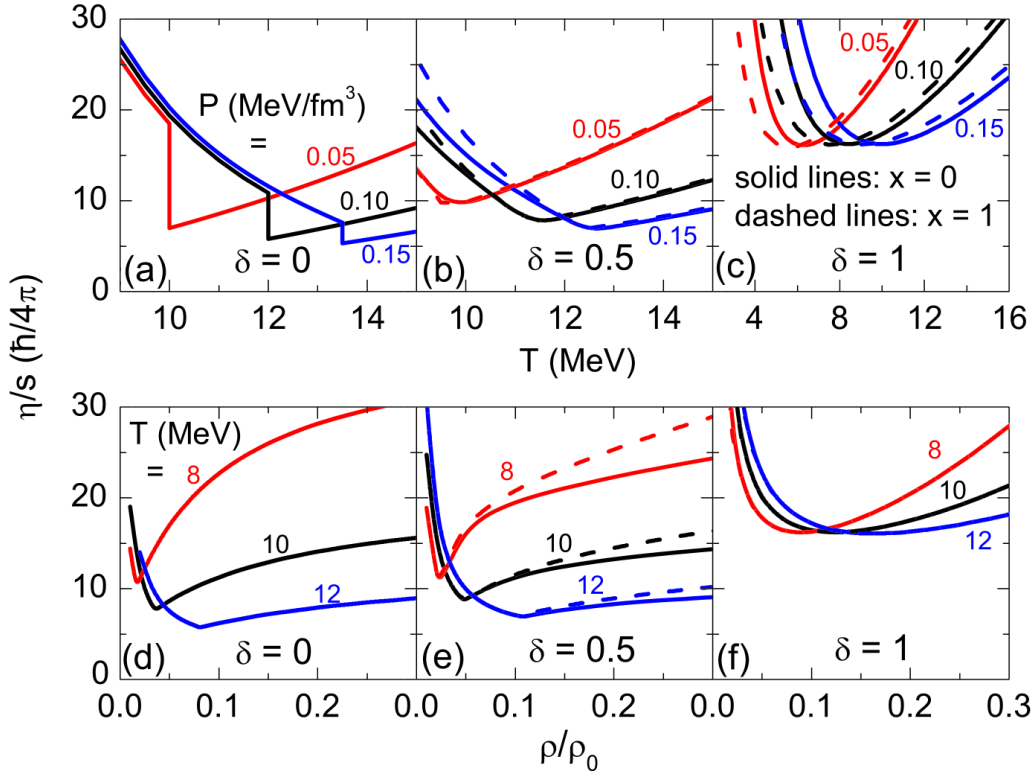


Figure 3.9: (Color online) The specific shear viscosity as functions of temperature (upper panels) and density (lower panels) at different fixed pressures and temperatures, respectively, in isospin symmetric matter ($\delta = 0$), neutron-rich matter ($\delta = 0.5$), and pure neutron matter ($\delta = 1$) for both symmetry energies $x = 0$ and $x = 1$ [83].

From the above discussions, one can get that Pauli blocking, intermediate cross-section, the asymmetry of nucleonic matters have an effect on the shear viscosity. Both of the Pauli blocking and inter-mediate cross-section affect nucleon-nucleon collisions and then the shear viscosity. A system with different asymmetries of nucleonic matters would have different nucleon-nucleon potentials and different nucleon-nucleon cross-sections which would make shear viscosity different. However, one can notice that these calculations are with uniform nucleonic matter. There are no fragment effects considered in those calculations. The nuclear matter in the gas phase is different from the gas of classical fluids (as the water vapour), which is composed of not only single nucleons, neutrons, and protons, but also complex particles like alpha-particles and light fragments depending on the temperature conditions [145, 146]. In this case, one extracts the shear viscosity coefficient by using the shear strain rate method and setting up a periodic cubic box within the improved quantum molecular dynamic (ImQMD) model [84]. In the framework of ImQMD, potential energy density [147, 148] without the spin-orbit term can be written

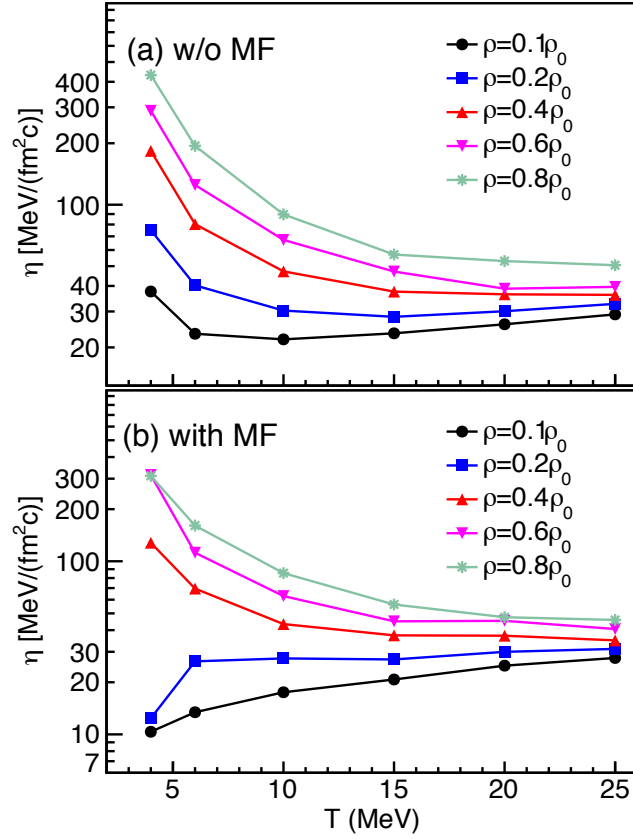


Figure 3.10: (Color online) Shear viscosity as a function of temperature at different densities in the calculations without (a) and with (b) mean field. [84].

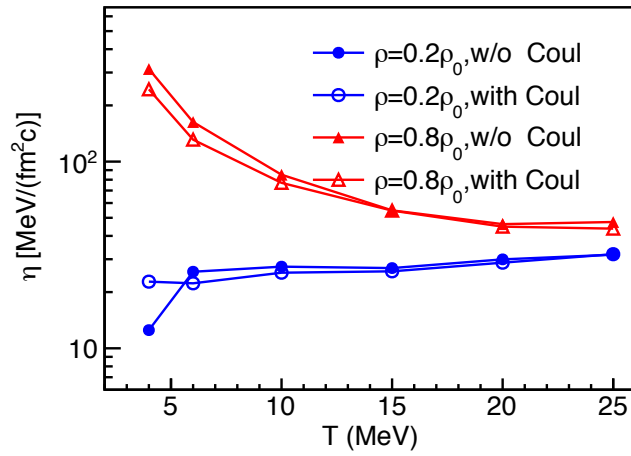


Figure 3.11: (Color online) Shear viscosity as a function of temperature in the calculations without and with the Coulomb interaction [84].

as,

$$\begin{aligned}
V_{loc} = & \frac{\alpha}{2} \frac{\rho^2}{\rho_0} + \frac{\beta}{\gamma + 1} \frac{\rho^{\gamma+1}}{\rho_0^\gamma} + \frac{g_{sur}}{2\rho_0} (\nabla\rho)^2 \\
& + g_\tau \frac{\rho^{\eta+1}}{\rho_0^\eta} + \frac{g_{sur,iso}}{\rho_0} [\nabla(\rho_n - \rho_p)]^2 + \frac{C_s}{2\rho_0} \rho^2 \delta^2,
\end{aligned} \tag{3.17}$$

where $\rho = \rho_n + \rho_p$ is the net nucleon density, ρ_n and ρ_p are the proton and neutron densities, respectively, and $\delta = (\rho_n - \rho_p)/\rho$ is the normalized asymmetry of neutron and proton. The Skyrme density functional with interactions such as Eq. (3.17), as well as other approaches for nuclear systems, yield the liquid-gas phase transition at the subnormal densities for the near-symmetric nuclear matter. By switching on and off the mean field and thus inducing the phase transition, it can be able to observe the impact of clumping on viscosity in the phase transition region. The calculations are only for the isospin-symmetric nucleonic matters with the nucleon-nucleon cross section fixed at 40 mb.

In the case without mean field and in cascade mode, there is no phase transition and fragment only when mean field is taken into account. However, when the mean field is turned on, the nucleon potential and kinetic energy will change due to the fragment formation which is one of the challenges for simulations. To avoid the system being heated up, it needs to adjust this transient state temperature to the initial temperature by introducing the cooling factor ‘h’, which can be nominally positive and less than ‘1’.

Without mean field and in cascade mode, the viscosity is that of a gas of nucleons, as shown in Fig.3.10 (a) and it is similar to that in Fig.3.1 (b) and (d). From the results with mean field in Ref. [84] as shown in Fig.3.10 (b), it is seen that the shear viscosities are similar to those without mean field at high temperatures and densities. However, at densities below $0.4\rho_0$ and temperatures less than 10 MeV, it is found that the shear viscosity has a strong reduction when the mean field is switched on. The reasons could be understood in the following way: in the region of the phase transition, separated fragments, which move slowly, absorb most of the mass for the box system and stall the transport of momentum. Since those fragments are moving slowly, they play only a passive role in transporting the momentum. In the phase coexistence state, except for liquid-like fragments, there are gas phase nucleons in the system, which could become the primarily transported part. These gas phase nucleons rather collide with the fragments than with each other, which shortens their mean free path. In addition, with most mass in the fragments, the role of the Pauli principle in the gas is reduced which decreases the path further. Thus, in these cases, shear viscosity would be reduced. As density increases, the fragments would connect to each other, and the low-density gas phase is contained in voids in the liquid. Then momentum transport can progress, and the Pauli principle can be restored.

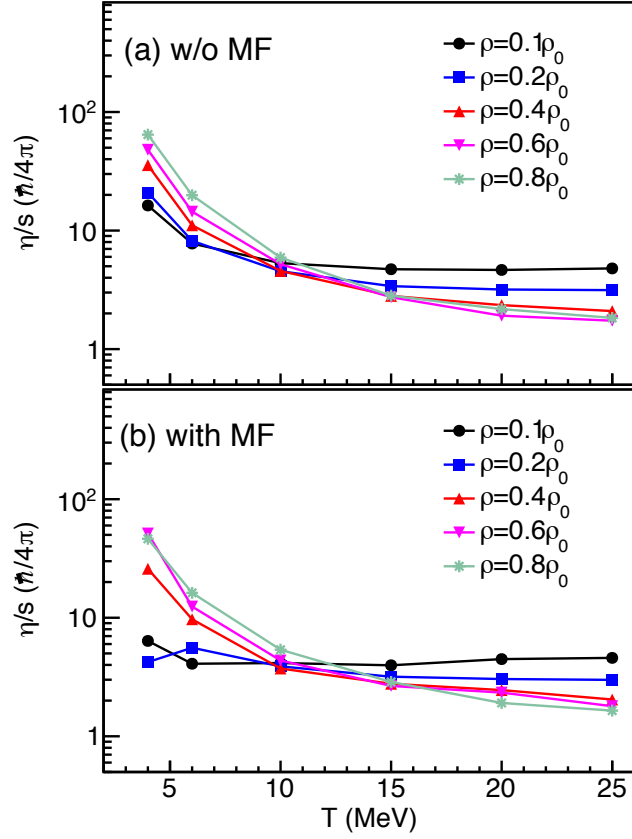


Figure 3.12: (Color online) The specify shear viscosity over entropy density η/s as a function of temperature at different densities in the calculations without (a) and with (b) mean field [84].

Moreover, when the fragments form, the long-range Coulomb interaction may play a role for shear viscosity [84]. It is worth to mentioning that in most of the calculations for the infinite and symmetric nuclear-matter systems, the Coulomb interactions are switched off, and the near-symmetric matter has comparable numbers of neutrons and protons. In Ref. [84], the effect of Coulomb interaction on the shear viscosity in coexistence nucleonic matter has been investigated. From the results with and without Coulomb interaction, as shown in Fig. 3.11, it is found that shear viscosity is reduced by the Coulomb interaction in the region of low temperature. For an understanding of this phenomena, one can imagine that two fluid layers pass from one to another. However, the repulsive Coulomb interaction among protons will reduce momentum transformation or momentum flux between two layers, which will decrease shear viscosity. In low-temperature region, the Coulomb interaction could be important in comparison with thermal motion. With the increasing of temperature, the Coulomb interaction effect becomes smaller since nuclear matter at higher temperature is more uniform and the effect of Coulomb interaction becomes negligible. Based on the above arguments, we can explain the temperature dependence of Coulomb correction on shear viscosity.

Table 3.1: η/s of different atomic and molecular systems: Helium, Nitrogen and H₂O in certain ranges of temperature and pressure [48, 84].

Systems [Ref.]	T (K)	Pressure (MPa)	η/s ($\hbar/4\pi$)
Helium [48]	2–20	0.1–1	8.8–126
Nitrogen [48]	50–600	0.1–10	11.9–7000
H ₂ O [48]	300–1200	10–100	25.5–377

For the simulation system investigated in Ref. [84], it is easy to extract the entropy density by Eq.(3.9). Then one can obtain the specific shear viscosity η/s which is an interesting topic for a bound value of $\hbar/4\pi$, known as the Kovtun-Son-Starinets (KSS) bound [24] as mentioned above. To briefly summarize the values of ratios of shear viscosity over entropy density for different systems, including atomic and molecular systems, QGP matter, finite nucleonic matter (FNM), as well as infinite nuclear matter (INM), are summarized in Tables 3.1 and 3.2 (The specific shear viscosities for QGP matter and finite nucleonic matter are discussed in later sections). It is worth to mentioning that the FNM is matter in a system with finite size like a single nucleus or a heavy-ion collision system. The hot quark gluon plasma (QGP) has a very low η/s which is very close to $\hbar/4\pi$ and behaves as a nearly perfect fluid [44]. When the QGP cools down and coalesces into a relativistic hadron gas state, specific shear viscosity η/s increases and becomes significantly higher than the KSS bound [77, 155]. When

Table 3.2: η/s of different quark matter (QGP) and finite nucleonic matter (FNM) as well as infinite nucleonic matter (INM) in certain ranges of temperature and density. Here $T_c \approx 170$ GeV is transition temperature from the hadronic phase to QGP phase [84, 149].

Systems [Refs.]	T (MeV)	ρ/ρ_0	$\eta/s (\hbar/4\pi)$
QGP1 [149–152]	$\leq T_c$	—	3.77–25.1
QGP2 [149–153]	$> T_c$	—	1.00–6.91
FNM1 [80, 92]	0.8–2.1	~ 1.0	2.5–6.5
FNM2 [154]	3.5–16	0.9–1.25	3.0–70.0
FNM3 [91]	6–16	0.2–0.3	9.5–20.0
INM1 [83]	8–14	0.01–0.3	4–30
INM2 [84]	4–25	0.1–0.8	2–55

the temperature goes down, we would get some hot finite nucleonic matter; the η/s is around 3.0 - 70 times of $\hbar/4\pi$ for the density of 0.2 - 1.25 ρ_0 [91, 154], in which the minimum η/s value corresponds to the liquid-gas phase transition as discussed in the previous model calculations. And here the value of η/s is larger than 2 times of $\hbar/4\pi$ for the infinite nuclear matter, which is consistent with the results in Ref. [78, 79, 83, 91]. For the finitely colder nuclear matter around the saturation density at much lower temperature (0.8–2.1 MeV), it is 2.5–6.5 times of $\hbar/4\pi$ [80, 92]. From the two tables, one can see that the QGP matter at around 170 MeV has the lowest η/s which is close to the KSS bound ($\hbar/4\pi$). However, the nuclear matter at around a few to a few tens MeV, which is in a liquid gas phase transition range, has also relative low η/s , i.e., about several times the KSS bound. The above low η/s may reflect the universal property of strong interaction matter regardless of partonic and nucleonic level. On the contrary, for atomic and molecular substances of He, Ni, and water, they have relatively large η/s which are dominated by electromagnetic interaction [84].

3.2. Finite nuclear matter

A nucleus is a many-body quantum system in which the constituents with finite nucleons are governed by strong interaction. A useful way to investigate the shear viscosity of finite nuclear matter is through heavy-ion collisions. In the past decades, different model-dependent calculations for shear viscosity, especially for the specific shear viscosity η/s , have been studied in intermediate-energy heavy-ion collisions.

Within the framework of the Boltzmann-Uehling-Uhlenbeck model, Li *et al.* [78] calculated the shear viscosity in Au + Au collisions below 100 MeV/A by using the Green-Kubo formula as Eq. (2.9). In their calculations, an isolated volume is chosen from a spherical space with a radius of 5 fm. For simplicity, the correlation functions can be rewritten in exponential form [76],

$$\langle T_{\alpha\beta}(t_0)T_{\alpha\beta}(t_0 + t') \rangle \propto \exp(-\frac{t'}{\tau_\pi}); \quad \alpha, \beta = x, y, z, \alpha \neq \beta. \quad (3.18)$$

The calculations of the stress tensor here only include the momentum part, and the mean field part is neglected. And the shear viscosity coefficient can be rewritten in a simple form:

$$\eta = \frac{V}{T} \langle T_{\alpha\beta}(t_0)T_{\alpha\beta}(t_0) \rangle \tau_\pi; \quad \alpha, \beta = x, y, z, \alpha \neq \beta. \quad (3.19)$$

where τ_π is the relaxation time of the shear flux. With the phase space information, one could get the time evolution of the correlation function. By fitting with $\exp(-\frac{t'}{\tau_\pi})$, τ_π and the shear viscosity can be obtained. And the entropy density can be calculated by the Gibbs formula,

$$s = \frac{\epsilon + P - \mu_n \rho}{T}, \quad (3.20)$$

where ϵ is energy density inside the volume with 5 fm radius. And μ_n is the nucleon chemical potential, ρ is nucleon density of system within the given sphere. As shown in Fig.3.13, the results for η/s show a rapid fall with the increasing of incident energy up to $E < 70$ MeV/A and then drop slowly to a value close to 0.5 when $E > 70$ MeV/A. Here it is worth to mentioning that η/s is a dimensionless quantity since it has been divided by \hbar in some figures blow. The results show a strong dependence of η/s on the equation of state (EoS) and a harder EoS would give a larger η/s . In the inset of Fig.3.13, there seems to be a turning point around $E \sim 65$ MeV/A. This turning point may indicate a change in the dynamical behavior of the system that is not caused by a phase transition. Since the BUU model is based on one body theory, there is no fluctuation, correlation, or the phase transition behavior. Compared to the KSS bound, here η/s is larger than 6 times of $1/4\pi$ (here \hbar is set to '1') in the energy region of $E < 100$ MeV/A.

With the same method of Green-Kubo formulas, Guo *et al.* investigated the specific shear viscosity in low-energy $^{40}\text{Ca} + ^{100}\text{Mo}$ heavy-ion collision by using an extended quantum molecular dynamics model [92]. As shown in Fig. 3.14, the ratio of shear viscosity to entropy density of the nuclear fireball shows a slight drop as temperature or beam energy increases. The results are consistent with those in

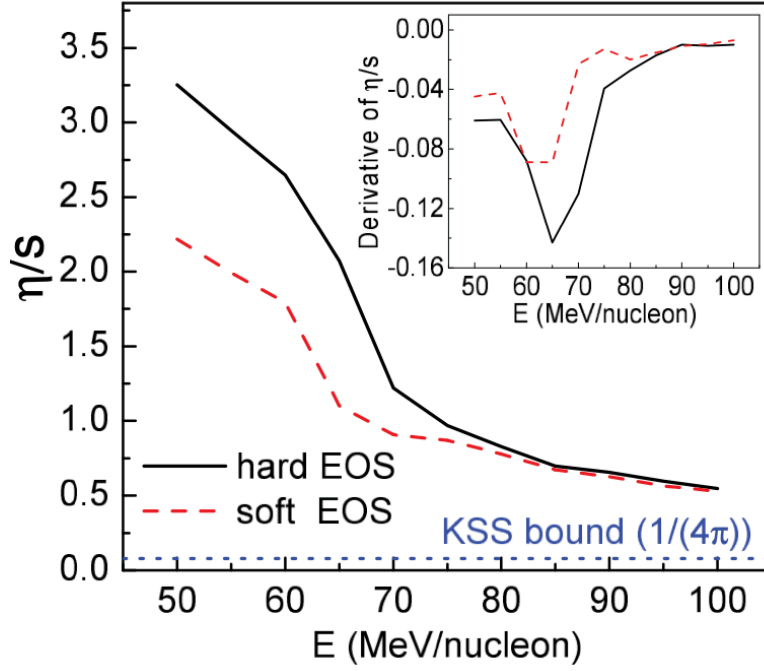


Figure 3.13: (Color online) η/s (here η/s is divided by \hbar and thus without unit) as a function of beam energy for the central Au + Au collision in a spherical volume with radius of 5 fm. The inset shows the derivative of η/s versus beam energy [78].

Ref. [134, 156]. Here the specific shear viscosity shows 2 times $1/4\pi$ ($\hbar=1$) which is very close to the KSS limit.

Later, Zhou et al. [91], investigated the thermodynamic and transport properties of nuclear fireballs created in the central region of heavy-ion collisions below 400 MeV/A within the isospin-dependent quantum molecular dynamic (IQMD) model. By fitting the results from Eq.(2.51), one can get shear viscosity in a numerical form [74],

$$\eta = \frac{1700}{T^2} \left(\frac{\rho}{\rho_0}\right)^2 + \frac{2}{1 + 0.001T^2} \left(\frac{\rho}{\rho_0}\right)^{0.7} + \frac{5.8\sqrt{T}}{1 + 160T^{-2}} \quad (3.21)$$

where η is in unit of MeV/(fm²c), and T is in unit of MeV. Combined temperature and density in the collision process, one can obtain shear viscosity. In the simulations, temperature and entropy density are calculated by the generalized hot Thomas Fermi formalism (GHTFF) [157]. In order to study the effect of cross section on shear viscosity, the nucleon-nucleon (NN) cross section is multiplied by a coefficient C_σ , $\sigma_{NN} = C_\sigma \sigma_{NN}^{free}$ [91]. In this case, the expression for shear viscosity changes to,

$$\eta(T, \rho, C_\sigma) = \frac{\eta(T, \rho)}{C_\sigma}, \quad (3.22)$$

The coefficient C_σ is set to 0.5, 1.0, or 1.5 in the simulations. As shown in Fig.3.15, shear viscosity

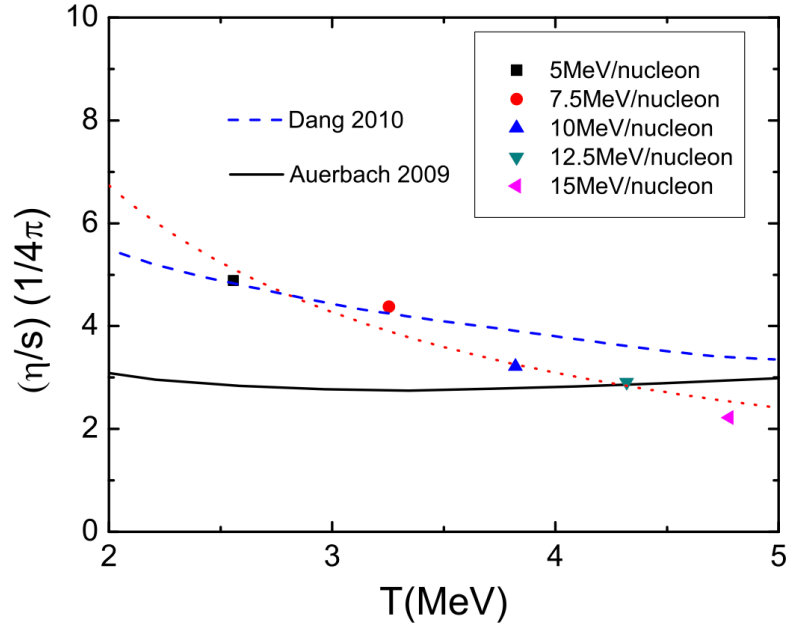


Figure 3.14: (Color online) η/s as a function of temperature in a central region for head on $^{40}\text{Ca} + ^{100}\text{Mo}$ collisions [92]. The solid line (Auerbach and Shlomo) is taken from Ref. [156], and the dashed line (Dinh Dang) is an extrapolation of the phonon-damping model prediction for ^{208}Pb in Ref. [134].

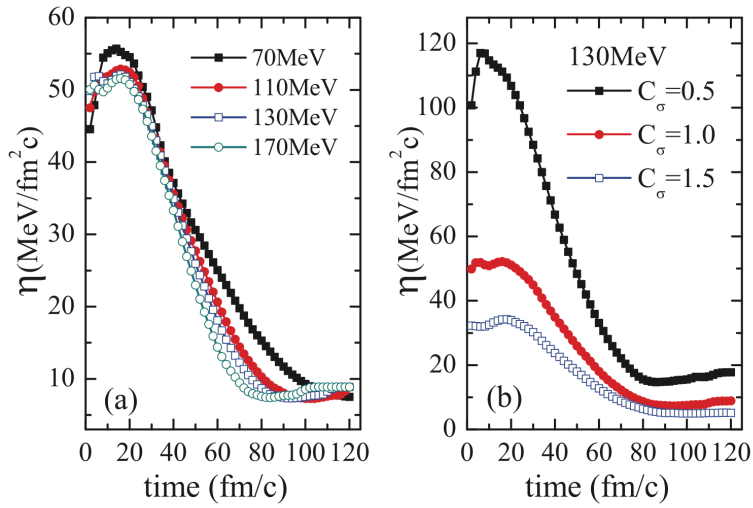


Figure 3.15: (Color online) Time evolution of shear viscosity at different beam energies and cross section factors [91].

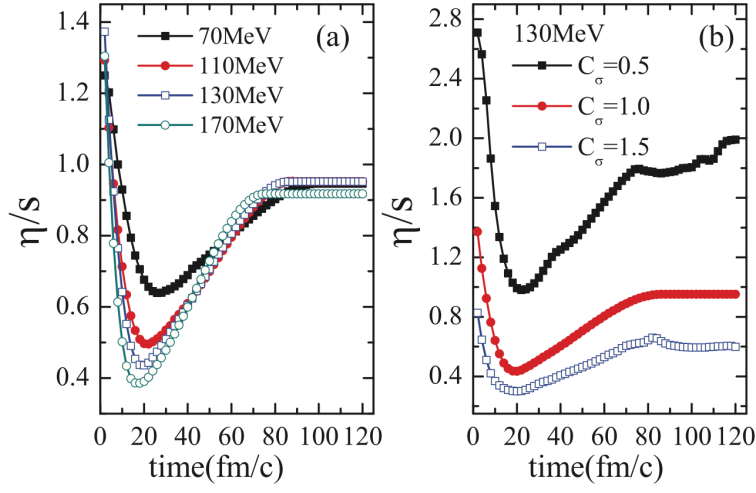


Figure 3.16: (Color online) Time evolution of specific shear viscosity at different beam energies and cross section factors [91].

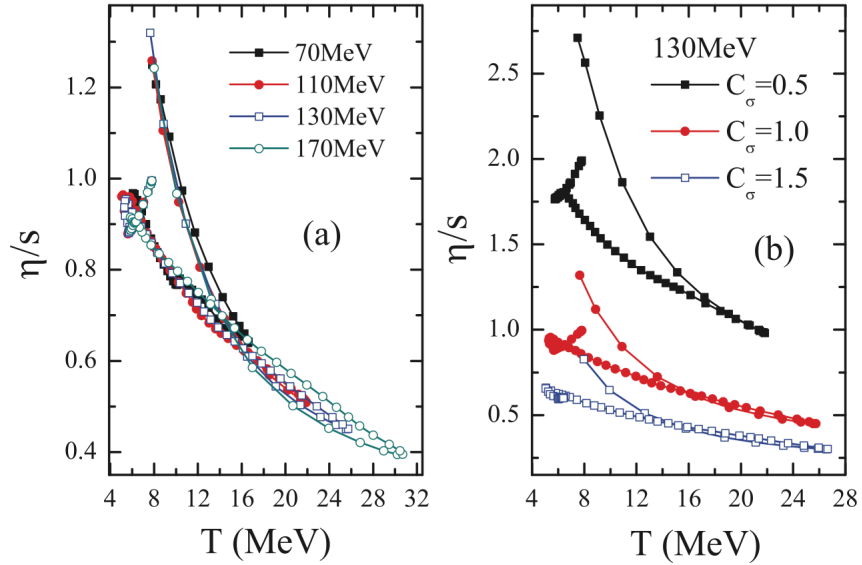


Figure 3.17: (Color online) Specific shear viscosity as a function of temperature at different beam energies and cross section factors [91].

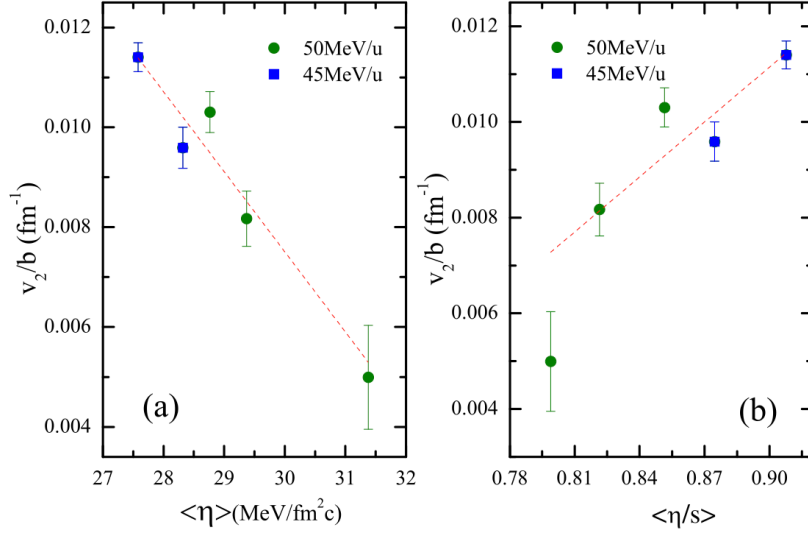


Figure 3.18: (Color online) The scaled elliptic flow as a function of the average shear viscosity and specific viscosity at 45 MeV/u and 50 MeV/u (Here MeV/u is the same with MeV/A) and corresponding impact parameters [158]. The red-dash lines are linear fits.

reaches the maximum value at the compression stage during the collision process. But specific shear viscosity shows the minimum value as in Fig.3.17. As shown in Fig.3.17, specific shear viscosity shows a transient minimal $\eta/s = (5-10)1/4\pi$ in the largest compression stage. It can be noticed that the shear viscosity of nuclear matter in heavy-ion collisions is time-dependent.

In a fluid, shear viscosity plays a resistance role to the flow. As we know, in non-central heavy-ion collisions, particles have collective behavior. Indeed, in a heavy-ion collision, there are two distinct ways for shear viscosity to influence the final emitted particles [159]. One is that it increases the magnitude and decreases the anisotropies of the hydrodynamically generated transverse flow which reflects the amount of shear viscosity over the entire expansion history of the fireball. Another is that it causes a deviation, δf , of the final phase-space distribution $f(x, p)$ from its isotropic local equilibrium form, $f(x, p) = f_0(x, p) + \delta f(x, p)$. In heavy-ion collisions, anisotropic flow can be defined as the orders of harmonic coefficients of Fourier expansion of the particle azimuthal distribution, such as the second-order elliptic flow v_2 ,

$$v_2 = \langle \cos(2\phi) \rangle = \left\langle \frac{p_x^2 + p_y^2}{p_x^2 - p_y^2} \right\rangle, \quad (3.23)$$

where ϕ is the azimuthal angle, p_x and p_y are the momenta of the particle at the x and y axes, respectively. For the further work from Zhou *et al.* [158], they consider the correlation between the elliptic flow v_2 scaled by the impact parameter b and the shear viscosity η as well as the specific viscosity η/s . Here v_2 is reduced by impact parameter b for reducing influence from b. As shown in Fig. 3.17,

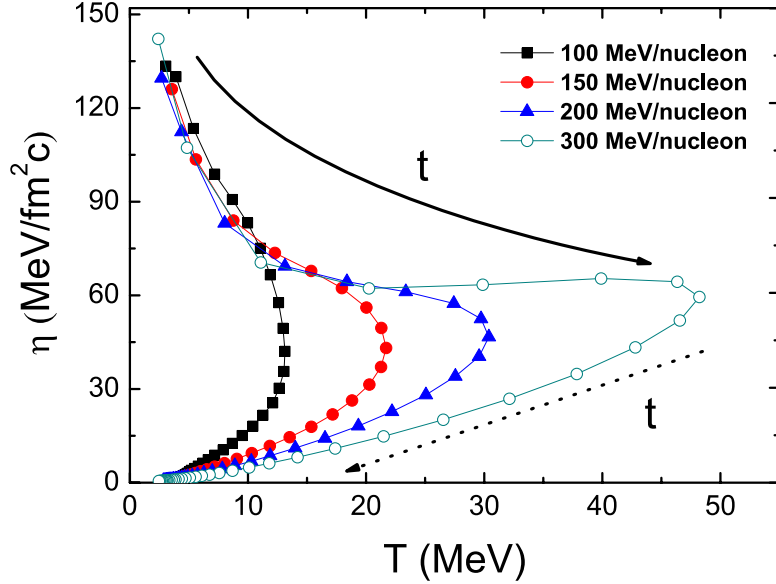


Figure 3.19: (Color online) Time evolution of specific shear viscosity at different beam energies for the soft EoS in the central region of X[5,5], Y[5,5], and Z[5,5] [79]. Solid and dotted arrows indicate the compression process and expansion process, respectively.

it is seen that v_2/b decreases linearly with increasing of average shear viscosity $\langle \eta \rangle$. It is also found that v_2/b mostly increases with increasing of average specific viscosity $\langle \eta/s \rangle$. So it presents a strong correlation between the elliptic flow and the shear viscosity or specific viscosity η/s . Somehow, larger shear viscosities quickly reduce collective flow. In relativistic heavy-ion collisions, the large elliptic flow observed at RHIC energies provides compelling evidence for strongly interacting matter that behaves as an almost perfect liquid [25–27, 159–161]. Here for the v_2/b versus $\langle \eta \rangle$ consistent with the findings in relativistic heavy-ion collisions, and it is opposite for the v_2/b versus specific viscosity η/s . For the later one, the authors argued that it is due to the stronger dissipation in the hadronic phase than in the partonic phase [158].

A similar work is done in Ref. [79] but with an extension model of Boltzmann-Uehling-Uhlenbeck, namely the Van der Waals Boltzmann-Uehling-Uhlenbeck (VdWBUU) model. In this model, its cross section within the nucleonic medium is derived from the mean field, which is given,

$$\sigma = \left(\frac{9\pi}{16}\right)^{1/3} b'^{2/3}, \quad (3.24)$$

where b' denotes the proper volume of the constituent particle, which can be related geometrically to

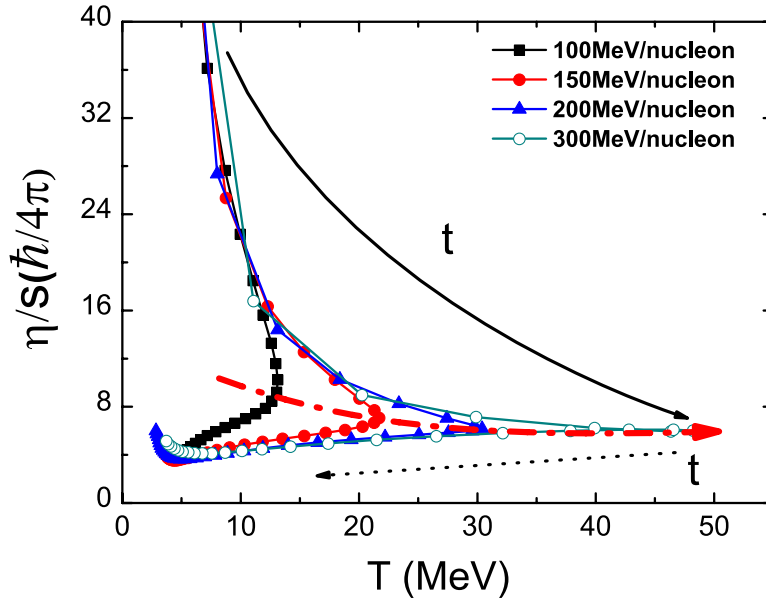


Figure 3.20: (Color online) The same as in Fig. 3.19 but for the correlation between specific shear viscosity (in units of $\hbar/4\pi$) and temperature [79].

its cross section for interaction with other particles and reads as,

$$a' = -a, \quad (3.25)$$

$$b' = \frac{b\kappa\rho^\kappa + 2\gamma a_s \left(\frac{\rho}{\rho_0}\right)^{1+\gamma} \tau_z I}{\left(\frac{f_{5/2}(z)}{f_{3/2}(z)}\right)\rho T + b\kappa\rho^{1+\kappa} + 2\gamma a_s \rho_0 \left(\frac{\rho}{\rho_0}\right)^{1+\gamma} \tau_z I}. \quad (3.26)$$

where a' is related to attractive interaction among particles; $z = \mu/T$ is the fugacity value of nucleons and $f_{5/2(3/2)}$ are Fermi integrals; a_s is coefficient of the symmetry energy term; γ describes the density dependence; and $a, b,$ and κ are parameters for the nuclear equation of state (EoS). The more detail can be seen in Ref. [79]. In simulations, shear viscosity is calculated in a central region which is defined as a $[-5, 5]^3 \text{ fm}^3$ or $[-3, 3]^3 \text{ fm}^3$ box with its center located in the c.m. with a numerical expression with isospin asymmetry taken into account as Eq. (3.6). And temperature for shear viscosity calculation is extracted by a quantum Fermion fluctuation approach, which is proposed in Ref. [162]. The entropy density can be determined by the density and temperature [163]:

$$s = \frac{U - A}{T} \frac{1}{V} = \left[\frac{5}{2} \frac{f_{5/2}(z)}{f_{3/2}(z)} - \ln z \right] \rho. \quad (3.27)$$

where $f_m(z) = \frac{1}{\Gamma(m)} \int_0^\infty \frac{x^{m-1}}{z^{-1}e^x + 1} dx$, and $z = e^{\frac{\mu}{T}}$ is fugacity. U is the internal energy and A is Helmholtz free energy [164].

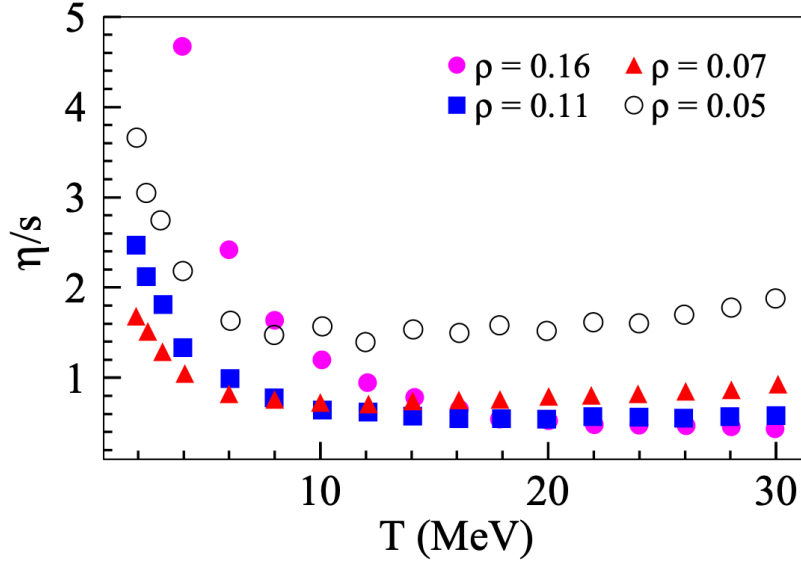


Figure 3.21: (Color online) Specific shear viscosity as a function of temperature at different densities [154].

From the results of Ref. [79] as shown in Fig. 3.19, it can be seen that in the compression process, shear viscosity decreases with increasing temperature. While in the expansion process, the behavior is inverted. It is also noticed that in the classical liquid, as the temperature goes higher, the particles become separated over larger distances, they lose local orientation order, and their interactions become weaker, hence the decrease in shear viscosity. A more microcosmic interpretation is the competition between Pauli blocking and collision as for higher density cases as in Fig. 2.5. On the contrary, the shear viscosity of gas increases with increasing of temperature due to the momentum of nucleons increasing. Thus, it is assumed that nuclear matter is in the liquid-like phase state during the compression process and in a gas-like phase during the later process. Around the inflection point, it should be in mixed-like phase [79]. But we cannot say there is a phase transition since the one-body theory for BUU model used in that work [79]. In Fig. 3.20, specific shear viscosity at a maximum compress stage tends to remain constant as beam energy increases, as the red-dot arrow shows. It is different from the shear viscosity versus T , as in Fig. 3.19.

In addition, Fang et al. [154] extracted shear viscosities of finite-size nuclear sources by using the mean free path method within the framework of the isospin-dependent quantum molecular dynamics model, and the entropy density is from the Gibbs formula as Eq. (3.20). The classical kinetic theory relates η of the system with the mean free path of the particle, as in Eq. (2.8). From the results as shown in Fig. 3.21, η/s is larger than 7 times KSS bound. And the authors found that a minimum of η/s is seen at around $T = 10$ MeV for $\rho \sim 1/2\rho_0$. For higher densities, $\rho = 0.16, 0.11 \text{ fm}^{-3}$, no minimum of η/s is seen, but instead η/s approaches an asymptotical value at higher temperatures.

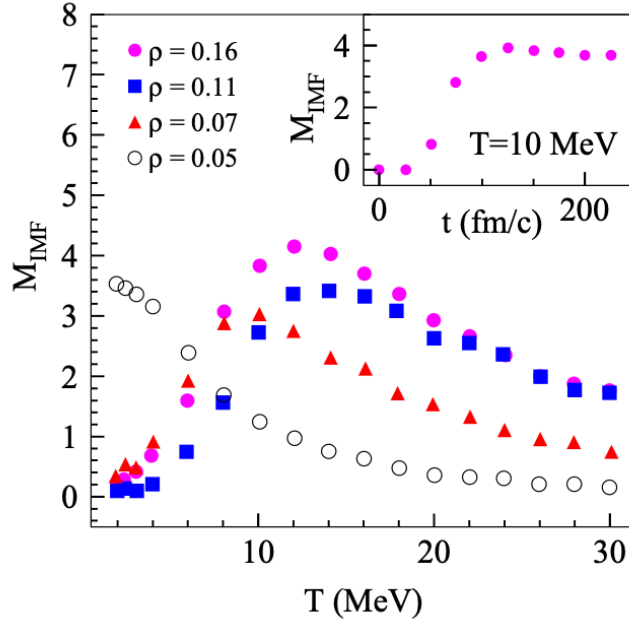


Figure 3.22: (Color online) Temperature dependence of the multiplicity of intermediate mass fragment (IMF) after the freeze-out of the system for nuclear sources at different densities. Inset is the time evolution of multiplicity of IMF at $T=10$ MeV for $\rho = 0.16\text{fm}^{-3}$ [154].

There may be a relation between the minimum of η/s as a function of T and liquid-gas phase transition of nuclear matter. And the authors have checked the multiplicity of the intermediate mass fragment (IMF), which is a widely studied observable for liquid-gas phase transition in heavy-ion collisions. As shown in Fig. 3.22, when the density is around $1/2 \rho_0$ and at the same temperature, the multiplicity of the IMF of the system after freezing-out shows a maximum value which could be the signal of a liquid-gas phase transition [165]. However, for the low density of 0.05 fm^{-3} , there is no maximum value for multiplicity of IMF as shown in Fig. 3.22 but shows a minimum of η/s in Fig. 3.21. It may indicate that the minimum of η/s here is more than the liquid-gas phase transition.

Further, Liu et al. [166] investigated the thermal and transport properties of central $^{129}\text{Xe} + ^{119}\text{Sn}$ collisions around the Fermi energy using the mean free path method and numerical expression [74] in the framework of an isospin-dependent quantum molecular dynamical model. As shown in Fig. 3.23 which has been corrected for the value of specific shear viscosity, it is seen that η/s is larger than 8 times the KSS bound. And it decreases as the beam energy increases, which is consistent with that in Refs.[78, 91].

In this section, shear viscosity is extracted in QMD or BUU type model with numerical equations (3.19), (3.21), and (2.8). It can be seen that these results are consistent. However, these formulas can not be utilized from the experimental side and are hard to check with data.

To summarize this part of the discussion, the shear viscosity in infinite and finite nucleonic matter,

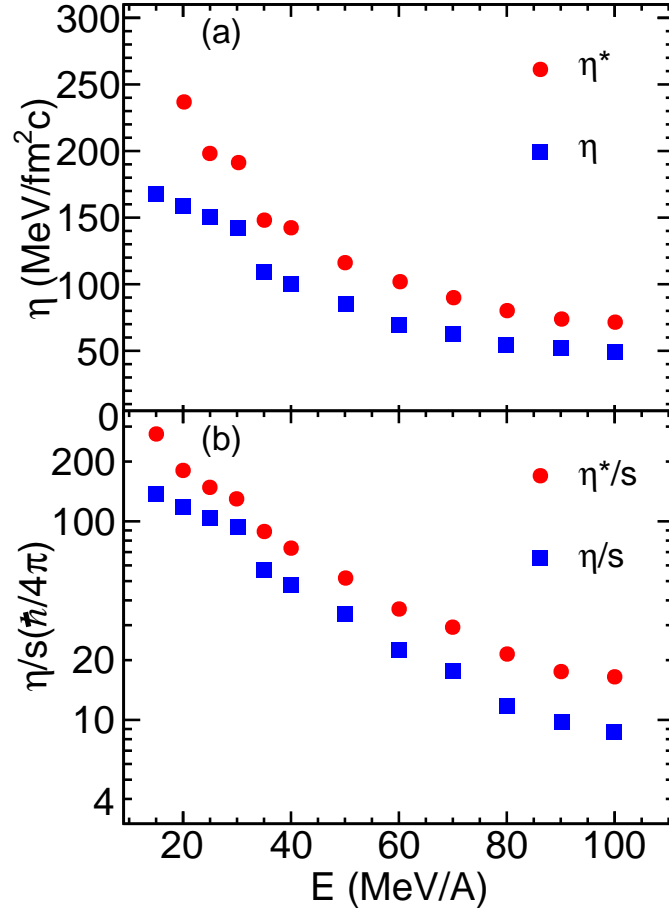


Figure 3.23: (Color online) Shear viscosity and specific shear viscosity as functions of temperature with two different methods [166]. But the result for specific shear viscosity in (b) has been modified.

Pauli blocking and nucleon-nucleon cross section play important roles. The values of specific shear viscosity by different methods or models are several times of $\hbar/4\pi$ and they are not very different from those of QGP matter.

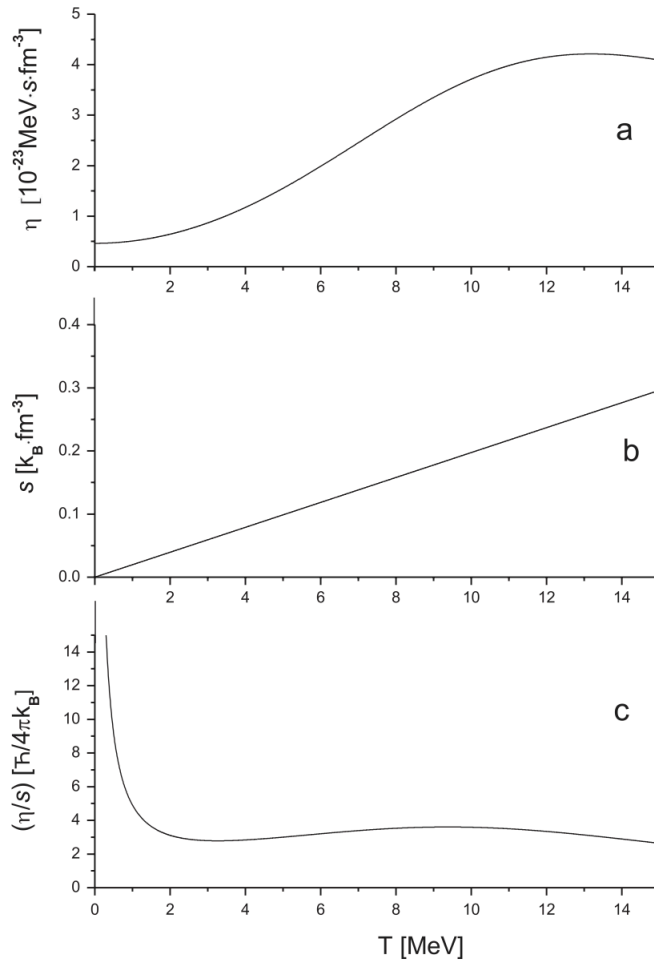


Figure 4.1: (Color online) The nuclear shear viscosity η (a), entropy density s (b) and their ratio, (η/s) (c), in units of $\hbar/4\pi k_B$, as functions of the temperature, T . The values of the parameters used in the calculations are $\epsilon_F = 40$ MeV, $\rho = 0.16$ fm $^{-3}$, $\alpha = 9.2$ MeV, and $\hbar\omega = 20$ MeV [156].

4. Experimental aspects of shear viscosity in nucleonic matter

4.1. Analysis method by experiment

In the previous section, we reviewed some calculations for shear viscosity (η) and the ratio of shear viscosity to entropy density (η/s) in nucleonic matter. As mentioned above, the analysis of the state of matter produced by the ultra-relativistic heavy-ion collisions at the Relativistic Heavy Ion Collider (RHIC) shows the matter has very small values of η/s [44]. How is it for finite nucleonic matter or infinite nuclear matter? The finite nucleonic matter like a finite nucleus, with the constituent nucleons being a many-body quantum system, is governed by strong interaction and shows highly correlated behavior [80]. It can be an ideal system to search for near-perfect fluidity in matter. The search for the universal characteristic of the strong interaction of the many-body quantum systems with shear viscosity is significant.

Auerbach and Sholomo have done earlier theoretical work [156] regarding the value of η/s for finite nuclear matter in which the nucleons are governed by strong interaction. The authors have extracted shear viscosity within a generalized Fermi liquid drop model by employing a collision kinetic equation, where the dissipative propagation of sound waves is taken into account in finite nuclei and nuclear matter [156]. In the Fermi liquid drop model, shear viscosity is expressed as,

$$\eta = \frac{2}{5}\rho\epsilon_F \frac{\tau_{coll}}{1 + (\omega\tau_{coll})^2}, \quad (4.1)$$

with

$$\tau_{coll} = \frac{\tau_0}{1 + \left(\frac{\hbar\omega}{2\pi T}\right)^2}. \quad (4.2)$$

where $\hbar\omega$ is the excitation energy of a sound wave and ω -dependent terms are related to the dynamical distortion of the particle momentum distribution due to memory effects [156]. In Eqs. (4.1) and (4.2), τ_{coll} is the Landau approximation for the collision relaxation time. And $\tau_0 = \hbar\alpha/T^2$ and the value of α is sensitive to the in-medium-nucleon-nucleon scattering cross section. α is taken to be 9.2 MeV in Ref. [167]. As displayed in Fig.4.1, shear viscosity increases as temperature increases at density of $\rho=0.16 \text{ fm}^{-3}$. Here the unit $10^{-23} \text{ MeV}\cdot\text{s}\cdot\text{fm}^{-3}$ is equal to $3 \text{ MeV}/(\text{fm}^2\text{c})$, and c is speed of light. From Fig.4.1(c), the authors found that the specific shear viscosity is not drastically different from the RHIC result. So it could be a general characteristic feature in a many-body nuclear system with strong interaction, not just for the state created in the relativistic heavy-ion collisions [156].

It raises a lot of interest in both theory and experiment. In 2011, Dang [134] proposed a formalism based on the Green-Kubo relation and the fluctuation dissipation theorem (FDT). With the Green-Kubo formula [22], one can obtain the expression for the linear transport coefficient of any system at a given temperature T and density ρ in terms of the time dependence of equilibrium fluctuations in the conjugate flux [134]. The Green-Kubo formula has been mentioned above. Here we write the shear viscosity $\eta(T)$ as,

$$\eta(T) = \lim_{\omega \rightarrow 0} \frac{1}{2\omega} \int dt d^3x e^{i\omega t} \langle T_{xy}(\mathbf{x}, t) T_{xy}(\mathbf{x}, t_0) \rangle \quad (4.3)$$

where $\langle \dots \rangle$ denotes average over an equilibrium ensemble of events. From the fluctuation dissipation theorem, the right-hand side of Eq. (4.3) can be written as proportion to the absorption cross section

$\sigma(\omega, T)$,

$$\begin{aligned}
\eta(T) &= \lim_{\omega \rightarrow 0} \frac{1}{2\omega i} [G_A(\omega) - G_R(\omega)] \\
&= - \lim_{\omega \rightarrow 0} \frac{\text{Im } G_R(\omega)}{\omega} \\
&= \lim_{\omega \rightarrow 0} \frac{\sigma(\omega, T)}{C}
\end{aligned} \tag{4.4}$$

where G_A and G_R are the advanced and retarded Green functions, respectively, with

$$G_R = -i \int dt d^3x e^{i\omega t} \langle T_{xy}(\mathbf{x}, t) T_{xy}(\mathbf{x}, t_0) \rangle \tag{4.5}$$

and $G_A(\omega) = G_R^*(\omega)$. The C in Eq. (4.4) is equal to $16\pi G$ with G being the ten-dimensional gravitational constant. As in Ref. [134], one can obtain the final expression for the shear viscosity at temperature T ,

$$\eta(T) = \eta(0) \frac{\Gamma(T)}{\Gamma(0)} \frac{E_{GDR}(0)^2 + [\Gamma(0)/2]^2}{E_{GDR}(T)^2 + [\Gamma(T)/2]^2}, \tag{4.6}$$

where Γ is the full width at half maximum (FWHM) of the giant dipole resonance (GDR), and E_{GDR} is its peak energy. The $\eta(0)$ is shear viscosity at $T=0$. It is worth to mentioning that in the calculations, an uncertainty is in extracting the value $\eta(0)$ of the shear viscosity $\eta(T)$ at $T = 0$ and it can be given different dissipation mechanisms [134]. By using Eq. (4.6), one can calculate the shear viscosity η of a finite hot nucleus directly from the width and energy of the GDR of this nucleus in the experimental data which gives model-independent estimation. The entropy density (entropy per volume V) is calculated,

$$s = \frac{S}{V} = \rho \frac{S}{A}. \tag{4.7}$$

with the nuclear density $\rho = 0.16 \text{ fm}^{-3}$. In Ref. [134], two formulas in different methods were used to determine the entropy. One is from phonon-damping model (PDM) [168–170] and another is from the Fermi-gas formula,

$$S = 2a_T T \tag{4.8}$$

where a_T the temperature-dependent parametrization of the density parameter as in Refs. [171–173]. This formula (4.8) is used in the FLDM and the analysis of experimental data. Combined Eq. (4.7) and Eq. (4.8), one can obtain the entropy density $s = 2\rho \frac{a_T}{A} T$. T is the temperature corresponding to the final excitation energy E^* and is given by $T = \sqrt{E^*/a_T}$, where $E^* = E_0^* - E_{rot} - E_{GDR} - \Delta P$,

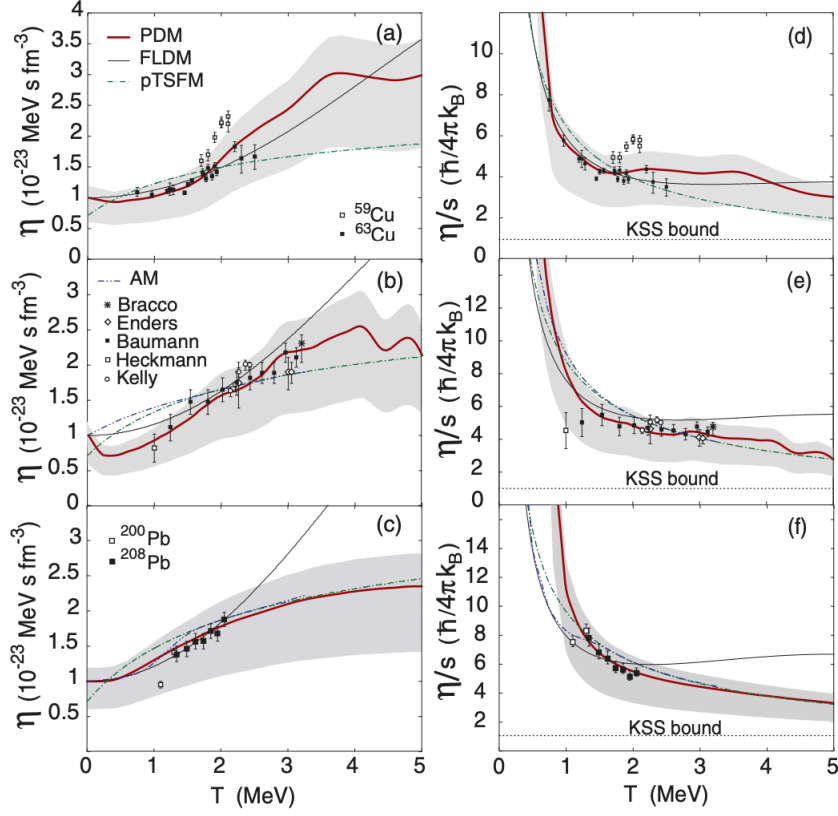


Figure 4.2: (Color online) Shear viscosity $\eta(T)$ [(a)–(c)] and ratio of η/s [(d)–(f)] as functions of T for nuclei in [(a) and (d)] copper, [(b) and (e)] tin, and [(c) and (f)] lead regions. The gray areas are the PDM predictions by using $0.6u < \eta(0) < 1.2u$ [134]. Here u is an unit 10^{-23} MeV s fm^3 . The experimental data for the calculations of η/s are from copper (^{59}Cu [171] and ^{63}Cu [172]), tin (by Bracco et al. [174], Enders et al. [175], Baumann et al. [173], Heckmann et al. [176], and Kelly et al. [177]), and lead (^{208}Pb [173] and ^{200}Pb [178]).

E_0^* , E_{rot} and ΔP being average excitation energy, the average rotational energy and the pairing energy, respectively [80]. For a given hot nucleus, one can extract the experimental temperature, the width, and the energy of the GDR. When substituted these quantities into Eq. (4.6) and the equation for entropy density $s = 2\rho \frac{a_T}{A} T$, it can be given a model-independent estimation of the ratio η/s .

4.2. Shear viscosities of finite nuclei in experiment

The predictions for the shear viscosity η and the ratio η/s by the phonon-damping model (PDM), the Fermi-liquid-drop model (FLDM), the two versions of TSFM, namely, the adiabatic model (AM), and the phenomenological parametrization of the two thermal-shape fluctuation models (pTSFM) for ^{63}Cu , ^{120}Sn , and ^{208}Pb are plotted as functions of T in comparison with the empirical results. The empirical values for η in Figs. 4.2(a)–(c) are extracted from the experimental systematics for the GDR in copper, tin, and lead regions [171–178], making use of Eq. (4.6). The theoretical results show agreement with that of experiment. And shear viscosities for nuclei increase with temperature. The specific shear

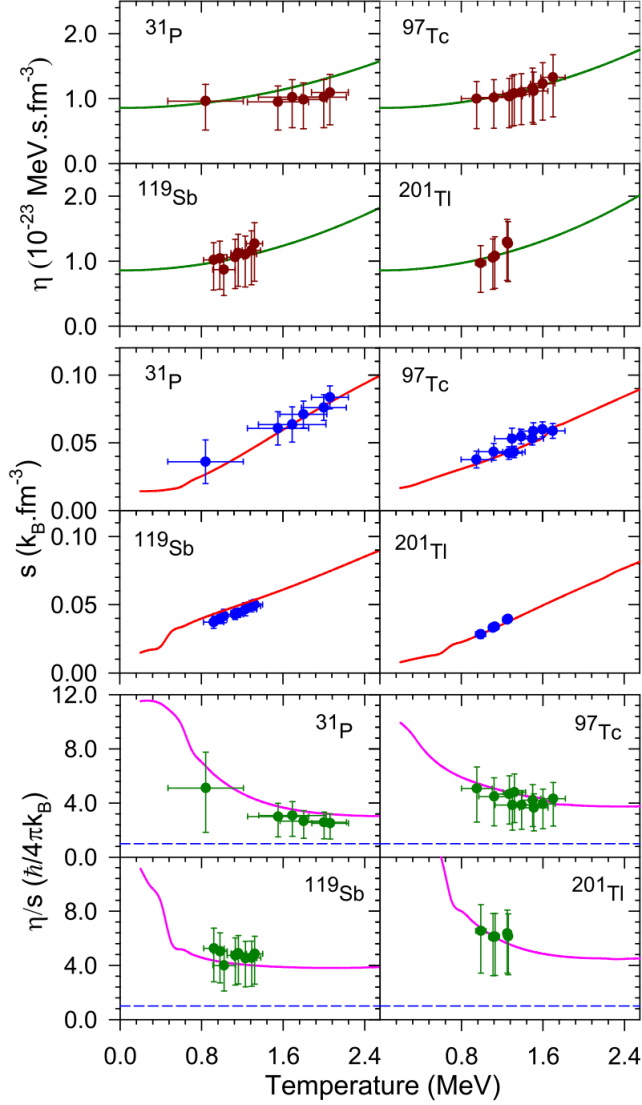


Figure 4.3: (Color online) Experimental data (symbols) along with the theoretical predictions (solid lines) for shear viscosity η (upper panel), entropy density s (middle panel), and specific shear viscosity (η/s) (lower panel). Blue short-dashed line (lower panel) is the KSS bound. The errors in η and η/s include the statistical errors as well as the systematic error due to the lower and upper bounds of $\eta(0)$ [80].

viscosity shows a mild decrease with temperature and is larger than 3 times the KSS bound.

Heavier nuclear systems from $A \sim 30$ to $A \sim 208$ are investigated in Ref. [80] for the shear viscosity and ratio of shear viscosity over entropy density by using the formalism as Eq. (4.6). Shear viscosity, entropy density, and the ratio of shear viscosity to entropy density are well reproduced for the systems. Here, shear viscosity also shows an increase as temperature increases. It is interpreted by the kinetic theoretical calculations $\eta = \frac{1}{3} \rho m v \lambda$ as Eq. 2.8. For an equilibrated nucleus, the mean free path $\lambda \sim v/N_{coll}$, where N_{coll} is the collision number, and is not sensitive to temperature. Thus, shear viscosity increases with temperature for both the mean free path λ and v increasing with temperature with $v \sim \sqrt{T}$. One can notice that the finite nucleus system is not a dilute gas system but a fermion

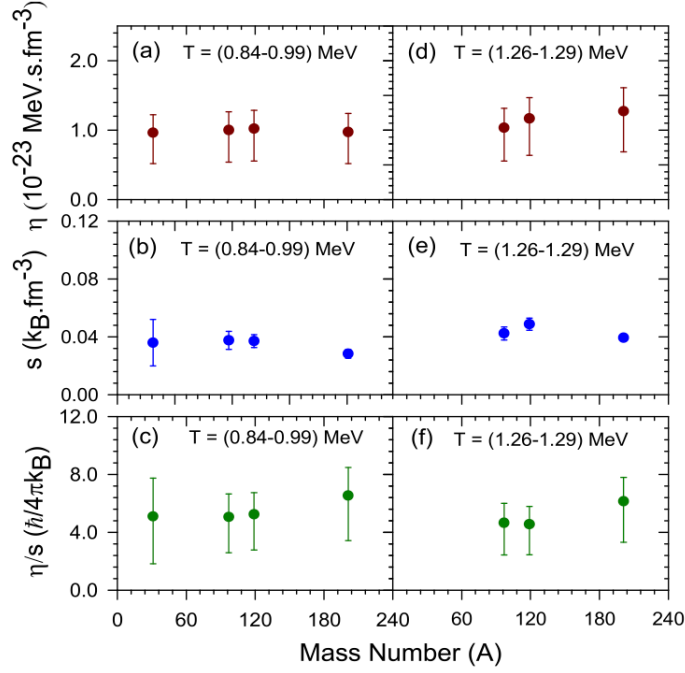


Figure 4.4: (Color online) Shear viscosity (a), entropy density (b) and specific shear viscosity (c) as functions of mass number (A) in the different temperature regions [80].

system with nucleon density reaching 0.16 fm^{-3} and Pauli blocking effect. However, the results for shear viscosity of finite nucleus shown in Fig. 4.3 and Fig. 4.4 are different from those in Fig. 2.5, Fig. 3.8 and Fig. 3.10. From the calculations with Green-Kubo, Chapman-Enskog and relaxation time approximation methods, shear viscosity at temperature $T = 0$ is a large value. Here, η at $T = 0$ has a small finite value. Moreover, it is confined in the range $(2.5-6.5) \hbar/(4\pi k_B)$ for the finite nuclear matter within the temperature range of $\sim(0.8-2.1) \text{ MeV}$ [80]. For the dependence of mass number, it is seen that η increases with the mass number at the highest available temperature for heavier nuclei, as in Fig. 4.4 (d). However, η/s is still within $(5.1-6.5) \hbar/(4\pi k_B)$ and shows independence with the nuclear size and the neutron-proton asymmetry at a given temperature [80].

In other aspects, the effect of high angular momentum on shear viscosity is discussed by Bhattacharya et al. [179]. With the help of the critical temperature included fluctuation model (CTFM) and FLDM, the predictions for shear viscosity at different angular momenta can be given, and comparison is done with the experimental data by using experimental giant dipole resonance (GDR) width (Γ) at high angular momenta ($J = 12-54 \hbar$) and temperatures ($T = 1.2-2.1 \text{ MeV}$) collected from the existing literature. As displayed in Fig. 4.5, it can be seen that the shear viscosity (η) increases with T and J . The results from the critical temperature included fluctuation model (CTFM) well describe J -induced η . However, the shear viscosity from FLDM, which is an extension of the liquid drop model (LDM) to quantum Fermi liquid, displays a large deviation in the higher angular momentum region and is

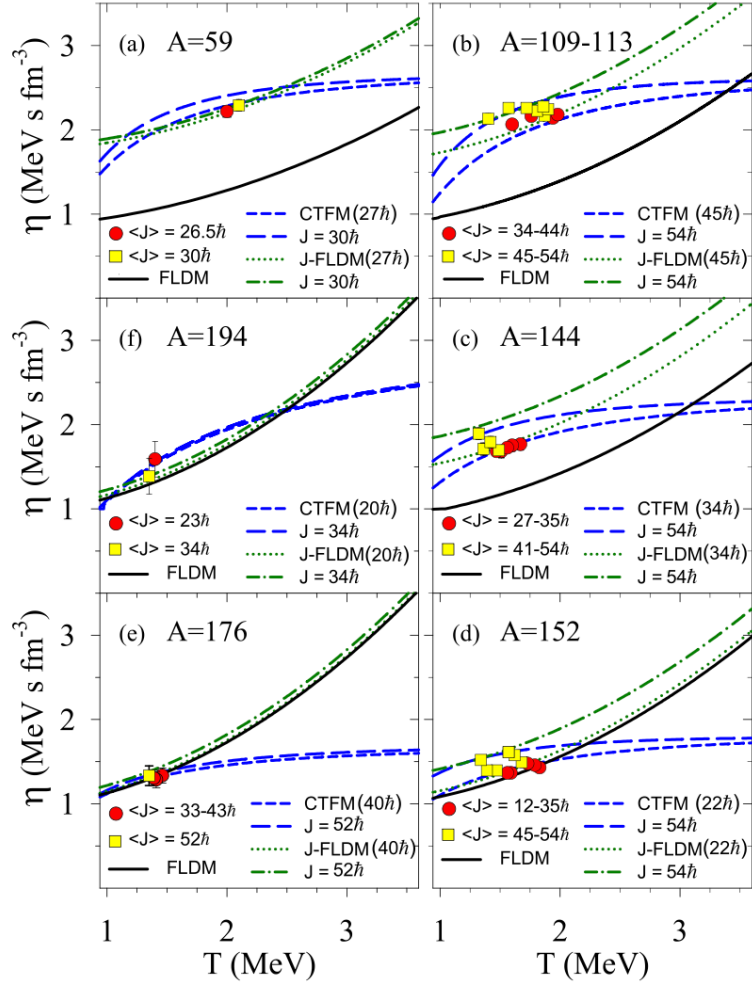


Figure 4.5: (Color online) Shear viscosity as a function of temperature for different mass nuclei at different angular momenta (J) [179].

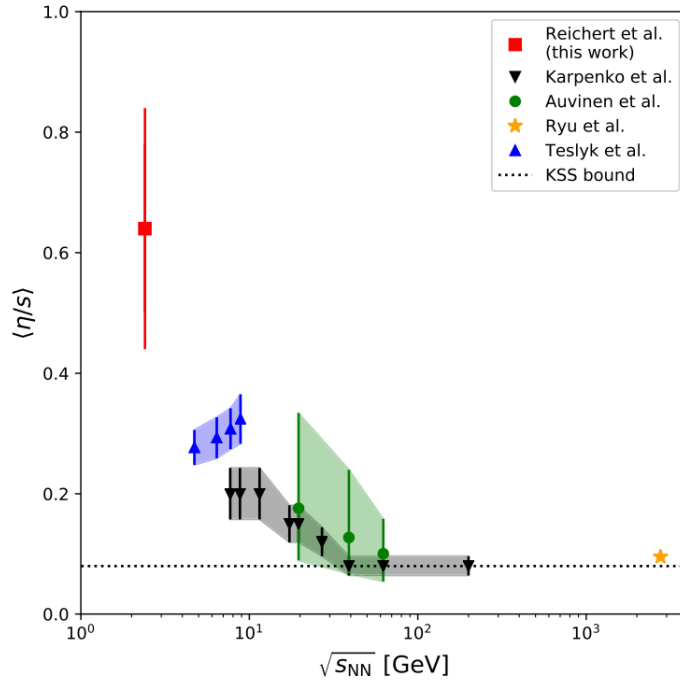


Figure 4.6: (Color online) Ratio of shear viscosity to entropy density η/s as a function of collision energy $\sqrt{s_{\text{NN}}}$ [81]. The blue triangles-up are extracted from [184] at full overlap, while the black triangles-down are from [185] and the green circles are from [186]. The orange star denotes an estimate from [187], and the dotted black line shows the KSS bound [24].

failing to describe the experimental data. From Fig. 4.5, one could also learn that the effect of J in η is important for lighter mass nuclei. The reason given by the author is due to smaller moment of inertia for the lighter mass nuclei in comparison to that of the heavier mass nuclei.

Recently, Reichert *et al.* [81] estimated η/s from data provided by the HADES experiment at GSI on the flow coefficients v_1, \dots, v_4 for protons in $^{197}\text{Au}+^{197}\text{Au}$ reactions at $E_{\text{lab}} = 1.23 \text{ AGeV}$ (or $\sqrt{s_{\text{NN}}} = 2.4 \text{ GeV}$). Through the coarse graining analysis of the UrQMD [180–183] transport simulations of the flow harmonics in comparison to the experimental data, it was obtained that $\eta/s \approx 0.65 \pm 0.15$ (or $(8 \pm 2) 1/4\pi$) as shown by the red-square point in Fig.4.6. It is seen that even in the higher collision energy, η/s shows a decrease as beam energy increases. Reichert *et al.* pointed out that one could explore Λ , $\bar{\Lambda}$ polarization from the spatial distribution of η/s in the transverse plane. Also, one can get information on the contributions of η/s to the collective flow components since the flow components were created at different times of the collision. For instance, v_1 is mainly created during the maximal compression phase, where η/s is lowest and v_2 gains further contributions during the expansion phase, where η/s moderately increases [81]. Moreover, one could investigate the effects of shear viscosity on the Fourier-decomposition of azimuthal particle distribution [81].

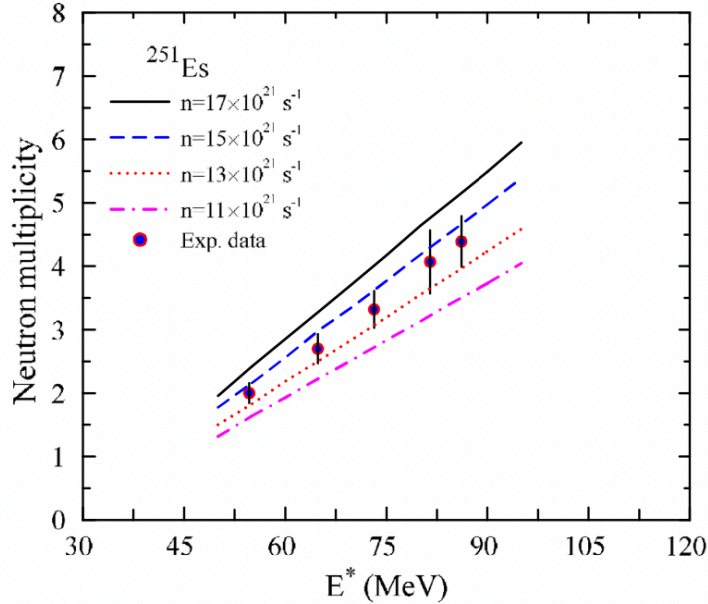


Figure 4.7: (Color online) The pre-scission fission neutron multiplicity for the compound nucleus ^{251}Es as a function of energy calculated with different values of the post-saddle friction [195]. The experimental data with filled symbols is from [196].

4.3. Others

Fission is an important subject in the studies of nuclear physics, nuclear astrophysics, and nuclear applications [188–191]. Lots of work has attempted to reproduce experimental data on fission in heavy ion collisions by adjusting the properties of the viscosity of hot nuclear matter [188, 189, 192–195]. It is well known that the standard statistical model underestimates the number of measured pre-scission particles emitted in heavy-ion reactions [193–195]. The main reason could be due to the nuclear viscosity. For the fission, it has two main processes: one is the time needed for transition from equilibrium compound state to saddle point called the transient time (τ_{tr}) and the other is the time of descent from saddle to scission point, called τ_{ssc} [194]. And such processes have been investigated and it is indicated that dissipative in nature at high excitation energy is important [194]. In Ref. [195], Eslamizadeh and Pirpour simulated the fission process of the excited compound nucleus ^{251}Es produced in $^{19}\text{F}+^{232}\text{Th}$ reaction with a stochastic approach based on two-dimensional Langevin equations. Within the framework, it contains a friction coefficient (n) as a free parameter which depends on the nuclear viscosity. As shown in Fig. 4.7, it is shown that the results of calculations are in good agreement with the experimental data by applying values of the post-saddle friction equal to $13\text{--}15 \times 10^{21} \text{ s}^{-1}$ [195]. In Ref. [195], the author did not give the value of the nuclear viscosity but the post-saddle friction, which indicates that nuclear viscosity plays an important role in fission dynamics.

In this section, we have reviewed some results for shear viscosity η and specific shear viscosity η/s . Shear viscosity in terms of the width and energy of GDR can help us extract it from experiments. Shear

viscosity of finite nuclei shows an increase as temperature increases at low temperatures with a density $\rho=0.16 \text{ fm}^{-3}$. However, for the shear viscosity of infinite nuclear matter as shown in Figs. 3.9 and 3.10, it can be seen that at density $\rho=0.16 \text{ fm}^{-3}$, shear viscosity decreases as a function of temperature in the low temperature region since there is a competition between Pauli blocking and nucleon-nucleon collisions. Whether it is a finite-size effect or not should be checked in future investigations. And from the experimental results for specific shear viscosity η/s , it is not so different from that of QGP matter produced in relativistic heavy-ion collisions. Also, we have presented some previous results about the effects of mass and angular momentum on shear viscosity and the effect of nuclear viscosity in fission dynamics studies.

5. η/s in relativistic heavy–ion collision

This review focuses mainly on the shear viscosity and ratio of shear viscosity to the entropy density η/s of nucleonic matter. However, there is a strong connection between η/s of nucleonic matter and QGP in relativistic heavy-ion collisions. For completion, we will shortly review η/s in relativistic heavy-ion collisions. In heavy-ion collision, the exact shear viscosity and ratio of shear viscosity to the entropy density should be time dependence and depend on matter density, system temperature, the presence of magnetic fields, and possibly other system conditions since the collision system compression or expansion (in relativistic heavy-ion collisions as the QGP expands and goes through a transition into a hadron phase) [197].

5.1. Ratio of shear viscosity to entropy density across the QCD phase diagram

After the KSS bound proposed by Kovtun, Son, and Starinets [24], lots of efforts were paid to the ratio of shear viscosity to entropy density η/s , the fluidity of QGP matter, the relation between η/s and phase diagram, etc. According to the results in Ref. [48], the ratio of shear viscosity to entropy density near the phase transition from hadrons to quarks and gluons shows a similar behavior to helium, nitrogen, and water. As seen in Fig. 5.1, the experimental and calculated η/s values for nuclear matter show a minimum in the vicinity of the critical temperature T_c [198]. This value of η/s for QGP and that in relativistic heavy-ion collision in RHIC is much lower than that obtained from helium, nitrogen, and water. It has been interpreted that the QGP created in the early phase of RHIC collisions is more strongly coupled than atomic and molecular substances. From Fig. 5.1, η/s for RHIC collisions at T_c , is rather close to the conjectured lower bound of $1/4\pi$ (generally, in relativistic heavy-ion collisions $\hbar=1$). The authors concluded that it is compatible with the minimum expected if the hot and dense QCD matter produced in RHIC collisions follows decay trajectories that are close to the critical end point (CEP) [198].

5.2. The dependence of ratio of shear viscosity to entropy density on collision centrality

According to the work [197], the author gives the dependence of specific shear viscosity on collision centrality in ultra-relativistic heavy-ion collisions at RHIC and LHC by using the Gavin ansatz, which relates the longitudinal broadening of transverse momentum two-particle correlators, G_2 . The G_2

Table 5.1: Compilation table [197] for measured charged particle densities, $dN_{ch}/d\eta$, and longitudinal widths, $\sigma_{\Delta\eta}$, of the charge independent correlator G_2^{CI} , interpolated freezeout times, τ_f , and computed values of η/s as a function of the centrality of Pb+Pb collisions at $\sqrt{s_{NN}}=2.76$ TeV [200–203] and Au+Au at $\sqrt{s_{NN}}=200$ GeV [204, 205].

Centrality	$dN_{ch}/d\eta$	$\sigma_{\Delta\eta}$ of G_2^{CI}	τ_f (fm/c)	η/s
LHC				
0-5%	1601.00 ± 60.00	$0.68 \pm 0.01^{sta} + 0.11^{sys} - 0.03^{sys}$	$10.33 \pm 0.10 \pm 1.03^{fit}$	$0.05 \pm 0.00^{sta} \pm 0.04^{sys}$
5-10%	1294.00 ± 49.00	$0.73 \pm 0.01^{sta} + 0.54^{sys} - 0.03^{sys}$	$9.62 \pm 0.09 \pm 0.91^{fit}$	$0.07 \pm 0.00^{sta} \pm 0.03^{sys}$
10-20%	966.00 ± 37.00	$0.71 \pm 0.01^{sta} + 0.04^{sys} - 0.03^{sys}$	$8.73 \pm 0.08 \pm 0.75^{fit}$	$0.06 \pm 0.00^{sta} \pm 0.02^{sys}$
20-30%	649.00 ± 23.00	$0.73 \pm 0.01^{sta} + 0.03^{sys} - 0.03^{sys}$	$7.64 \pm 0.07 \pm 0.56^{fit}$	$0.07 \pm 0.00^{sta} \pm 0.03^{sys}$
30-40%	426.00 ± 15.00	$0.70 \pm 0.01^{sta} + 0.03^{sys} - 0.03^{sys}$	$6.64 \pm 0.06 \pm 0.39^{fit}$	$0.06 \pm 0.00^{sta} \pm 0.02^{sys}$
40-50%	261.00 ± 9.00	$0.69 \pm 0.01^{sta} + 0.03^{sys} - 0.03^{sys}$	$5.64 \pm 0.05 \pm 0.23^{fit}$	$0.06 \pm 0.00^{sta} \pm 0.02^{sys}$
50-60%	149.00 ± 6.00	$0.65 \pm 0.01^{sta} + 0.03^{sys} - 0.03^{sys}$	$4.68 \pm 0.04 \pm 0.13^{fit}$	$0.05 \pm 0.00^{sta} \pm 0.02^{sys}$
60-70%	76.00 ± 4.00	$0.63 \pm 0.01^{sta} + 0.03^{sys} - 0.03^{sys}$	$3.74 \pm 0.04 \pm 0.20^{fit}$	$0.05 \pm 0.00^{sta} \pm 0.02^{sys}$
70-80%	35.00 ± 2.00	$0.59 \pm 0.01^{sta} + 0.02^{sys} - 0.02^{sys}$	$2.89 \pm 0.03 \pm 0.33^{fit}$	$0.04 \pm 0.00^{sta} \pm 0.02^{sys}$
RHIC				
0-5%	691.00 ± 49.00	$0.94 \pm 0.06^{sta} \pm 0.17^{sys}$	$7.24 \pm 0.07 \pm 0.50^{fit}$	$0.14 \pm 0.03^{sta} \pm 0.09^{sys}$
5-10%	558.00 ± 40.00	$0.99 \pm 0.07^{sta} \pm 0.06^{sys}$	$6.81 \pm 0.06 \pm 0.41^{fit}$	$0.16 \pm 0.03^{sta} \pm 0.07^{sys}$
10-20%	421.00 ± 30.00	$0.93 \pm 0.06^{sta} \pm 0.07^{sys}$	$6.27 \pm 0.05 \pm 0.30^{fit}$	$0.14 \pm 0.03^{sta} \pm 0.06^{sys}$
20-30%	287.00 ± 20.00	$0.84 \pm 0.05^{sta} \pm 0.03^{sys}$	$5.62 \pm 0.04 \pm 0.17^{fit}$	$0.10 \pm 0.02^{sta} \pm 0.04^{sys}$
30-40%	195.00 ± 14.00	$0.67 \pm 0.03^{sta} \pm 0.02^{sys}$	$5.05 \pm 0.04 \pm 0.12^{fit}$	$0.04 \pm 0.01^{sta} \pm 0.02^{sys}$
40-50%	126.00 ± 60.00	$0.59 \pm 0.02^{sta} \pm 0.03^{sys}$	$4.48 \pm 0.05 \pm 0.17^{fit}$	$0.01 \pm 0.01^{sta} \pm 0.02^{sys}$
50-60%	78.00 ± 9.00	$0.57 \pm 0.02^{sta} \pm 0.02^{sys}$	$3.95 \pm 0.06 \pm 0.27^{fit}$	$0.01 \pm 0.01^{sta} \pm 0.02^{sys}$
60-70%	45.00 ± 6.00	$0.55 \pm 0.02^{sta} \pm 0.04^{sys}$	$3.43 \pm 0.08 \pm 0.38^{fit}$	$0.003 \pm 0.009^{sta} \pm 0.022^{sys}$

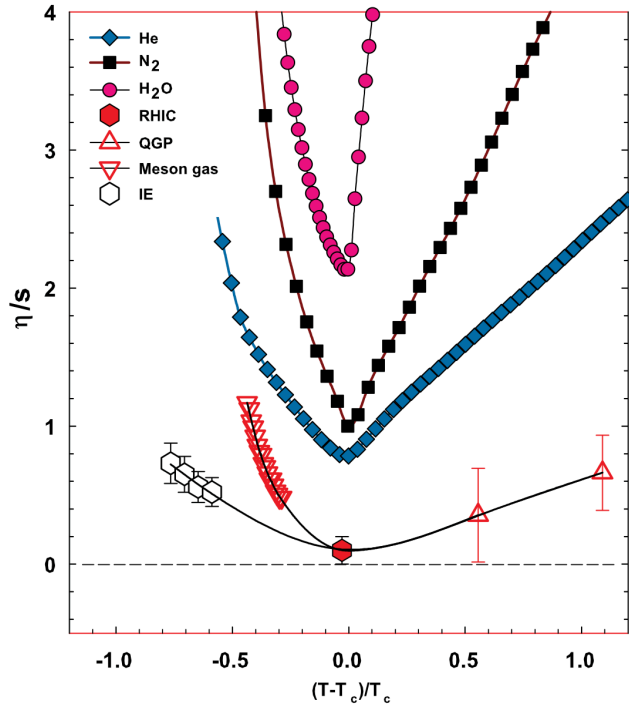


Figure 5.1: (Color online) Ratio of shear viscosity to entropy density (η/s) as a function of reduce temperature $(T-T_c)/T_c$ for several substances [198]. The lattice QCD value critical temperature T_c for nuclear matter is set at 170 MeV [199].

correlator [206, 207] is designed to be proportional to the covariance of momentum currents and is as such sensitive to dissipative viscous forces at play during the transverse and longitudinal expansion of the matter formed in A+A collisions. And these forces lead to a longitudinal broadening of G_2 measured as a function of the pseudorapidity difference of measured charged particles [197]. Through this G_2 correlator, Gavin gave a clear image for relation between G_2 and system expansion. As the matter expands, neighboring fluid cells drag one another. Fast fluid cells tend to slow down whereas slow fluid cells accelerate. This has the effect of dampening the expansion and produces a progressive broadening of the G_2 correlator with time. The longer the system lives, the longer viscous effects play a role, and the broader the G_2 correlator becomes [197]. It means that one can get the difference in the variance of the correlator among different collision centralities. For the Gavin ansatz, one can write it as,

$$\sigma_c^2 - \sigma_0^2 = \frac{4}{T_c} \frac{\eta}{s} \left(\frac{1}{\tau_0} - \frac{1}{\tau_{c,f}} \right) \quad (5.1)$$

where σ_c is the longitudinal width of the correlator measured in most central collisions whereas σ_0 is the longitudinal width of the correlator at formation time τ_0 which is set 1.0 ± 0.5 fm/c [208]. The critical temperature T_c is used at $160 \text{ MeV} \pm 5 \text{ MeV}$ [208]. $\tau_{c,f}$ is the freeze-out time in most central collisions which can be obtained from two pion Bose-Einstein measurements from AGS to LHC energies [209].

With Eq. 5.1, it gives one way to compare model simulations and experimental data. Based on RHIC and LHC data and with Gavin ansatz, the estimates for specific shear viscosity are given as in table 5.1. Seeing from table 5.1, η/s based on ALICE (A Large Ion Collider Experiment) data exhibits very weak or no dependence on collision centrality at LHC energy, while estimates obtained from STAR data hint that η/s might be a function of collision centrality at top RHIC energy. However, given the large systematic uncertainties of these data, one cannot draw a strong conclusion about the dependence on collision centrality. For the precision of estimates of the dependence of η/s , one needs to improve the accuracy of the STAR measurement of G_2 . Additionally, it can be found that the mean values of η/s at some collision centralities are less than the KSS bound of $1/4\pi \approx 0.08$ and it is more obvious from LHC results than from STAR data. If one neglects the systematic uncertainties, it could raise the question of how the universal bound of $1/4\pi$ is for QGP matter.

5.3. Magnetic field effect on ratio of shear viscosity to entropy density

In noncentral relativistic heavy-ion collisions, an extremely strong magnetic field up to $\sim 10^{18}$ G can be created [210–213]. As in Pb+Pb collisions at LHC, the computation shows that the strength of the magnetic field can reach $eB \sim 15m_\pi^2$ [210], where $m_\pi = 140$ MeV is the mass of pion. With such a strong electromagnetic field, it could induce some anomalous transport phenomena in hot quantum chromodynamic (QCD) matter [214, 215], such as the chiral magnetic effect (CME) [216, 217], chiral separation effect (CSE) [218], chiral electric separation effect (CESE) [219], chiral magnetic waves (CMW) [220], chiral vortical effect (CVE) [221] and particle polarization [222]. The magnetic field created in noncentral collisions is perpendicular to the reaction plane and Lorentz force can vanish in the direction parallel to the field. Lorentz force lay down in the reaction plane which makes azimuthal anisotropy for transverse flow of QGP [223]. And also, it would significantly influence on the properties of strange quark matter. With strong magnetic field, the condensates for light quarks/antiquarks (as u and d quark) degree of freedom are affected [224]. If the condensates increase with the magnetic field at low temperatures, it refers to magnetic catalysis (MC), and decrease for temperatures close to TPC which refers to inverse magnetic catalysis (IMC) [214, 225]. These effects would change the masses of the u and d quarks which in turn play an important role to the transport feature [226].

There is lots of work to investigate the influence of the magnetic field on the QCD phase diagram. And also, the impact of magnetic field on the shear viscosity of quark matter has been investigated in Refs. [223, 226–228]. The simulations are in the framework of Nambu–Jona–Lasinio model (NJL) where magnetohydrodynamics is considered. Under the relaxation time approximation, one can obtain

shear viscosity for the QGP system [226, 227],

$$\eta = \frac{1}{15T} \sum_a g_a \int \frac{d^3p}{(2\pi)^3} \frac{p^4}{E_a^2} \tau_a f_a^0 (1 - f_a^0) \quad (5.2)$$

where ‘a’ is index for quark and antiquark, τ_a^c is the relaxation time of the quark generated by the collision mechanism and g_a is degeneracy factor for quark and antiquark which is equal to $N_s \times N_f \times N_c = 2 \times 2 \times 3$ where N_s is spin freedom; N_f is flavor freedom [u and d, for SU(2)]; N_c is color freedom [226, 227, 229]. Here only two-flavor (isospin-symmetric) quark matter is considered for a system medium mainly with u and d quarks and their antiquarks. In Eq. (5.2), f^0 is the equilibrium distribution function, which is written as covariant form [226],

$$f^0(x, p) = \frac{1}{\exp\left[\frac{u_\mu p^\mu \mp \mu}{T}\right] + 1}. \quad (5.3)$$

where $u_\mu(x) = \gamma_\mu(1, \mathbf{u}(x))$; $u_\mu(x)$ is the four velocities of the fluid. The symbol \mp is for quark (‘-’) and antiquark (‘+’). With magnetic field, the shear viscosity coefficient of the dissipative fluid system can be decomposed into five different components (n=0,1,2,3,4) [226]. The $n = 0$ component remains undisturbed by magnetic field. The other four components can be expressed [226],

$$\eta_2 = 4\eta_1 = \frac{1}{15T} \sum_a g_a \int \frac{d^3p}{(2\pi)^3} \frac{p^4}{E_a^2} f_a^0 (1 - f_a^0) \frac{(\tau_a^B)^2}{\tau_a^c} \quad (5.4)$$

and

$$\eta_4 = 2\eta_3 = \frac{1}{15T} \sum_a g_a \int \frac{d^3p}{(2\pi)^3} \frac{p^4}{E_a^2} f_a^0 (1 - f_a^0) \tau_a^B \quad (5.5)$$

where τ_a^B is the relaxation time induced by the magnetic field.

As shown in Fig. 5.2, without magnetic field, specific shear viscosity decreases as temperature increases in the range of 100–300 MeV. Here at eB=0, due to the increase in collisional frequency with temperature, relaxation time decreases with T. Being proportional with the decreasing function τ_c for eB=0, η/s decreases with temperature [227]. When the magnetic field is taken into account, the components of shear viscosity over entropy increase with the increasing of temperature. One can notice that in Eq. (5.4), η_2 becomes inverse to the τ^c with the magnetic field. Thus, η_2/s increases with temperature. For the Hall-type viscosity, $\eta_{3,4} \propto \tau^B$, $\eta_{3,4}$ increases as temperature increases because of its phase space part [227]. The η_4/s in Fig. 5.2 shows a value that crosses the KSS bound. It indicates

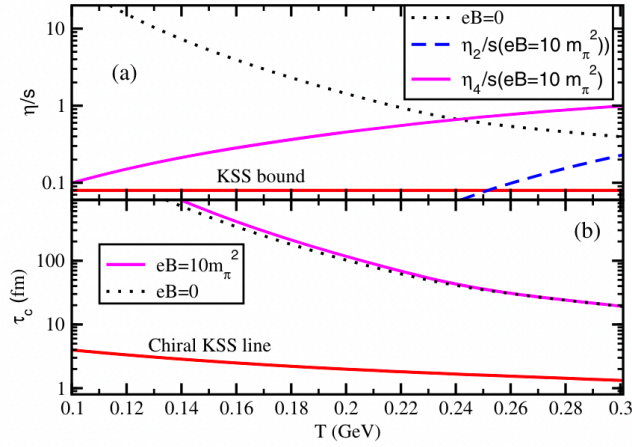


Figure 5.2: (Color online) The ratio of shear viscosity to entropy density η/s (a) and relaxation time τ_c (b) as functions of temperature at $eB=0$ and $eB=10 m_\pi^2$ [227].

that the effect of magnetic field could make the quark matter system a more perfect fluid.

5.4. Bayesian estimation of ratio of shear viscosity to entropy density

First principles for the transport properties of QGP matter in heavy-ion collisions remain challenging [232, 233]. In recent years, machine learning and Bayesian analysis methods have attracted lots of attention on the study of nuclear physics [230, 234–237]. With the application of Bayesian analysis [230, 237], one can give a meaningful credibility region for the ratio of shear viscosity to entropy density η/s for the QGP matter [230, 232, 233, 238]. In Ref. [230], the authors used Bayesian parameter estimation methods to constrain temperature-dependent specific shear and bulk viscosity $\eta/s(T)$ and $\zeta/s(T)$, which are fundamental properties of the QGP. In Bayes' theorem, one has to give the posterior distributions as,

$$P(\mathbf{x}|\mathbf{y}_{\text{exp}}) = \frac{P(\mathbf{y}_{\text{exp}}|\mathbf{x})P(\mathbf{x})}{P(\mathbf{y}_{\text{exp}})}, \quad (5.6)$$

where $P(\mathbf{y}_{\text{exp}}|\mathbf{x})$ is a likelihood function that quantifies how well the model describes the experimental measurement and $P(\mathbf{x})$ is a prior function. And the normalization $P(\mathbf{y}_{\text{exp}})$ is called the ‘Bayesian evidence’ [232]. Then, one needs to build up a vector of model parameters \mathbf{x} and do the simulations with parameters (\mathbf{x}). With the model calculations, we could do the comparison with a set of experimental data \mathbf{y} . The desired parameter estimates may be extracted from the posterior distribution. How to constraint the parameters in a Bayesian analysis process? In Ref. [233], the authors from JETSCAPE Collaboration have given some ways: first, this can be achieved with better external constraints on the model’s parameters \mathbf{x} , reflected in a more realistic prior distribution $P(\mathbf{x})$; second, new or more

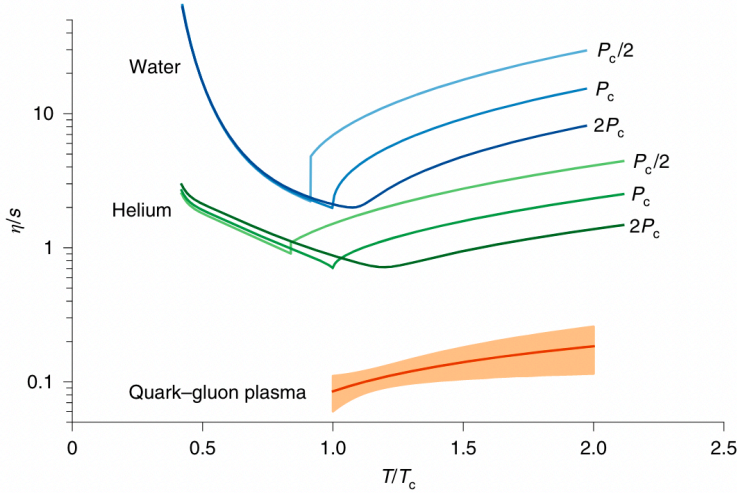


Figure 5.3: (Color online) Specific shear viscosity as a function of reduce temperature T/T_c for water, Helium and QGP [230]. The water and Helium are with different pressures which calculated from NIST data [231]. The orange line and band show the posterior median and 90% credible region for the QGP $\eta/s(T)$ estimated from PbPb collision data at $\sqrt{s_{NN}}=2.76$ and 5.02 TeV.

precise experimental data can tighten the likelihood $P(\mathbf{y}_{\text{exp}}|\mathbf{x})$; third, theoretical progress on the model and better quantification of the model' s uncertainties lead to more reliable constraints through the likelihood as well.

In Ref. [230], the authors calibrate the model with a diverse set of experimental data measured by ALICE at LHC from Pb+Pb collisions at beam energies of both $\sqrt{s_{NN}}=2.76$ and 5.02 TeV. As the orange band shows in Fig. 5.3, the η/s is constrained in a 90% credible region. Here it can be seen that near the T_c , η/s is very close to the KSS bound ($1/4\pi \approx 0.08$) and even lower than it. With the help of hybrid model, denoted as T_RENTo + VISH (2 + 1) + UrQMD [237] which has successfully described the previous ALICE measurements [232], the authors give more results for transport properties in ultra-relativistic heavy-ion collisions using the Bayesian analysis method. They argued that the improved statistical uncertainties both on the experimental data and hydrodynamic calculations with additional observables do not help to reduce the final credibility ranges much, which indicates a need for improving the dynamical collision model before the hydrodynamic takes place [237].

In the Bayesian analysis method, some uncertainties would come from different models. In Ref. [233], JETSCAPE Collaboration extended the Bayesian inference framework and proposed Bayesian model averaging method, in which the posterior distribution is defined by,

$$P(\mathbf{x}|\mathbf{y}_{\text{exp}}) \sim \sum_i P^{(i)}(\mathbf{y}_{\text{exp}})P^{(i)}(\mathbf{x}|\mathbf{y}_{\text{exp}}) \quad (5.7)$$

where i is the index for different models. The authors with three kinds of hadronic phase-space distribu-

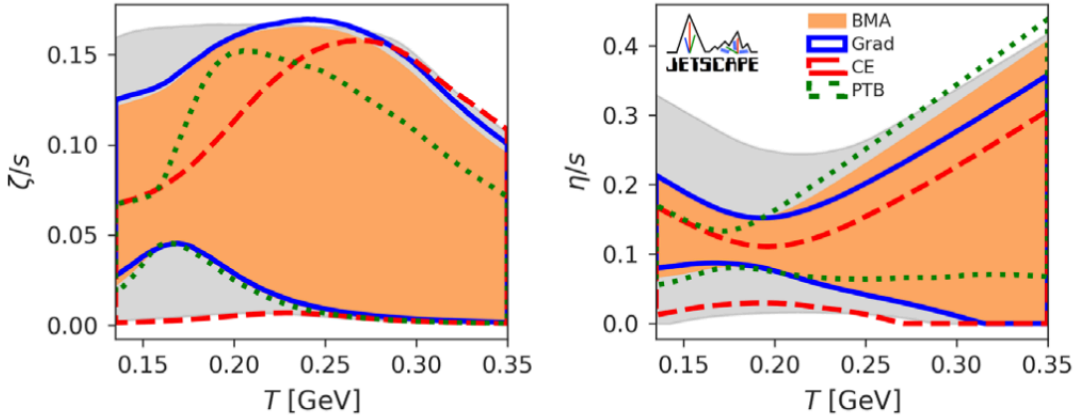


Figure 5.4: (Color online) Specific bulk (left) and shear (right) viscosities of QGP as functions of temperature. The 90% credible intervals for the prior (gray), the posteriors of the Grad (blue), Chapman-Enskog (red), and Pratt-Torrieri-Bernhard (green) models, and their Bayesian model average (orange) [233].

tions: the 14-moment Grad approximation, relativistic Chapman-Enskog series in the relaxation-time approximation (“RTA Chapman-Enskog”), and Pratt-Torrieri-Bernhard models, are for the particlization process which is the transition from hydrodynamics to hadronic kinetics and constrain the shear and bulk viscosities of quark-gluon plasma (QGP) at temperatures of 150–350 MeV by using combined data of Au+Au collisions at $\sqrt{s_{\text{NN}}}=200$ GeV from the RHIC and Pb+Pb collisions at $\sqrt{s_{\text{NN}}}=2.76$ TeV from the LHC. The results are shown in Fig 5.4. It can be seen that different particlization models show similar qualitative features. In the deconfinement region, one can obtain the most likely values for η/s of order 0.1 and ζ/s of 0.05-0.1 [233]. For specific shear viscosity, the experimental data are significant constraints for $150 \lesssim T \lesssim 250$ MeV. However, at higher or lower temperature region, the constraint becomes less. And the constraints on the specific bulk viscosity are weaker. Though the constrain from the orange region in Fig 5.4 does not reach a very narrow band yet, the Bayesian model average method including both experimental and known theoretical uncertainties provides a better way to constrain the transport properties of the quark-gluon plasma.

6. Summary and outlook

In this review, we have presented the shear viscosity and specific shear viscosity of nucleonic matter. Shear viscosity is an important transport property for classical and quantum systems. There are mainly two research directions on shear viscosity. One is the universality of the specific shear viscosity and the conjecture value $\hbar/4\pi$. Another is specific shear viscosity for the phase transition. By some methods, such as the mean free path, Green-Kubo method, shear strain rate method, Chapman-Enskog method and relaxation time approximation, one can extract shear viscosity for the infinite nuclear matter. Also, one can estimate shear viscosity and specific shear viscosity for finite nuclear matter or nuclear matter formed in heavy-ion collisions with the mean free path and Green-Kubo methods. From these results, it can be found that the viscosity of the nucleonic matter is mainly affected by four physical sources, i.e., density, temperature, isospin asymmetry, and nucleon-nucleon cross section. For lower-density systems, shear viscosity increases with temperature. For nucleonic matter at higher density, shear viscosity shows a minimum structure due to competition between temperature and collision. And lower isospin asymmetry or a higher nucleon-nucleon cross section leads to smaller shear viscosity. There are some extended effects on shear viscosity, such as the mean free path and Pauli blocking which can be fixed in a system with given density, temperature, isospin asymmetry, and nucleon-nucleon cross section. Actually, from a microscopic view, it rises by potential and nucleon-nucleon collision among particles.

Moreover, it can be found that specific shear viscosity for nucleonic matter has no more difference from that of the state created in relativistic heavy-ion collisions. The value of specific shear viscosity for nucleonic matter is several times of $\hbar/4\pi$ which indicates the KSS bound postulate being an universal limit. For phase transition investigations, even though some substances show minimum values around critical temperature, the liquid state and pure neutron matter without phase transition can display minimum value from dependence on temperature due to the existence of the Pauli Block effect. Such a turning point is from the dynamic effect; thus, one should be careful when considering phase transition with specific shear viscosity.

It may be easier to determine shear viscosity with an analytic formula. However, how to get the shear viscosity in heavy-ion collisions, which includes compression and expansion processes and is far from equilibrium, could be a challenge. In the heavy-ion collision process, shear viscosity and other transport properties have time and spatial dependence. From the experimental aspect, it is also hard to extract shear viscosity from heavy-ion collision, even though one can calculate shear viscosity with the width of giant dipole resonance or constrain shear viscosity within a hybrid model by comparing it with experimental data. For the later one, the accuracy of shear viscosity is dependent on the models.

The estimation for shear viscosity with the width of giant dipole resonance from experimental data is only for the range of about several MeV. Moreover, it can be found that the dependence of shear viscosity with the width of giant dipole resonance on temperature for finite nuclear matter shows an inverse trend to the result of the theoretical calculations in the low temperature region. Therefore, the experimental investigations on shear viscosity for finite nuclear matter are expected.

Shear viscosity and specific shear viscosity in relativistic heavy-ion collisions have also been briefly presented in this review. It is an important subject in relativistic heavy-ion collision, which is dependent on temperature as well as magnetic field effects etc. The strong magnetic field significantly affects the shear viscosity of QGP matter. It could be interesting to pay attention to that in intermediate-energy heavy-ion collisions. There are more issues for shear viscosity to be considered in the future for asymmetric nuclear matter which the fragment effect is taken into account. And it could be worth observing its correlations with dipole resonance or collective flow. As nucleons with spin degree, however, up to now, less work has been done considering how the spin and spin potential act on shear viscosity and specific shear viscosity. Especially in non-central heavy-ion collisions with large angular momentum, the effect of spin-orbit coupling on shear viscosity is also worthy of consideration.

Acknowledgements

This work is supported by the National Natural Science Foundation of China under Contracts Nos. 11890710, 11890714, 12205049, 12147101, 11925502, 11961141003, and 11935001, the Strategic Priority Research Program of CAS under Grant No. XDB34000000, National Key R&D Program of China under Grant No. 2018YFE0104600, and by Guangdong Major Project of Basic and Applied Basic Research No. 2020B0301030008.

Author's contributions (*optional section*)

Detailing here the contributions of the authors of the review.

References

- [1] M. Prakash, M. Prakash, R. Venugopalan, G. Welke, [Non-equilibrium properties of hadronic mixtures](#), *Physics Reports* 227 (6) (1993) 321–366. doi:[https://doi.org/10.1016/0370-1573\(93\)90092-R](https://doi.org/10.1016/0370-1573(93)90092-R).
URL <https://www.sciencedirect.com/science/article/pii/037015739390092R>
- [2] T. Schäfer, [Fluid dynamics and viscosity in strongly correlated fluids](#), *Annual Review of Nuclear and Particle Science* 64 (1) (2014) 125–148. arXiv:<https://doi.org/10.1146/annurev-nucl-102313-025439>, doi:10.1146/annurev-nucl-102313-025439.
URL <https://doi.org/10.1146/annurev-nucl-102313-025439>
- [3] R. E. McKinnie, J. S. Olson, [Effects of solvent composition and viscosity on the rates of CO binding to heme proteins](#), *Journal of Biological Chemistry* 256 (17) (1981) 8928–8932. doi:[https://doi.org/10.1016/S0021-9258\(19\)52488-7](https://doi.org/10.1016/S0021-9258(19)52488-7).
URL <https://www.sciencedirect.com/science/article/pii/S0021925819524887>
- [4] H. Kyushiki, A. Ikai, [The effect of solvent viscosity on the rate-determining step of fatty acid synthetase](#), *Proteins: Structure, Function, and Bioinformatics* 8 (3) (1990) 287–293. arXiv:<https://onlinelibrary.wiley.com/doi/pdf/10.1002/prot.340080310>, doi:<https://doi.org/10.1002/prot.340080310>.
URL <https://onlinelibrary.wiley.com/doi/abs/10.1002/prot.340080310>

- [5] C. Malosso, L. Zhang, R. Car, S. Baroni, D. Tisi, [Viscosity in water from first-principles and deep-neural-network simulations](#), npj Computational Materials 8 (1) (2022) 139. doi:10.1038/s41524-022-00830-7.
URL <https://doi.org/10.1038/s41524-022-00830-7>
- [6] P. S. Shternin, D. G. Yakovlev, [Shear viscosity in neutron star cores](#), Phys. Rev. D 78 (2008) 063006. doi:10.1103/PhysRevD.78.063006.
URL <https://link.aps.org/doi/10.1103/PhysRevD.78.063006>
- [7] P. S. Shternin, M. Baldo, P. Haensel, [Transport coefficients of nuclear matter in neutron star cores](#), Phys. Rev. C 88 (2013) 065803. doi:10.1103/PhysRevC.88.065803.
URL <https://link.aps.org/doi/10.1103/PhysRevC.88.065803>
- [8] P. S. Shternin, M. Baldo, H. J. Schulze, [Transport coefficients in neutron star cores in BHF approach. Comparison of different nucleon potentials](#), Journal of Physics: Conference Series 932 (1) (2017) 012042. doi:10.1088/1742-6596/932/1/012042.
URL <https://dx.doi.org/10.1088/1742-6596/932/1/012042>
- [9] E.-B. Huo, K.-R. Li, X.-Y. Qu, Y. Zhang, T.-T. Sun, [Continuum Skyrme Hartree-Fock-Bogoliubov theory with Green's function method for neutron-rich Ca, Ni, Zr, and Sn isotopes](#), Nucl. Sci. Tech. 34 (2023) 105. doi:10.1007/s41365-023-01261-9.
- [10] X. Qu, H. Tong, C. Wang, S. Wang, [Neutron matter properties from relativistic brueckner-hartree-fock theory in the full dirac space](#), SCIENCE CHINA-PHYSICS MECHANICS and ASTRONOMY 66 (2023) 242011. doi:10.1007/s11433-022-2048-3.
- [11] E. E. Kolomeitsev, D. N. Voskresensky, [Viscosity of neutron star matter and \$r\$ -modes in rotating pulsars](#), Phys. Rev. C 91 (2015) 025805. doi:10.1103/PhysRevC.91.025805.
URL <https://link.aps.org/doi/10.1103/PhysRevC.91.025805>
- [12] D. D. Ofengeim, D. G. Yakovlev, [Shear viscosity in magnetized neutron star crust](#), Europhysics Letters 112 (5) (2015) 59001. doi:10.1209/0295-5075/112/59001.
URL <https://dx.doi.org/10.1209/0295-5075/112/59001>
- [13] N. T. Bishop, P. J. van der Walt, M. Naidoo, [Effect of a viscous fluid shell on the propagation of gravitational waves](#), Phys. Rev. D 106 (2022) 084018. doi:10.1103/PhysRevD.106.084018.
URL <https://link.aps.org/doi/10.1103/PhysRevD.106.084018>

- [14] The LIGO Scientific Collaboration and Virgo Collaboration, [GW170817: Observation of gravitational waves from a binary neutron star inspiral](#), *Phys. Rev. Lett.* 119 (2017) 161101. doi:
[10.1103/PhysRevLett.119.161101](https://doi.org/10.1103/PhysRevLett.119.161101).
URL <https://link.aps.org/doi/10.1103/PhysRevLett.119.161101>
- [15] P. Shternin, D. Ofengeim, [Transport coefficients of magnetized neutron star cores](#), *The European Physical Journal A* 58 (3) (2022) 42. doi:[10.1140/epja/s10050-022-00687-w](https://doi.org/10.1140/epja/s10050-022-00687-w).
URL <https://doi.org/10.1140/epja/s10050-022-00687-w>
- [16] R. N. Manchester, G. B. Hobbs, A. Teoh, M. Hobbs, [The Australia telescope national facility pulsar catalogue](#), *The Astronomical Journal* 129 (4) (2005) 1993. doi:[10.1086/428488](https://doi.org/10.1086/428488).
URL <https://dx.doi.org/10.1086/428488>
- [17] D. N. Zubarev, [The method of the non-equilibrium statistical operator and its applications. I](#), *Fortschritte der Physik* 18 (3) (1970) 125–147. arXiv:<https://onlinelibrary.wiley.com/doi/pdf/10.1002/prop.19700180302>, doi:<https://doi.org/10.1002/prop.19700180302>.
URL <https://onlinelibrary.wiley.com/doi/abs/10.1002/prop.19700180302>
- [18] L. D. Landau, E. M. Lifshitz, [CHAPTER II - VISCOUS FLUIDS](#), in: L. D. Landau, E. M. Lifshitz (Eds.), *Fluid Mechanics (Second Edition)*, Pergamon, 1987, pp. 44–94. doi:[10.1016/B978-0-08-033933-7.50010-6](https://doi.org/10.1016/B978-0-08-033933-7.50010-6).
URL <https://www.sciencedirect.com/science/article/pii/B9780080339337500106>
- [19] J.-P. Hansen, I. R. McDonald, [Chapter 8-hydrodynamics and transport coefficients](#), in: J.-P. Hansen, I. R. McDonald (Eds.), *Theory of Simple Liquids (Fourth Edition)*, fourth edition Edition, Academic Press, Oxford, 2013, pp. 311–361. doi:<https://doi.org/10.1016/B978-0-12-387032-2.00008-8>.
URL <https://www.sciencedirect.com/science/article/pii/B9780123870322000088>
- [20] Z. Haralson, J. Goree, [Overestimation of viscosity by the Green-Kubo method in a dusty plasma experiment](#), *Phys. Rev. Lett.* 118 (2017) 195001. doi:[10.1103/PhysRevLett.118.195001](https://doi.org/10.1103/PhysRevLett.118.195001).
URL <https://link.aps.org/doi/10.1103/PhysRevLett.118.195001>
- [21] G. Pan, C. McCabe, [Prediction of viscosity for molecular fluids at experimentally accessible shear rates using the transient time correlation function formalism](#), *The Journal of Chemical Physics* 125 (19) (2006) 194527. arXiv:<https://doi.org/10.1063/1.2364899>, doi:[10.1063/1.2364899](https://doi.org/10.1063/1.2364899)

1.2364899.

URL <https://doi.org/10.1063/1.2364899>

- [22] R. Kubo, *The fluctuation-dissipation theorem*, Reports on Progress in Physics 29 (1) (1966) 255. doi:10.1088/0034-4885/29/1/306.
URL <https://dx.doi.org/10.1088/0034-4885/29/1/306>
- [23] C. M. Tenney, E. J. Maginn, *Limitations and recommendations for the calculation of shear viscosity using reverse nonequilibrium molecular dynamics*, The Journal of Chemical Physics 132 (1), 014103 (01 2010). arXiv:https://pubs.aip.org/aip/jcp/article-pdf/doi/10.1063/1.3276454/13366073/014103\>_1_online.pdf, doi:10.1063/1.3276454.
URL <https://doi.org/10.1063/1.3276454>
- [24] P. K. Kovtun, D. T. Son, A. O. Starinets, *Viscosity in strongly interacting quantum field theories from black hole physics*, Phys. Rev. Lett. 94 (2005) 111601. doi:10.1103/PhysRevLett.94.111601.
URL <https://link.aps.org/doi/10.1103/PhysRevLett.94.111601>
- [25] The PHENIX Collaboration, *Formation of dense partonic matter in relativistic nucleus–nucleus collisions at RHIC: Experimental evaluation by the PHENIX Collaboration*, Nuclear Physics A 757 (1) (2005) 184–283, first Three Years of Operation of RHIC. doi:<https://doi.org/10.1016/j.nuclphysa.2005.03.086>.
URL <https://www.sciencedirect.com/science/article/pii/S0375947405005300>
- [26] The PHOBOS Collaboration, *The PHOBOS perspective on discoveries at RHIC*, Nuclear Physics A 757 (1) (2005) 28–101, first Three Years of Operation of RHIC. doi:<https://doi.org/10.1016/j.nuclphysa.2005.03.084>.
URL <https://www.sciencedirect.com/science/article/pii/S0375947405005282>
- [27] The STAR Collaboration, *Experimental and theoretical challenges in the search for the quark-gluon plasma: The STAR Collaboration’s critical assessment of the evidence from RHIC collisions*, Nuclear Physics A 757 (1) (2005) 102–183, first Three Years of Operation of RHIC. doi:<https://doi.org/10.1016/j.nuclphysa.2005.03.085>.
URL <https://www.sciencedirect.com/science/article/pii/S0375947405005294>
- [28] J. Chen, D. Keane, Y. G. Ma, A. Tang, Z. Xu, *Antinuclei in heavy-ion collisions*, Phys. Rep. 760 (2018) 1. doi:10.1016/j.physrep.2018.07.002.

- [29] C. M. Ko, [Searching for QCD critical point with light nuclei](#), Nuclear Science and Techniques 34 (5) (2023) 80. doi:[10.1007/s41365-023-01231-1](https://doi.org/10.1007/s41365-023-01231-1).
URL <https://doi.org/10.1007/s41365-023-01231-1>
- [30] R. Rapp, [Bottomonium suppression in heavy-ion collisions and the in-medium strong force](#), Nucl. Sci. Tech. 34 (2023) 63. doi:[10.1007/s41365-023-01213-3](https://doi.org/10.1007/s41365-023-01213-3).
- [31] G. Y. Qin, [3D wakes on the femtometer scale by supersonic jets.](#), Nuclear Science and Techniques 34 (2023) 22. doi:[10.1007/s41365-023-01182-7](https://doi.org/10.1007/s41365-023-01182-7).
- [32] H. X. Zhang, Y. X. Xiao, J. W. Kang, et al., [Phenomenological study of the anisotropic quark matter in the two-flavor NambuJonaLasinio model](#), Nuclear Science and Techniques 33 (2022) 150. doi:[10.1007/s41365-022-01129-4](https://doi.org/10.1007/s41365-022-01129-4).
- [33] The ATLAS Collaboration, [The ATLAS Experiment at the CERN Large Hadron Collider](#), Journal of Instrumentation 3 (08) (2008) S08003. doi:[10.1088/1748-0221/3/08/S08003](https://doi.org/10.1088/1748-0221/3/08/S08003).
URL <https://dx.doi.org/10.1088/1748-0221/3/08/S08003>
- [34] The CMS Collaboration, [The CMS experiment at the CERN LHC](#), Journal of Instrumentation 3 (08) (2008) S08004. doi:[10.1088/1748-0221/3/08/S08004](https://doi.org/10.1088/1748-0221/3/08/S08004).
URL <https://dx.doi.org/10.1088/1748-0221/3/08/S08004>
- [35] The ALICE Collaboration, [The ALICE experiment at the CERN LHC](#), Journal of Instrumentation 3 (08) (2008) S08002. doi:[10.1088/1748-0221/3/08/S08002](https://doi.org/10.1088/1748-0221/3/08/S08002).
URL <https://dx.doi.org/10.1088/1748-0221/3/08/S08002>
- [36] The LHCb Collaboration, [The LHCb Detector at the LHC](#), Journal of Instrumentation 3 (08) (2008) S08005. doi:[10.1088/1748-0221/3/08/S08005](https://doi.org/10.1088/1748-0221/3/08/S08005).
URL <https://dx.doi.org/10.1088/1748-0221/3/08/S08005>
- [37] H. Wang, J.-H. Chen, [Anisotropy flows in Pb–Pb collisions at LHC energies from parton scatterings with heavy quark trigger](#), Nuclear Science and Techniques 33 (2) (2022) 15. doi:[10.1007/s41365-022-00999-y](https://doi.org/10.1007/s41365-022-00999-y).
URL <https://doi.org/10.1007/s41365-022-00999-y>
- [38] L.-L. Zhu, B. Wang, M. Wang, H. Zheng, [Energy and centrality dependence of light nuclei production in relativistic heavy-ion collisions](#), Nuclear Science and Techniques 33 (4) (2022) 45.

doi:10.1007/s41365-022-01028-8.

URL <https://doi.org/10.1007/s41365-022-01028-8>

- [39] A. Nakamura, S. Sakai, [Transport coefficients of a gluon plasma](#), Phys. Rev. Lett. 94 (2005) 072305. doi:10.1103/PhysRevLett.94.072305.
URL <https://link.aps.org/doi/10.1103/PhysRevLett.94.072305>
- [40] N. Christiansen, M. Haas, J. M. Pawłowski, N. Strodthoff, [Transport Coefficients in Yang-Mills Theory and QCD](#), Phys. Rev. Lett. 115 (2015) 112002. doi:10.1103/PhysRevLett.115.112002.
URL <https://link.aps.org/doi/10.1103/PhysRevLett.115.112002>
- [41] K. J. Eskola, [Nearly perfect quark–gluon fluid](#), Nature Physics 15 (11) (2019) 1111–1112. doi:10.1038/s41567-019-0643-0.
URL <https://doi.org/10.1038/s41567-019-0643-0>
- [42] W. Busza, K. Rajagopal, , W. van der Schee, [Heavy ion collisions: The big picture and the big questions](#), Annual Review of Nuclear and Particle Science 68 (2018) 339. doi:<https://doi.org/10.1146/annurev-nucl-101917-020852>.
- [43] B. Müller, J. L. Nagle, [Results from the relativistic heavy ion collider](#), Annu. Rev. Nucl. Part. Sci. 56 (2006) 93. doi:10.1146/annurev.nucl.56.080805.140556.
- [44] T. Schäfer, D. Teaney, [Nearly perfect fluidity: from cold atomic gases to hot quark gluon plasmas](#), Reports on Progress in Physics 72 (12) (2009) 126001. doi:10.1088/0034-4885/72/12/126001.
URL <https://dx.doi.org/10.1088/0034-4885/72/12/126001>
- [45] P. Romatschke, U. Romatschke, [Viscosity information from relativistic nuclear collisions: How Perfect is the Fluid Observed at RHIC?](#), Phys. Rev. Lett. 99 (2007) 172301. doi:10.1103/PhysRevLett.99.172301.
URL <https://link.aps.org/doi/10.1103/PhysRevLett.99.172301>
- [46] H. Song, U. Heinz, [Causal viscous hydrodynamics in 2 + 1 dimensions for relativistic heavy-ion collisions](#), Phys. Rev. C 77 (2008) 064901. doi:10.1103/PhysRevC.77.064901.
URL <https://link.aps.org/doi/10.1103/PhysRevC.77.064901>
- [47] C. Shen, U. Heinz, P. Huovinen, H. Song, [Systematic parameter study of hadron spectra and elliptic flow from viscous hydrodynamic simulations of Au+Au collisions at \$\sqrt{s_{NN}} = 200\$ GeV](#),

Phys. Rev. C 82 (2010) 054904. doi:10.1103/PhysRevC.82.054904.

URL <https://link.aps.org/doi/10.1103/PhysRevC.82.054904>

[48] L. P. Csernai, J. I. Kapusta, L. D. McLerran, [Strongly interacting low-viscosity matter created in relativistic nuclear collisions](#), Phys. Rev. Lett. 97 (2006) 152303. doi:10.1103/PhysRevLett.97.152303.

URL <https://link.aps.org/doi/10.1103/PhysRevLett.97.152303>

[49] J. A. Joseph, E. Elliott, J. E. Thomas, [Shear viscosity of a unitary fermi gas near the superfluid phase transition](#), Phys. Rev. Lett. 115 (2015) 020401. doi:10.1103/PhysRevLett.115.020401.

URL <https://link.aps.org/doi/10.1103/PhysRevLett.115.020401>

[50] A. D. B. Woods, A. C. H. Hallett, [THE VISCOSITY OF LIQUID HELIUM II BETWEEN 0.79 °K AND THE LAMBDA POINT](#), Canadian Journal of Physics 41 (4) (1963) 596–609. arXiv:<https://doi.org/10.1139/p63-062>, doi:10.1139/p63-062.

URL <https://doi.org/10.1139/p63-062>

[51] T. A. Alvesalo, H. K. Collan, M. T. Loponen, M. C. Veuro, [Experimental determination of the viscosity and density of the normal component of superfluid \$^3\text{He}\$ at the melting curve](#), Phys. Rev. Lett. 32 (1974) 981–985. doi:10.1103/PhysRevLett.32.981.

URL <https://link.aps.org/doi/10.1103/PhysRevLett.32.981>

[52] T. A. Alvesalo, H. K. Collan, M. T. Loponen, O. V. Lounasmaa, M. C. Veuro, [The viscosity and some related properties of liquid \$^3\text{He}\$ at the melting curve between 1 and 100 mK](#), Journal of Low Temperature Physics 19 (1) (1975) 1–37. doi:10.1007/BF00115527.

URL <https://doi.org/10.1007/BF00115527>

[53] P. Wolfle, [Low-temperature properties of liquid \$^3\text{He}\$](#) , Reports on Progress in Physics 42 (2) (1979) 269. doi:10.1088/0034-4885/42/2/002.

URL <https://dx.doi.org/10.1088/0034-4885/42/2/002>

[54] B. Immanuel, D. Jean, Z. Wilhelm, [Many-body physics with ultracold gases](#), Rev. Mod. Phys. 80 (2008) 885–964. doi:10.1103/RevModPhys.80.885.

URL <https://link.aps.org/doi/10.1103/RevModPhys.80.885>

[55] G. Stefano, P. L. P., S. Sandro, [Theory of ultracold atomic Fermi gases](#), Rev. Mod. Phys. 80 (2008) 1215–1274. doi:10.1103/RevModPhys.80.1215.

URL <https://link.aps.org/doi/10.1103/RevModPhys.80.1215>

- [56] M. Horikoshi, S. Nakajima, M. Ueda, T. Mukaiyama, [Measurement of universal thermodynamic functions for a unitary Fermi gas](#), *Science* 327 (5964) (2010) 442–445. [arXiv:https://www.science.org/doi/pdf/10.1126/science.1183012](#), [doi:10.1126/science.1183012](#).
URL [https://www.science.org/doi/abs/10.1126/science.1183012](#)
- [57] C. Cao, E. Elliott, J. Joseph, H. Wu, J. Petricka, T. Schäfer, J. E. Thomas, [Universal quantum viscosity in a unitary Fermi gas](#), *Science* 331 (6013) (2011) 58–61. [arXiv:https://www.science.org/doi/pdf/10.1126/science.1195219](#), [doi:10.1126/science.1195219](#).
URL [https://www.science.org/doi/abs/10.1126/science.1195219](#)
- [58] T. Enss, R. Haussmann, W. Zwerger, [Viscosity and scale invariance in the unitary Fermi gas](#), *Annals of Physics* 326 (3) (2011) 770–796. [doi:https://doi.org/10.1016/j.aop.2010.10.002](#).
URL [https://www.sciencedirect.com/science/article/pii/S000349161000179X](#)
- [59] L. Salasnich, F. Toigo, [Viscosity-entropy ratio of the unitary Fermi gas from zero-temperature elementary excitations](#), *Journal of Low Temperature Physics* 165 (5) (2011) 239–248. [doi:10.1007/s10909-011-0391-8](#).
URL [https://doi.org/10.1007/s10909-011-0391-8](#)
- [60] H. Guo, L. D. Wu, C. C. Chien, K. Levin, [Microscopic approach to shear viscosities of unitary fermi gases above and below the superfluid transition](#), *Phys. Rev. Lett.* 107 (2011) 020403. [doi:10.1103/PhysRevLett.107.020403](#).
URL [https://link.aps.org/doi/10.1103/PhysRevLett.107.020403](#)
- [61] K. Schoenberg, V. Bagnoud, A. Blazevic, V. E. Fortov, D. O. Gericke, A. Golubev, D. H. H. Hoffmann, D. Kraus, I. V. Lomonosov, V. Mintsev, S. Neff, P. Neumayer, A. R. Piriz, R. Redmer, O. Rosmej, M. Roth, T. Schenkel, B. Sharkov, N. A. Tahir, D. Varentsov, Y. Zhao, [High-energy-density-science capabilities at the Facility for Antiproton and Ion Research](#), *Physics of Plasmas* 27 (4) (2020) 043103. [arXiv:https://pubs.aip.org/aip/pop/article-pdf/doi/10.1063/1.5134846/15926936/043103\1\1_online.pdf](#), [doi:10.1063/1.5134846](#).
URL [https://doi.org/10.1063/1.5134846](#)
- [62] J. Pouthas, B. Borderie, R. Dayras, E. Plagnol, M. Rivet, F. Saint-Laurent, J. Steckmeyer, G. Auger, C. Bacri, S. Barbey, A. Barbier, A. Benkirane, J. Benlliure, B. Berthier, E. Bougamont, P. Bourgault, P. Box, R. Bzyl, B. Cahan, Y. Cassagnou, D. Charlet, J. Charvet, A. Chbihi, T. Clerc, N. Copinet, D. Cussol, M. Engrand, J. Gautier, Y. Huguet, O. Jouniaux, J. Lav-

ille, P. Le Botlan, A. Leconte, R. Legrain, P. Lelong, M. Le Guay, L. Martina, C. Mazur, P. Mosrin, L. Olivier, J. Passerieux, S. Pierre, B. Piquet, E. Plaige, E. Pollacco, B. Raine, A. Richard, J. Ropert, C. Spitaels, L. Stab, D. Sznajderman, L. Tassan-got, J. Tillier, M. Tripon, P. Vallerand, C. Volant, P. Volkov, J. Wieleczko, G. Wittwer, [INDRA, a \$4\pi\$ charged product detection array at GANIL](#), Nuclear Instruments and Methods in Physics Research Section A: Accelerators, Spectrometers, Detectors and Associated Equipment 357 (2) (1995) 418–442. doi:[https://doi.org/10.1016/0168-9002\(94\)01543-0](https://doi.org/10.1016/0168-9002(94)01543-0).

URL <https://www.sciencedirect.com/science/article/pii/0168900294015430>

[63] S.-W. Bai, X.-F. Yang, S.-J. Wang, Y.-C. Liu, P. Zhang, Y.-S. Liu, H.-R. Hu, Y.-F. Guo, J. Wang, Z.-Y. Du, Z. Yan, Y.-K. Zhang, Y.-L. Ye, Q.-T. Li, Y.-C. Ge, C.-Y. He, [Commissioning of a high-resolution collinear laser spectroscopy apparatus with a laser ablation ion source](#), Nuclear Science and Techniques 33 (1) (2022) 9. doi:[10.1007/s41365-022-00992-5](https://doi.org/10.1007/s41365-022-00992-5).

URL <https://doi.org/10.1007/s41365-022-00992-5>

[64] M.-T. Tang, L.-J. Mao, H.-J. Lu, L.-X. Zhao, J. Li, X.-P. Sha, F. Ma, Y.-B. Zhou, K.-M. Yan, X.-M. Ma, X.-D. Yang, J.-C. Yang, [Design of an efficient collector for the HIAF electron cooling system](#), Nuclear Science and Techniques 32 (10) (2021) 116. doi:[10.1007/s41365-021-00949-0](https://doi.org/10.1007/s41365-021-00949-0).

URL <https://doi.org/10.1007/s41365-021-00949-0>

[65] P.-Y. Yu, B. Zhang, F.-F. Wang, C.-X. Li, G.-Z. Sun, Z.-J. Wang, L.-B. Liu, C.-Z. Yuan, Y. He, H.-S. Xu, [Fabrication and cold test of prototype of spatially periodic radio frequency quadrupole focusing linac](#), Nuclear Science and Techniques 32 (1) (2021) 8. doi:[10.1007/s41365-020-00835-1](https://doi.org/10.1007/s41365-020-00835-1).

URL <https://doi.org/10.1007/s41365-020-00835-1>

[66] L. Rezzolla, P. Pizzochero, D. I. Jones, N. Rea, I. Vidaña, [The Physics and Astrophysics of Neutron Stars](#), 1st Edition, no. XIX, 811 in Astrophysics and Space Science Library, Springer Cham, 2019.

URL <https://doi.org/10.1007/978-3-319-97616-7>

[67] S.-W. Lan, S.-S. Shi, [Anisotropic flow in high baryon density region](#), Nuclear Science and Techniques 33 (2) (2022) 21. doi:[10.1007/s41365-022-01006-0](https://doi.org/10.1007/s41365-022-01006-0).

URL <https://doi.org/10.1007/s41365-022-01006-0>

[68] Z. Yu, Z. Dingwei, L. Xiaofeng, Experimental study of the qcd phase diagram in relativistic

- heavy-ion collisions, Nuclear Techniques 46 (2023) 040001. doi:10.11889/j.0253-3219.2023.hjs.46.040001.
- [69] D. Hengtong, L. Shengtai, L. Junhong, Progress on qcd properties in strong magnetic fields from lattice qcd, Nuclear Techniques 46 (2023) 040008. doi:10.11889/j.0253-3219.2023.hjs.46.040008.
- [70] C. Qian, M. Guoliang, C. Jinhui, Transport model study of conserved charge fluctuations and qcd phase transition in heavy-ion collisions, Nuclear Techniques 46 (2023) 040013. doi:10.11889/j.0253-3219.2023.hjs.46.040013.
- [71] D. Yilun, L. Chengming, S. Chao, X. Shusheng, Y. Yan, Z. Zheng, Review of QCD phase diagram analysis using effective field theories, Nuclear Techniques 46 (2023) 040009. doi:10.11889/j.0253-3219.2023.hjs.46.040009.
- [72] K.-J. Sun, L.-W. Chen, C. M. Ko, F. Li, J. Xu, Z. Xu, Light nuclei production and qcd phase transition in heavy-ion collisions, Nuclear Techniques 46 (2023) 040012. doi:10.11889/j.0253-3219.2023.hjs.46.040012.
- [73] G. Bertsch, [The collision integral in nuclear matter at zero temperature](#), Zeitschrift für Physik A Atoms and Nuclei 289 (1) (1978) 103–105. doi:10.1007/BF01408501.
URL <https://doi.org/10.1007/BF01408501>
- [74] P. Danielewicz, [Transport properties of excited nuclear matter and the shock-wave profile](#), Physics Letters B 146 (3) (1984) 168–175. doi:[https://doi.org/10.1016/0370-2693\(84\)91010-4](https://doi.org/10.1016/0370-2693(84)91010-4).
URL <https://www.sciencedirect.com/science/article/pii/0370269384910104>
- [75] L. Shi, P. Danielewicz, [Nuclear isospin diffusivity](#), Phys. Rev. C 68 (2003) 064604. doi:10.1103/PhysRevC.68.064604.
URL <https://link.aps.org/doi/10.1103/PhysRevC.68.064604>
- [76] A. Muronga, [Shear viscosity coefficient from microscopic models](#), Phys. Rev. C 69 (2004) 044901. doi:10.1103/PhysRevC.69.044901.
URL <https://link.aps.org/doi/10.1103/PhysRevC.69.044901>
- [77] N. Demir, S. A. Bass, [Shear-viscosity to entropy-density ratio of a relativistic hadron gas](#), Phys. Rev. Lett. 102 (2009) 172302. doi:10.1103/PhysRevLett.102.172302.
URL <https://link.aps.org/doi/10.1103/PhysRevLett.102.172302>

- [78] S. X. Li, D. Q. Fang, Y. G. Ma, C. L. Zhou, [Shear viscosity to entropy density ratio in the Boltzmann-Uehling-Uhlenbeck model](#), Phys. Rev. C 84 (2011) 024607. doi:[10.1103/PhysRevC.84.024607](https://doi.org/10.1103/PhysRevC.84.024607).
URL <https://link.aps.org/doi/10.1103/PhysRevC.84.024607>
- [79] X. G. Deng, Y. G. Ma, M. Veselský, [Thermal and transport properties in central heavy-ion reactions around a few hundred MeV/nucleon](#), Phys. Rev. C 94 (2016) 044622. doi:[10.1103/PhysRevC.94.044622](https://doi.org/10.1103/PhysRevC.94.044622).
URL <https://link.aps.org/doi/10.1103/PhysRevC.94.044622>
- [80] D. Mondal, D. Pandit, S. Mukhopadhyay, S. Pal, B. Dey, S. Bhattacharya, A. De, S. Bhattacharya, S. Bhattacharyya, P. Roy, K. Banerjee, S. R. Banerjee, [Experimental determination of \$\eta/s\$ for finite nuclear matter](#), Phys. Rev. Lett. 118 (2017) 192501. doi:[10.1103/PhysRevLett.118.192501](https://doi.org/10.1103/PhysRevLett.118.192501).
URL <https://link.aps.org/doi/10.1103/PhysRevLett.118.192501>
- [81] T. Reichert, G. Inghirami, M. Bleicher, [A first estimate of \$\eta/s\$ in Au+Au reactions at Elab=1.23 AGeV](#), Physics Letters B 817 (2021) 136285. doi:<https://doi.org/10.1016/j.physletb.2021.136285>.
URL <https://www.sciencedirect.com/science/article/pii/S0370269321002252>
- [82] J. Xu, [Specific viscosity of neutron-rich nuclear matter from a relaxation time approach](#), Phys. Rev. C 84 (2011) 064603. doi:[10.1103/PhysRevC.84.064603](https://doi.org/10.1103/PhysRevC.84.064603).
URL <https://link.aps.org/doi/10.1103/PhysRevC.84.064603>
- [83] J. Xu, L.-W. Chen, C. M. Ko, B.-A. Li, Y. G. Ma, [Shear viscosity of neutron-rich nucleonic matter near its liquid-gas phase transition](#), Physics Letters B 727 (1) (2013) 244–248. doi:<https://doi.org/10.1016/j.physletb.2013.10.051>.
URL <https://www.sciencedirect.com/science/article/pii/S0370269313008587>
- [84] X. G. Deng, P. Danielewicz, Y. G. Ma, H. Lin, Y. X. Zhang, [Impact of fragment formation on shear viscosity in the nuclear liquid-gas phase transition region](#), Phys. Rev. C 105 (2022) 064613. doi:[10.1103/PhysRevC.105.064613](https://doi.org/10.1103/PhysRevC.105.064613).
URL <https://link.aps.org/doi/10.1103/PhysRevC.105.064613>
- [85] G. Bertsch, S. Das Gupta, [A guide to microscopic models for intermediate energy heavy ion collisions](#), Physics Reports 160 (4) (1988) 189–233. doi:[https://doi.org/10.1016/0370-1573\(88\)00000-0](https://doi.org/10.1016/0370-1573(88)00000-0)

- [86] J. Aichelin, “quantum” molecular dynamics—a dynamical microscopic n-body approach to investigate fragment formation and the nuclear equation of state in heavy ion collisions, *Physics Reports* 202 (5) (1991) 233–360. doi:[https://doi.org/10.1016/0370-1573\(91\)90094-3](https://doi.org/10.1016/0370-1573(91)90094-3).
URL <https://www.sciencedirect.com/science/article/pii/0370157391900943>
- [87] Y.-X. Zhang, Y.-J. Wang, M. Colonna, P. Danielewicz, A. Ono, M. B. Tsang, H. Wolter, J. Xu, L.-W. Chen, D. Cozma, Z.-Q. Feng, S. Das Gupta, N. Ikeno, C.-M. Ko, B.-A. Li, Q.-F. Li, Z.-X. Li, S. Mallik, Y. Nara, T. Ogawa, A. Ohnishi, D. Oliinychenko, M. Papa, H. Petersen, J. Su, T. Song, J. Weil, N. Wang, F.-S. Zhang, Z. Zhang, [Comparison of heavy-ion transport simulations: Collision integral in a box](#), *Phys. Rev. C* 97 (2018) 034625. doi:[10.1103/PhysRevC.97.034625](https://doi.org/10.1103/PhysRevC.97.034625).
URL <https://link.aps.org/doi/10.1103/PhysRevC.97.034625>
- [88] J. Xu, [Transport approaches for the description of intermediate-energy heavy-ion collisions](#), *Progress in Particle and Nuclear Physics* 106 (2019) 312–359. doi:<https://doi.org/10.1016/j.pnpnp.2019.02.009>.
URL <https://www.sciencedirect.com/science/article/pii/S0146641019300213>
- [89] M. Colonna, Y.-X. Zhang, Y.-J. Wang, D. Cozma, P. Danielewicz, C. M. Ko, A. Ono, M. B. Tsang, R. Wang, H. Wolter, J. Xu, Z. Zhang, L.-W. Chen, H.-G. Cheng, H. Elfner, Z.-Q. Feng, M. Kim, Y. Kim, S. Jeon, C.-H. Lee, B.-A. Li, Q.-F. Li, Z.-X. Li, S. Mallik, D. Oliinychenko, J. Su, T. Song, A. Sorensen, F.-S. Zhang, [Comparison of heavy-ion transport simulations: Mean-field dynamics in a box](#), *Phys. Rev. C* 104 (2021) 024603. doi:[10.1103/PhysRevC.104.024603](https://doi.org/10.1103/PhysRevC.104.024603).
URL <https://link.aps.org/doi/10.1103/PhysRevC.104.024603>
- [90] H. Wolter, M. Colonna, D. Cozma, P. Danielewicz, C. M. Ko, R. Kumar, A. Ono, M. B. Tsang, J. Xu, Y.-X. Zhang, E. Bratkovskaya, Z.-Q. Feng, T. Gaitanos, A. Le Fèvre, N. Ikeno, Y. Kim, S. Mallik, P. Napolitani, D. Oliinychenko, T. Ogawa, M. Papa, J. Su, R. Wang, Y.-J. Wang, J. Weil, F.-S. Zhang, G.-Q. Zhang, Z. Zhang, J. Aichelin, W. Cassing, L.-W. Chen, H.-G. Cheng, H. Elfner, K. Gallmeister, C. Hartnack, S. Hashimoto, S. Jeon, K. Kim, M. Kim, B.-A. Li, C.-H. Lee, Q.-F. Li, Z.-X. Li, U. Mosel, Y. Nara, K. Niita, A. Ohnishi, T. Sato, T. Song, A. Sorensen, N. Wang, W.-J. Xie, [Transport model comparison studies of intermediate-energy heavy-ion collisions](#), *Progress in Particle and Nuclear Physics* 125 (2022)

103962. doi:<https://doi.org/10.1016/j.ppnp.2022.103962>.

URL <https://www.sciencedirect.com/science/article/pii/S0146641022000230>

- [91] C. L. Zhou, Y. G. Ma, D. Q. Fang, G. Q. Zhang, *Thermodynamic properties and shear viscosity over entropy-density ratio of the nuclear fireball in a quantum-molecular dynamics model*, Phys. Rev. C 88 (2013) 024604. doi:[10.1103/PhysRevC.88.024604](https://doi.org/10.1103/PhysRevC.88.024604).
URL <https://link.aps.org/doi/10.1103/PhysRevC.88.024604>
- [92] C. Q. Guo, Y. G. Ma, W. B. He, X. G. Cao, D. Q. Fang, X. G. Deng, C. L. Zhou, *Isovector dipole resonance and shear viscosity in low energy heavy-ion collisions*, Phys. Rev. C 95 (2017) 054622. doi:[10.1103/PhysRevC.95.054622](https://doi.org/10.1103/PhysRevC.95.054622).
URL <https://link.aps.org/doi/10.1103/PhysRevC.95.054622>
- [93] P. Danielewicz, *Shoek waves in a hydrodynamic model of central heavy ion collisions*, Nuclear Physics A 314 (2) (1979) 465–484. doi:[https://doi.org/10.1016/0375-9474\(79\)90608-0](https://doi.org/10.1016/0375-9474(79)90608-0).
URL <https://www.sciencedirect.com/science/article/pii/0375947479906080>
- [94] J. Pochodzalla, T. Möhlenkamp, T. Rubehn, A. Schüttauf, A. Wörner, E. Zude, M. Begemann-Blaich, T. Blaich, H. Emling, A. Ferrero, C. Gross, G. Immé, I. Iori, G. J. Kunde, W. D. Kunze, V. Lindenstruth, U. Lynen, A. Moroni, W. F. J. Müller, B. Ocker, G. Raciti, H. Sann, C. Schwarz, W. Seidel, V. Serfling, J. Stroth, W. Trautmann, A. Trzcinski, A. Tucholski, G. Verde, B. Zwieglinski, *Probing the nuclear liquid-gas phase transition*, Phys. Rev. Lett. 75 (1995) 1040–1043. doi:[10.1103/PhysRevLett.75.1040](https://doi.org/10.1103/PhysRevLett.75.1040).
URL <https://link.aps.org/doi/10.1103/PhysRevLett.75.1040>
- [95] J. B. Natowitz, R. Wada, K. Hagel, T. Keutgen, M. Murray, A. Makeev, L. Qin, P. Smith, C. Hamilton, *Caloric curves and critical behavior in nuclei*, Phys. Rev. C 65 (2002) 034618. doi:[10.1103/PhysRevC.65.034618](https://doi.org/10.1103/PhysRevC.65.034618).
URL <https://link.aps.org/doi/10.1103/PhysRevC.65.034618>
- [96] Y. G. Ma, *Application of information theory in nuclear liquid gas phase transition*, Phys. Rev. Lett. 83 (1999) 3617–3620. doi:[10.1103/PhysRevLett.83.3617](https://doi.org/10.1103/PhysRevLett.83.3617).
URL <https://link.aps.org/doi/10.1103/PhysRevLett.83.3617>
- [97] Y. G. Ma, J. B. Natowitz, R. Wada, K. Hagel, J. Wang, T. Keutgen, Z. Majka, M. Murray, L. Qin, P. Smith, R. Alfaro, J. Cibor, M. Cinausero, Y. E. Masri, D. Fabris, E. Fioretto, A. Keksis, M. Lunardon, A. Makeev, N. Marie, E. Martin, A. Martinez-Davalos, A. Menchaca-Rocha,

- G. Nebbia, G. Prete, V. Rizzi, A. Ruangma, D. V. Shetty, G. Souliotis, P. Staszal, M. Veselsky, G. Viesti, E. M. Winchester, S. J. Yennello, [Critical behavior in light nuclear systems: Experimental aspects](#), Phys. Rev. C 71 (2005) 054606. doi:[10.1103/PhysRevC.71.054606](https://doi.org/10.1103/PhysRevC.71.054606).
URL <https://link.aps.org/doi/10.1103/PhysRevC.71.054606>
- [98] B. Borderie, J. Frankland, [Liquid–gas phase transition in nuclei](#), Progress in Particle and Nuclear Physics 105 (2019) 82–138. doi:<https://doi.org/10.1016/j.ppnp.2018.12.002>.
URL <https://www.sciencedirect.com/science/article/pii/S0146641018301030>
- [99] R. Wang, Y.-G. Ma, R. Wada, L.-W. Chen, W.-B. He, H.-L. Liu, K.-J. Sun, [Nuclear liquid–gas phase transition with machine learning](#), Phys. Rev. Res. 2 (2020) 043202. doi:[10.1103/PhysRevResearch.2.043202](https://doi.org/10.1103/PhysRevResearch.2.043202).
URL <https://link.aps.org/doi/10.1103/PhysRevResearch.2.043202>
- [100] C. Liu, X.-G. Deng, Y.-G. Ma, [Density fluctuations in intermediate-energy heavy-ion collisions](#), Nuclear Science and Techniques 33 (5) (2022) 52. doi:[10.1007/s41365-022-01040-y](https://doi.org/10.1007/s41365-022-01040-y).
URL <https://doi.org/10.1007/s41365-022-01040-y>
- [101] H. Caines, [The search for critical behavior and other features of the QCD phase diagram – current status and future prospects](#), Nuclear Physics A 967 (2017) 121–128, the 26th International Conference on Ultra-relativistic Nucleus-Nucleus Collisions: Quark Matter 2017. doi:<https://doi.org/10.1016/j.nuclphysa.2017.05.116>.
URL <https://www.sciencedirect.com/science/article/pii/S0375947417302580>
- [102] D. C. Zhang, H. G. Cheng, Z. Q. Feng, [Hyperon dynamics in heavy-ion collisions near threshold energy](#), Chin. Phys. Lett. 38 (2021) 092501. doi:[10.1088/0256-307X/38/9/092501](https://doi.org/10.1088/0256-307X/38/9/092501).
- [103] Y.-G. Ma, [Hypernuclei as a laboratory to test hyperon–nucleon interactions](#), Nuclear Science and Techniques 34 (6) (2023) 97. doi:[10.1007/s41365-023-01248-6](https://doi.org/10.1007/s41365-023-01248-6).
URL <https://doi.org/10.1007/s41365-023-01248-6>
- [104] J. Y. Jia, G. Giacalone, C. J. Zhang, [Precision tests of the nonlinear mode coupling of anisotropic flow via high-energy collisions of isobars](#), Chin. Phys. Lett. 40 (2023) 042501. doi:[10.1088/0256-307X/40/4/042501](https://doi.org/10.1088/0256-307X/40/4/042501).
- [105] Y.-G. Ma, [New type of double-slit interference experiment at fermi scale](#), Nuclear Science and Techniques 34 (1) (2023) 16. doi:[10.1007/s41365-023-01167-6](https://doi.org/10.1007/s41365-023-01167-6).
URL <https://doi.org/10.1007/s41365-023-01167-6>

- [106] J.-W. Chen, Y.-H. Li, Y.-F. Liu, E. Nakano, *QCD viscosity to entropy density ratio in the hadronic phase*, Phys. Rev. D 76 (2007) 114011. doi:[10.1103/PhysRevD.76.114011](https://doi.org/10.1103/PhysRevD.76.114011).
URL <https://link.aps.org/doi/10.1103/PhysRevD.76.114011>
- [107] H. B. Meyer, *Density, short-range order, and the quark-gluon plasma*, Phys. Rev. D 79 (2009) 011502. doi:[10.1103/PhysRevD.79.011502](https://doi.org/10.1103/PhysRevD.79.011502).
URL <https://link.aps.org/doi/10.1103/PhysRevD.79.011502>
- [108] S. Ghosh, A. Lahiri, S. Majumder, R. Ray, S. K. Ghosh, *Shear viscosity due to Landau damping from the quark-pion interaction*, Phys. Rev. C 88 (2013) 068201. doi:[10.1103/PhysRevC.88.068201](https://doi.org/10.1103/PhysRevC.88.068201).
URL <https://link.aps.org/doi/10.1103/PhysRevC.88.068201>
- [109] P. Danielewicz, B. Barker, L. Shi, *From stopping to viscosity in nuclear reactions*, AIP Conference Proceedings 1128 (1) (2009) 104–111. arXiv:<https://aip.scitation.org/doi/pdf/10.1063/1.3146204>, doi:[10.1063/1.3146204](https://doi.org/10.1063/1.3146204).
URL <https://aip.scitation.org/doi/abs/10.1063/1.3146204>
- [110] J. Ryckaert, A. Bellemans, G. Ciccotti, G. V. Paolini, *Evaluation of transport coefficients of simple fluids by molecular dynamics: Comparison of Green-Kubo and nonequilibrium approaches for shear viscosity.*, Phys. Rev. C 39 (1989) 259–267. doi:[10.1103/physreva.39.259](https://doi.org/10.1103/physreva.39.259).
URL <https://link.aps.org/doi/10.1103/physreva.39.259>
- [111] B. Hess, *Determining the shear viscosity of model liquids from molecular dynamics simulations*, The Journal of Chemical Physics 116 (1) (2002) 209–217. arXiv:<https://aip.scitation.org/doi/pdf/10.1063/1.1421362>, doi:[10.1063/1.1421362](https://doi.org/10.1063/1.1421362).
URL <https://aip.scitation.org/doi/abs/10.1063/1.1421362>
- [112] K. Paech, S. Pratt, *Origins of bulk viscosity in relativistic heavy ion collisions*, Phys. Rev. C 74 (2006) 014901. doi:[10.1103/PhysRevC.74.014901](https://doi.org/10.1103/PhysRevC.74.014901).
URL <https://link.aps.org/doi/10.1103/PhysRevC.74.014901>
- [113] D. J. Evans, G. Morriss, *Statistical mechanics of nonequilibrium liquids*, 2nd Edition, Cambridge University Press, 2008. doi:[10.1017/CB09780511535307](https://doi.org/10.1017/CB09780511535307).
- [114] A. Hosoya, M. aki Sakagami, M. Takao, *Nonequilibrium thermodynamics in field theory: Transport coefficients*, Annals of Physics 154 (1) (1984) 229–252. doi:<https://doi.org/10.1016/>

0003-4916(84)90144-1.

URL <https://www.sciencedirect.com/science/article/pii/0003491684901441>

- [115] X. G. Deng, Y. G. Ma, Y. X. Zhang, *Green–Kubo formula for Boltzmann and Fermi–Dirac statistics*, The European Physical Journal A 57 (7) (2021) 242. doi:10.1140/epja/s10050-021-00550-4.
URL <https://doi.org/10.1140/epja/s10050-021-00550-4>
- [116] A. A. Abrikosov, I. M. Khalatnikov, *The theory of a fermi liquid (the properties of liquid ^3He at low temperatures)*, Reports on Progress in Physics 22 (1) (1959) 329. doi:10.1088/0034-4885/22/1/310.
URL <https://dx.doi.org/10.1088/0034-4885/22/1/310>
- [117] L. P. Kadanoff, P. C. Martin, *Hydrodynamic equations and correlation functions*, Annals of Physics 24 (1963) 419–469. doi:[https://doi.org/10.1016/0003-4916\(63\)90078-2](https://doi.org/10.1016/0003-4916(63)90078-2).
URL <https://www.sciencedirect.com/science/article/pii/0003491663900782>
- [118] A. Ito, H. Nakamura, *Calculation of microscopic stress tensor with non-equilibrium molecular dynamics*, Theoretical and Applied Mechanics Japan 57 (2009) 159–167. doi:10.11345/nctam.57.159.
- [119] D. J. Evans, G. Morriss, *Statistical Mechanics of Nonequilibrium Liquids*, 2nd Edition, Cambridge University Press, 2008.
URL <https://doi.org/10.1017/CB09780511535307>
- [120] S. Chapman, T. G. Cowling, *The Mathematical Theory of Non-uniform Gases*, Cambridge University Press, Cambridge, UK, 1952.
- [121] N. M. MacKay, Z.-W. Lin, *The shear viscosity of parton matter under anisotropic scatterings*, The European Physical Journal C 82 (10) (2022) 918. doi:10.1140/epjc/s10052-022-10892-y.
URL <https://doi.org/10.1140/epjc/s10052-022-10892-y>
- [122] E. A. Uehling, G. E. Uhlenbeck, *Transport phenomena in Einstein-Bose and Fermi-Dirac gases. I*, Phys. Rev. 43 (1933) 552–561. doi:10.1103/PhysRev.43.552.
URL <https://link.aps.org/doi/10.1103/PhysRev.43.552>
- [123] D. Davesne, *Transport coefficients of a hot pion gas*, Phys. Rev. C 53 (1996) 3069–3084. doi:

[10.1103/PhysRevC.53.3069](https://doi.org/10.1103/PhysRevC.53.3069).

URL <https://link.aps.org/doi/10.1103/PhysRevC.53.3069>

[124] P. Chakraborty, J. I. Kapusta, [Quasiparticle theory of shear and bulk viscosities of hadronic matter](#), Phys. Rev. C 83 (2011) 014906. doi:[10.1103/PhysRevC.83.014906](https://doi.org/10.1103/PhysRevC.83.014906).

URL <https://link.aps.org/doi/10.1103/PhysRevC.83.014906>

[125] B. Barker, P. Danielewicz, [Shear viscosity from nuclear stopping](#), Phys. Rev. C 99 (2019) 034607. doi:[10.1103/PhysRevC.99.034607](https://doi.org/10.1103/PhysRevC.99.034607).

URL <https://link.aps.org/doi/10.1103/PhysRevC.99.034607>

[126] A. Wiranata, M. Prakash, [Shear viscosities from the Chapman-Enskog and the relaxation time approaches](#), Phys. Rev. C 85 (2012) 054908. doi:[10.1103/PhysRevC.85.054908](https://doi.org/10.1103/PhysRevC.85.054908).

URL <https://link.aps.org/doi/10.1103/PhysRevC.85.054908>

[127] S. Plumari, A. Puglisi, F. Scardina, V. Greco, [Shear viscosity of a strongly interacting system: Green-Kubo correlator versus Chapman-Enskog and relaxation-time approximations](#), Phys. Rev. C 86 (2012) 054902. doi:[10.1103/PhysRevC.86.054902](https://doi.org/10.1103/PhysRevC.86.054902).

URL <https://link.aps.org/doi/10.1103/PhysRevC.86.054902>

[128] C. Wesp, A. El, F. Reining, Z. Xu, I. Bouras, C. Greiner, [Calculation of shear viscosity using green-kubo relations within a parton cascade](#), Phys. Rev. C 84 (2011) 054911. doi:[10.1103/PhysRevC.84.054911](https://doi.org/10.1103/PhysRevC.84.054911).

URL <https://link.aps.org/doi/10.1103/PhysRevC.84.054911>

[129] J.-B. Rose, J. M. Torres-Rincon, A. Schäfer, D. R. Oliinychenko, H. Petersen, [Shear viscosity of a hadron gas and influence of resonance lifetimes on relaxation time](#), Phys. Rev. C 97 (2018) 055204. doi:[10.1103/PhysRevC.97.055204](https://doi.org/10.1103/PhysRevC.97.055204).

URL <https://link.aps.org/doi/10.1103/PhysRevC.97.055204>

[130] N. Auerbach, A. Yeverechyahu, [Nuclear viscosity and widths of giant resonances](#), Annals of Physics 95 (1) (1975) 35–52. doi:[https://doi.org/10.1016/0003-4916\(75\)90042-1](https://doi.org/10.1016/0003-4916(75)90042-1).

URL <https://www.sciencedirect.com/science/article/pii/0003491675900421>

[131] K. T. R. Davies, A. J. Sierk, J. R. Nix, [Effect of viscosity on the dynamics of fission](#), Phys. Rev. C 13 (1976) 2385–2403. doi:[10.1103/PhysRevC.13.2385](https://doi.org/10.1103/PhysRevC.13.2385).

URL <https://link.aps.org/doi/10.1103/PhysRevC.13.2385>

- [132] K. T. R. Davies, R. A. Managan, J. R. Nix, A. J. Sierk, Rupture of the neck in nuclear fission, Phys. Rev. C 16 (1977) 1890–1901. doi:10.1103/PhysRevC.16.1890.
URL <https://link.aps.org/doi/10.1103/PhysRevC.16.1890>
- [133] J. R. Nix, A. J. Sierk, Macroscopic description of isoscalar giant multipole resonances, Phys. Rev. C 21 (1980) 396–404. doi:10.1103/PhysRevC.21.396.
URL <https://link.aps.org/doi/10.1103/PhysRevC.21.396>
- [134] N. Dinh Dang, Shear-viscosity to entropy-density ratio from giant dipole resonances in hot nuclei, Phys. Rev. C 84 (2011) 034309. doi:10.1103/PhysRevC.84.034309.
URL <https://link.aps.org/doi/10.1103/PhysRevC.84.034309>
- [135] Y. Kikuchi, K. Tsumura, T. Kunihiro, Mesoscopic dynamics of fermionic cold atoms — quantitative analysis of transport coefficients and relaxation times, Physics Letters A 380 (24) (2016) 2075–2080. doi:<https://doi.org/10.1016/j.physleta.2016.04.027>.
URL <https://www.sciencedirect.com/science/article/pii/S0375960116301104>
- [136] P. Danielewicz, G. F. Bertsch, Production of deuterons and pions in a transport model of energetic heavy-ion reactions, Nuclear Physics A 533 (4) (1991) 712–748. doi:[https://doi.org/10.1016/0375-9474\(91\)90541-D](https://doi.org/10.1016/0375-9474(91)90541-D).
URL <https://www.sciencedirect.com/science/article/pii/037594749190541D>
- [137] P. Danielewicz, Q. Pan, Blast of light fragments from central heavy-ion collisions, Phys. Rev. C 46 (1992) 2002–2011. doi:10.1103/PhysRevC.46.2002.
URL <https://link.aps.org/doi/10.1103/PhysRevC.46.2002>
- [138] Q. Pan, P. Danielewicz, From sideward flow to nuclear compressibility, Phys. Rev. Lett. 70 (1993) 2062–2065. doi:10.1103/PhysRevLett.70.2062.
URL <https://link.aps.org/doi/10.1103/PhysRevLett.70.2062>
- [139] P. Danielewicz, Determination of the mean-field momentum-dependence using elliptic flow, Nuclear Physics A 673 (1) (2000) 375–410. doi:[https://doi.org/10.1016/S0375-9474\(00\)00083-X](https://doi.org/10.1016/S0375-9474(00)00083-X).
URL <https://www.sciencedirect.com/science/article/pii/S037594740000083X>
- [140] T. Alm, G. Röpke, M. Schmidt, Critical enhancement of the in-medium nucleon-nucleon cross section at low temperatures, Phys. Rev. C 50 (1994) 31–37. doi:10.1103/PhysRevC.50.31.
URL <https://link.aps.org/doi/10.1103/PhysRevC.50.31>

- [141] C. Fuchs, A. Faessler, M. El-Shabshiry, [Off-shell behavior of the in-medium nucleon-nucleon cross section](#), Phys. Rev. C 64 (2001) 024003. doi:[10.1103/PhysRevC.64.024003](https://doi.org/10.1103/PhysRevC.64.024003).
URL <https://link.aps.org/doi/10.1103/PhysRevC.64.024003>
- [142] W. Reisdorf, M. Stockmeier, A. Andronic, M. L. Benabderrahmane, O. Hartmann, N. Herrmann, K. Hildenbrand, Y. Kim, M. Kiš, P. Koczoń, T. Kress, Y. Leifels, X. Lopez, M. Merschmeyer, A. Schüttauf, V. Barret, Z. Basrak, N. Bastid, R. Čaplar, P. Crochet, P. Dupieux, M. Dželalija, Z. Fodor, Y. Grishkin, B. Hong, T. Kang, J. Kecskemeti, M. Kirejczyk, M. Korolija, R. Kotte, A. Lebedev, T. Matulewicz, W. Neubert, M. Petrovici, F. Rami, M. Ryu, Z. Seres, B. Sikora, K. Sim, V. Simion, K. Siwek-Wilczyńska, V. Smolyankin, G. Stoicea, Z. Tymiński, K. Wiśniewski, D. Wohlfarth, Z. Xiao, H. Xu, I. Yushmanov, A. Zhilin, [Systematics of pion emission in heavy ion collisions in the 1A GeV regime](#), Nuclear Physics A 781 (3) (2007) 459–508. doi:<https://doi.org/10.1016/j.nuclphysa.2006.10.085>.
URL <https://www.sciencedirect.com/science/article/pii/S0375947406007676>
- [143] W. Reisdorf, A. Andronic, R. Averbeck, M. L. Benabderrahmane, O. Hartmann, N. Herrmann, K. Hildenbrand, T. Kang, Y. Kim, M. Kiš, P. Koczoń, T. Kress, Y. Leifels, M. Merschmeyer, K. Piasecki, A. Schüttauf, M. Stockmeier, V. Barret, Z. Basrak, N. Bastid, R. Čaplar, P. Crochet, P. Dupieux, M. Dželalija, Z. Fodor, P. Gasik, Y. Grishkin, B. Hong, J. Kecskemeti, M. Kirejczyk, M. Korolija, R. Kotte, A. Lebedev, X. Lopez, T. Matulewicz, W. Neubert, M. Petrovici, F. Rami, M. Ryu, Z. Seres, B. Sikora, K. Sim, V. Simion, K. Siwek-Wilczyńska, V. Smolyankin, G. Stoicea, Z. Tymiński, K. Wiśniewski, D. Wohlfarth, Z. Xiao, H. Xu, I. Yushmanov, A. Zhilin, [Systematics of central heavy ion collisions in the 1 A GeV regime](#), Nuclear Physics A 848 (3) (2010) 366–427. doi:<https://doi.org/10.1016/j.nuclphysa.2010.09.008>.
URL <https://www.sciencedirect.com/science/article/pii/S0375947410006810>
- [144] J. Xu, L.-W. Chen, B.-A. Li, H.-R. Ma, [Effects of isospin and momentum dependent interactions on liquid–gas phase transition in hot asymmetric nuclear matter](#), Physics Letters B 650 (5) (2007) 348–353. doi:<https://doi.org/10.1016/j.physletb.2007.05.035>.
URL <https://www.sciencedirect.com/science/article/pii/S0370269307006132>
- [145] K. A. Bugaev, M. I. Gorenstein, I. N. Mishustin, W. Greiner, [Statistical multifragmentation in thermodynamic limit](#), Physics Letters B 498 (3) (2001) 144–148. doi:[10.1016/S0370-2693\(00\)01374-5](https://doi.org/10.1016/S0370-2693(00)01374-5).
URL <https://www.sciencedirect.com/science/article/pii/S0370269300013745>

- [146] B. Borderie, J. Frankland, [Liquid–gas phase transition in nuclei](#), *Progress in Particle and Nuclear Physics* 105 (2019) 82–138. doi:<https://doi.org/10.1016/j.pnpnp.2018.12.002>.
URL <https://www.sciencedirect.com/science/article/pii/S0146641018301030>
- [147] Y. Zhang, Z. Li, [Elliptic flow and system size dependence of transition energies at intermediate energies](#), *Phys. Rev. C* 74 (2006) 014602. doi:[10.1103/PhysRevC.74.014602](https://doi.org/10.1103/PhysRevC.74.014602).
URL <https://link.aps.org/doi/10.1103/PhysRevC.74.014602>
- [148] N. Wang, T. Wu, J. Zeng, Y. Yang, L. Ou, [Improvement on fermionic properties and new isotope production in molecular dynamics simulations](#), *Journal of Physics G: Nuclear and Particle Physics* 43 (6) (2016) 065101. doi:[10.1088/0954-3899/43/6/065101](https://doi.org/10.1088/0954-3899/43/6/065101).
URL <https://dx.doi.org/10.1088/0954-3899/43/6/065101>
- [149] J. Dey, S. Satapathy, A. Mishra, S. Paul, S. Ghosh, [From noninteracting to interacting picture of quark–gluon plasma in the presence of a magnetic field and its fluid property](#), *International Journal of Modern Physics E* 30 (06) (2021) 2150044. arXiv:<https://doi.org/10.1142/S0218301321500440>, doi:[10.1142/S0218301321500440](https://doi.org/10.1142/S0218301321500440).
URL <https://doi.org/10.1142/S0218301321500440>
- [150] C. Sasaki, K. Redlich, [Transport coefficients near chiral phase transition](#), *Nuclear Physics A* 832 (1) (2010) 62–75. doi:<https://doi.org/10.1016/j.nuclphysa.2009.11.005>.
URL <https://www.sciencedirect.com/science/article/pii/S0375947409008963>
- [151] R. Marty, E. Bratkovskaya, W. Cassing, J. Aichelin, H. Berrehrach, [Transport coefficients from the Nambu–Jona-Lasinio model for \$SU\(3\)_f\$](#) , *Phys. Rev. C* 88 (2013) 045204. doi:[10.1103/PhysRevC.88.045204](https://doi.org/10.1103/PhysRevC.88.045204).
URL <https://link.aps.org/doi/10.1103/PhysRevC.88.045204>
- [152] P. Deb, G. P. Kadam, H. Mishra, [Estimating transport coefficients in hot and dense quark matter](#), *Phys. Rev. D* 94 (2016) 094002. doi:[10.1103/PhysRevD.94.094002](https://doi.org/10.1103/PhysRevD.94.094002).
URL <https://link.aps.org/doi/10.1103/PhysRevD.94.094002>
- [153] J. Dias de Deus, A. S. Hirsch, C. Pajares, R. P. Scharenberg, B. K. Srivastava, [Clustering of color sources and the shear viscosity of the QGP in heavy ion collisions at RHIC and LHC energies](#), *The European Physical Journal C* 72 (8) (2012) 2123. doi:[10.1140/epjc/s10052-012-2123-x](https://doi.org/10.1140/epjc/s10052-012-2123-x).
URL <https://doi.org/10.1140/epjc/s10052-012-2123-x>

- [154] D. Q. Fang, Y. G. Ma, C. L. Zhou, [Shear viscosity of hot nuclear matter by the mean free path method](#), Phys. Rev. C 89 (2014) 047601. doi:[10.1103/PhysRevC.89.047601](https://doi.org/10.1103/PhysRevC.89.047601).
URL <https://link.aps.org/doi/10.1103/PhysRevC.89.047601>
- [155] K. Itakura, O. Morimatsu, H. Otomo, [Shear viscosity of a hadronic gas mixture](#), Phys. Rev. D 77 (2008) 014014. doi:[10.1103/PhysRevD.77.014014](https://doi.org/10.1103/PhysRevD.77.014014).
URL <https://link.aps.org/doi/10.1103/PhysRevD.77.014014>
- [156] N. Auerbach, S. Shlomo, [\$\eta/s\$ ratio in finite nuclei](#), Phys. Rev. Lett. 103 (2009) 172501. doi:[10.1103/PhysRevLett.103.172501](https://doi.org/10.1103/PhysRevLett.103.172501).
URL <https://link.aps.org/doi/10.1103/PhysRevLett.103.172501>
- [157] D. T. Khoa, N. Ohtsuka, A. Faessler, M. Matin, S. Huang, E. Lehmann, Y. Lofty, [Microscopic study of thermal properties of the nuclear matter formed in heavy-ion collisions](#), Nuclear Physics A 542 (4) (1992) 671–698. doi:[https://doi.org/10.1016/0375-9474\(92\)90263-J](https://doi.org/10.1016/0375-9474(92)90263-J).
URL <https://www.sciencedirect.com/science/article/pii/037594749290263J>
- [158] C. L. Zhou, Y. G. Ma, D. Q. Fang, G. Q. Zhang, J. Xu, X. G. Cao, W. Q. Shen, [Correlation between elliptic flow and shear viscosity in intermediate-energy heavy-ion collisions](#), Phys. Rev. C 90 (2014) 057601. doi:[10.1103/PhysRevC.90.057601](https://doi.org/10.1103/PhysRevC.90.057601).
URL <https://link.aps.org/doi/10.1103/PhysRevC.90.057601>
- [159] U. Heinz, R. Snellings, [Collective flow and viscosity in relativistic heavy-ion collisions](#), Annual Review of Nuclear and Particle Science 63 (1) (2013) 123–151. arXiv:<https://doi.org/10.1146/annurev-nucl-102212-170540>, doi:[10.1146/annurev-nucl-102212-170540](https://doi.org/10.1146/annurev-nucl-102212-170540).
URL <https://doi.org/10.1146/annurev-nucl-102212-170540>
- [160] The BRAHMS Collaboration, [Quark-gluon plasma and color glass condensate at RHIC? the perspective from the BRAHMS experiment](#), Nuclear Physics A 757 (1) (2005) 1–27, first Three Years of Operation of RHIC. doi:<https://doi.org/10.1016/j.nuclphysa.2005.02.130>.
URL <https://www.sciencedirect.com/science/article/pii/S0375947405002770>
- [161] M. Gyulassy, L. McLerran, [New forms of QCD matter discovered at RHIC](#), Nuclear Physics A 750 (1) (2005) 30–63, quark-Gluon Plasma. New Discoveries at RHIC: Case for the Strongly Interacting Quark-Gluon Plasma. Contributions from the RBRC Workshop held May 14-15, 2004. doi:<https://doi.org/10.1016/j.nuclphysa.2004.10.034>.
URL <https://www.sciencedirect.com/science/article/pii/S0375947404011480>

- [162] H. Zheng, A. Bonasera, [Density and temperature of fermions from quantum fluctuations](#), *Physics Letters B* 696 (1) (2011) 178–181. doi:<https://doi.org/10.1016/j.physletb.2010.12.019>. URL <https://www.sciencedirect.com/science/article/pii/S0370269310013663>
- [163] H. Zheng, A. Bonasera, [Higher order corrections to density and temperature of fermions from quantum fluctuations](#), *Phys. Rev. C* 86 (2012) 027602. doi:[10.1103/PhysRevC.86.027602](https://doi.org/10.1103/PhysRevC.86.027602). URL <https://link.aps.org/doi/10.1103/PhysRevC.86.027602>
- [164] E. Lifshitz, [PREFACE TO THE THIRD RUSSIAN EDITION](#), in: L. LANDAU, E. LIFSHITZ (Eds.), *Statistical Physics (Third Edition)*, third edition Edition, Butterworth-Heinemann, Oxford, 1980, pp. xiii–xiv. doi:<https://doi.org/10.1016/B978-0-08-057046-4.50004-X>. URL <https://www.sciencedirect.com/science/article/pii/B978008057046450004X>
- [165] Y. G. Ma, W. Q. Shen, [Onset of multifragmentation in intermediate energy light asymmetrical collisions](#), *Phys. Rev. C* 51 (1995) 710–715. doi:[10.1103/PhysRevC.51.710](https://doi.org/10.1103/PhysRevC.51.710). URL <https://link.aps.org/doi/10.1103/PhysRevC.51.710>
- [166] H. L. Liu, Y. G. Ma, A. Bonasera, X. G. Deng, O. Lopez, M. Veselský, [Mean free path and shear viscosity in central \$^{129}\text{Xe} + ^{119}\text{Sn}\$ collisions below 100 mev/nucleon](#), *Phys. Rev. C* 96 (2017) 064604. doi:[10.1103/PhysRevC.96.064604](https://doi.org/10.1103/PhysRevC.96.064604). URL <https://link.aps.org/doi/10.1103/PhysRevC.96.064604>
- [167] V. Kolomietz, S. Shlomo, [Nuclear fermi-liquid drop model](#), *Physics Reports* 390 (3) (2004) 133–233. doi:<https://doi.org/10.1016/j.physrep.2003.10.013>. URL <https://www.sciencedirect.com/science/article/pii/S0370157303004368>
- [168] N. D. Dang, A. Arima, [Quantal and thermal dampings of giant dipole resonances in \$^{90}\text{Zr}\$, \$^{120}\text{Sn}\$, and \$^{208}\text{Pb}\$](#) , *Phys. Rev. Lett.* 80 (1998) 4145–4148. doi:[10.1103/PhysRevLett.80.4145](https://doi.org/10.1103/PhysRevLett.80.4145). URL <https://link.aps.org/doi/10.1103/PhysRevLett.80.4145>
- [169] Nguyen Dinh Dang, A. Arima, [Temperature dependence of quantal and thermal dampings of the hot giant dipole resonance](#), *Nuclear Physics A* 636 (4) (1998) 427–451. doi:[https://doi.org/10.1016/S0375-9474\(98\)00211-5](https://doi.org/10.1016/S0375-9474(98)00211-5). URL <https://www.sciencedirect.com/science/article/pii/S0375947498002115>
- [170] N. D. Dang, A. Arima, [Pairing effect on the giant dipole resonance width at low temperature](#), *Phys. Rev. C* 68 (2003) 044303. doi:[10.1103/PhysRevC.68.044303](https://doi.org/10.1103/PhysRevC.68.044303). URL <https://link.aps.org/doi/10.1103/PhysRevC.68.044303>

- [171] Z. M. Drebi, K. A. Snover, A. W. Charlop, M. S. Kaplan, D. P. Wells, D. Ye, Y. Alhassid, [Spin-induced shape changes in light-medium mass compound nuclei](#), Phys. Rev. C 52 (1995) 578–594. doi:10.1103/PhysRevC.52.578.
URL <https://link.aps.org/doi/10.1103/PhysRevC.52.578>
- [172] M. Kicińska Habior, K. A. Snover, C. A. Gossett, J. A. Behr, G. Feldman, H. K. Glatzel, J. H. Gundlach, E. F. Garman, [Statistical giant dipole resonance decay of highly excited states of \$^{63}\text{Cu}\$](#) , Phys. Rev. C 36 (1987) 612–627. doi:10.1103/PhysRevC.36.612.
URL <https://link.aps.org/doi/10.1103/PhysRevC.36.612>
- [173] T. Baumann, E. Ramakrishnan, A. Azhari, J. Beene, R. Charity, J. Dempsey, M. Halbert, P.-F. Hua, R. Kryger, P. Mueller, R. Pfaff, D. Sarantites, L. Sobotka, D. Stracener, M. Thoennessen, G. Van Buren, R. Varner, S. Yokoyama, [Evolution of the giant dipole resonance in excited \$^{120}\text{Sn}\$ and \$^{208}\text{Pb}\$ nuclei populated by inelastic alpha scattering](#), Nuclear Physics A 635 (4) (1998) 428–445. doi:[https://doi.org/10.1016/S0375-9474\(98\)00197-3](https://doi.org/10.1016/S0375-9474(98)00197-3).
URL <https://www.sciencedirect.com/science/article/pii/S0375947498001973>
- [174] A. Bracco, J. J. Gaardhøje, A. M. Bruce, J. D. Garrett, B. Herskind, M. Pignanelli, D. Barnéoud, H. Nifenecker, J. A. Pinston, C. Ristori, F. Schussler, J. Bacelar, H. Hofmann, [Saturation of the width of the giant dipole resonance at high temperature](#), Phys. Rev. Lett. 62 (1989) 2080–2083. doi:10.1103/PhysRevLett.62.2080.
URL <https://link.aps.org/doi/10.1103/PhysRevLett.62.2080>
- [175] G. Enders, F. D. Berg, K. Hagel, W. Kühn, V. Metag, R. Novotny, M. Pfeiffer, O. Schwalb, R. J. Charity, A. Gobbi, R. Freifelder, W. Henning, K. D. Hildenbrand, R. Holzmann, R. S. Mayer, R. S. Simon, J. P. Wessels, G. Casini, A. Olmi, A. A. Stefanini, [Excitation-energy dependence of the giant dipole resonance width](#), Phys. Rev. Lett. 69 (1992) 249–252. doi:10.1103/PhysRevLett.69.249.
URL <https://link.aps.org/doi/10.1103/PhysRevLett.69.249>
- [176] P. Heckman, D. Bazin, J. Beene, Y. Blumenfeld, M. Chromik, M. Halbert, J. Liang, E. Mohrmann, T. Nakamura, A. Navin, B. Sherrill, K. Snover, M. Thoennessen, E. Tryggestad, R. Varner, [Low-temperature measurement of the giant dipole resonance width](#), Physics Letters B 555 (1) (2003) 43–48. doi:[https://doi.org/10.1016/S0370-2693\(03\)00017-0](https://doi.org/10.1016/S0370-2693(03)00017-0).
URL <https://www.sciencedirect.com/science/article/pii/S0370269303000170>

- [177] M. P. Kelly, K. A. Snover, J. P. S. van Schagen, M. Kicińska Habior, Z. Trznadel, [Giant dipole resonance in highly excited nuclei: Does the width saturate?](#), Phys. Rev. Lett. 82 (1999) 3404–3407. doi:10.1103/PhysRevLett.82.3404.
URL <https://link.aps.org/doi/10.1103/PhysRevLett.82.3404>
- [178] D. R. Chakrabarty, M. Thoennessen, N. Alamanos, P. Paul, S. Sen, [Evidence for prolate deformation in highly excited neutron-deficient Pb isotopes](#), Phys. Rev. Lett. 58 (1987) 1092–1095. doi:10.1103/PhysRevLett.58.1092.
URL <https://link.aps.org/doi/10.1103/PhysRevLett.58.1092>
- [179] S. Bhattacharya, D. Pandit, B. Dey, D. Mondal, S. Mukhopadhyay, S. Pal, A. De, S. R. Banerjee, [Effect of high angular momentum on \$\eta/s\$ of nuclear matter](#), Phys. Rev. C 103 (2021) 014305. doi:10.1103/PhysRevC.103.014305.
URL <https://link.aps.org/doi/10.1103/PhysRevC.103.014305>
- [180] S. A. Bass, M. Belkacem, M. Bleicher, M. Brandstetter, L. Bravina, C. Ernst, L. Gerland, M. Hofmann, S. Hofmann, J. Konopka, G. Mao, L. Neise, S. Soff, C. Spieles, H. Weber, L. Winkelmann, H. Stöcker, W. Greiner, C. Hartnack, J. Aichelin, N. Amelin, [Microscopic models for ultra-relativistic heavy ion collisions](#), Progress in Particle and Nuclear Physics 41 (1998) 255–369. doi:https://doi.org/10.1016/S0146-6410(98)00058-1.
URL <https://www.sciencedirect.com/science/article/pii/S0146641098000581>
- [181] M. Bleicher, E. Zabrodin, C. Spieles, S. A. Bass, C. Ernst, S. Soff, L. Bravina, M. Belkacem, H. Weber, H. Stöcker, W. Greiner, [Relativistic hadron-hadron collisions in the ultra-relativistic quantum molecular dynamics model](#), Journal of Physics G: Nuclear and Particle Physics 25 (9) (1999) 1859. doi:10.1088/0954-3899/25/9/308.
URL <https://dx.doi.org/10.1088/0954-3899/25/9/308>
- [182] H. Petersen, J. Steinheimer, G. Burau, M. Bleicher, H. Stöcker, [Fully integrated transport approach to heavy ion reactions with an intermediate hydrodynamic stage](#), Phys. Rev. C 78 (2008) 044901. doi:10.1103/PhysRevC.78.044901.
URL <https://link.aps.org/doi/10.1103/PhysRevC.78.044901>
- [183] J. Steinheimer, V. Vovchenko, J. Aichelin, M. Bleicher, H. Stöcker, [Final state hadronic rescattering with UrQMD](#), EPJ Web Conf. 171 (2018) 05003. doi:10.1051/epjconf/201817105003.
URL <https://doi.org/10.1051/epjconf/201817105003>

- [184] M. Teslyk, L. Bravina, O. Panova, O. Vitiuk, E. Zabrodin, [Shear viscosity in microscopic calculations of A+A collisions at energies available at the nuclotron-based ion collider facility \(NICA\)](#), Phys. Rev. C 101 (2020) 014904. doi:10.1103/PhysRevC.101.014904.
URL <https://link.aps.org/doi/10.1103/PhysRevC.101.014904>
- [185] I. A. Karpenko, P. Huovinen, H. Petersen, M. Bleicher, [Estimation of the shear viscosity at finite net-baryon density from A + A collision data at \$\sqrt{s_{NN}} = 7.7 - 200\$ GeV](#), Phys. Rev. C 91 (2015) 064901. doi:10.1103/PhysRevC.91.064901.
URL <https://link.aps.org/doi/10.1103/PhysRevC.91.064901>
- [186] J. Auvinen, J. E. Bernhard, S. A. Bass, I. Karpenko, [Investigating the collision energy dependence of \$\eta/s\$ in the beam energy scan at the BNL relativistic heavy ion collider using bayesian statistics](#), Phys. Rev. C 97 (2018) 044905. doi:10.1103/PhysRevC.97.044905.
URL <https://link.aps.org/doi/10.1103/PhysRevC.97.044905>
- [187] S. Ryu, J.-F. Paquet, C. Shen, G. S. Denicol, B. Schenke, S. Jeon, C. Gale, [Importance of the bulk viscosity of qcd in ultrarelativistic heavy-ion collisions](#), Phys. Rev. Lett. 115 (2015) 132301. doi:10.1103/PhysRevLett.115.132301.
URL <https://link.aps.org/doi/10.1103/PhysRevLett.115.132301>
- [188] E. Holub, D. Hilscher, G. Ingold, U. Jahnke, H. Orf, H. Rossner, [Neutron emission in central heavy-ion collisions of \$^{165}\text{Ho} + ^{20}\text{Ne}\$ at 11, 14.6, and 20.1 mev/nucleon](#), Phys. Rev. C 28 (1983) 252–270. doi:10.1103/PhysRevC.28.252.
URL <https://link.aps.org/doi/10.1103/PhysRevC.28.252>
- [189] W. P. Zank, D. Hilscher, G. Ingold, U. Jahnke, M. Lehmann, H. Rossner, [Fusion-fission dynamics at high excitation energies studied by neutron emission](#), Phys. Rev. C 33 (1986) 519–536. doi:10.1103/PhysRevC.33.519.
URL <https://link.aps.org/doi/10.1103/PhysRevC.33.519>
- [190] J. W. Chen, J. C. Pei, Y. Qiang, J. H. Chi, [Fission properties of neutron-rich nuclei around the end point of \$\beta\$ -process](#), Chin. Phys. Lett. 40 (2023) 012401. doi:10.1088/0256-307X/40/01/012401.
- [191] J. Y. Yi, C. Y. Qiao, J. C. Pei, Z. A. Wang, Y. J. Chen, N. C. Shu, Z. G. Ge, F. R. Xu, [Bayesian machine learning for the uncertainty evaluation of nuclear fission product yields](#), Sci. Sin.-Phys. Mech. Astron. 52 (2022) 252013. doi:10.1360/SSPMA-2021-0340.

- [192] A. Gavron, A. Gayer, J. Boissevain, H. Britt, J. Nix, A. Sierk, P. Grangé, S. Hassani, H. Weidenmüller, J. Beene, B. Cheynis, D. Drain, R. Ferguson, F. Obenshain, F. Plasil, G. Young, G. Petitt, C. Butler, [Neutron emission prior to fission](#), *Physics Letters B* 176 (3) (1986) 312–316. doi:[https://doi.org/10.1016/0370-2693\(86\)90170-X](https://doi.org/10.1016/0370-2693(86)90170-X).
URL <https://www.sciencedirect.com/science/article/pii/037026938690170X>
- [193] J. P. Lestone, S. G. McCalla, [Statistical model of heavy-ion fusion-fission reactions](#), *Phys. Rev. C* 79 (2009) 044611. doi:[10.1103/PhysRevC.79.044611](https://doi.org/10.1103/PhysRevC.79.044611).
URL <https://link.aps.org/doi/10.1103/PhysRevC.79.044611>
- [194] K. Kapoor, N. Bansal, C. Sharma, S. Verma, K. Rani, R. Mahajan, B. R. Behera, K. P. Singh, A. Kumar, H. Singh, R. Dubey, N. Saneesh, M. Kumar, A. Yadav, A. Jhingan, P. Sugathan, B. K. Nayak, A. Saxena, H. P. Sharma, S. K. Chamoli, [Role of viscosity in fusion-fission dynamics via simultaneously measured neutron and \$\alpha\$ -particle multiplicities](#), *Phys. Rev. C* 100 (2019) 014620. doi:[10.1103/PhysRevC.100.014620](https://doi.org/10.1103/PhysRevC.100.014620).
URL <https://link.aps.org/doi/10.1103/PhysRevC.100.014620>
- [195] H. Eslamizadeh, M. Pirpour, [Effect of viscosity on the fission dynamics of the excited compound nucleus \$^{251}\text{Es}\$ produced in fusion reaction](#), *Chinese Journal of Physics* 66 (2020) 527–533. doi:<https://doi.org/10.1016/j.cjph.2020.05.004>.
URL <https://www.sciencedirect.com/science/article/pii/S0577907320301209>
- [196] J. Newton, D. Hinde, R. Charity, J. Leigh, J. Bokhorst, A. Chatterjee, G. Foote, S. Ogaza, [Measurement and statistical model analysis of pre-fission neutron multiplicities](#), *Nuclear Physics A* 483 (1) (1988) 126–152. doi:[https://doi.org/10.1016/0375-9474\(88\)90068-1](https://doi.org/10.1016/0375-9474(88)90068-1).
URL <https://www.sciencedirect.com/science/article/pii/0375947488900681>
- [197] V. Gonzalez, S. Basu, A. Marin, J. Pan, P. Ladrón de Guevara, C. A. Pruneau, [Extraction of the specific shear viscosity of quark-gluon plasma from two-particle transverse momentum correlations](#), *The European Physical Journal C* 81 (5) (2021) 465. doi:[10.1140/epjc/s10052-021-09260-z](https://doi.org/10.1140/epjc/s10052-021-09260-z).
URL <https://doi.org/10.1140/epjc/s10052-021-09260-z>
- [198] R. A. Lacey, N. N. Ajitanand, J. M. Alexander, P. Chung, W. G. Holzmann, M. Issah, A. Taranenko, P. Danielewicz, H. Stöcker, [Has the QCD critical point been signaled by observations at the BNL relativistic heavy ion collider?](#), *Phys. Rev. Lett.* 98 (2007) 092301.

doi:10.1103/PhysRevLett.98.092301.

URL <https://link.aps.org/doi/10.1103/PhysRevLett.98.092301>

- [199] F. Karsch, E. Laermann, A. Peikert, Quark mass and flavour dependence of the QCD phase transition, Nuclear Physics B 605 (1) (2001) 579–599. doi:10.1016/S0550-3213(01)00200-0. URL <https://www.sciencedirect.com/science/article/pii/S0550321301002000>
- [200] K. Aamodt, (for ALICE Collaboration), Centrality dependence of the charged-particle multiplicity density at midrapidity in Pb-Pb collisions at $\sqrt{s_{NN}} = 2.76$ TeV, Phys. Rev. Lett. 106 (2011) 032301. doi:10.1103/PhysRevLett.106.032301. URL <https://link.aps.org/doi/10.1103/PhysRevLett.106.032301>
- [201] K. Aamodt, (for ALICE Collaboration), Two-pion Bose–Einstein correlations in central Pb+Pb collisions at $\sqrt{s_{NN}}=2.76$ TeV, Physics Letters B 696 (4) (2011) 328–337. doi:<https://doi.org/10.1016/j.physletb.2010.12.053>. URL <https://www.sciencedirect.com/science/article/pii/S0370269310014565>
- [202] E. Abbas, (for ALICE Collaboration), Centrality dependence of the pseudorapidity density distribution for charged particles in Pb+Pb collisions at $\sqrt{s_{NN}}=2.76$ TeV, Physics Letters B 726 (4) (2013) 610–622. doi:<https://doi.org/10.1016/j.physletb.2013.09.022>. URL <https://www.sciencedirect.com/science/article/pii/S0370269313007399>
- [203] S. Acharya, (for ALICE Collaboration), Longitudinal and azimuthal evolution of two-particle transverse momentum correlations in Pb+Pb collisions at $\sqrt{s_{NN}}=2.76$ TeV, Physics Letters B 804 (2020) 135375. doi:<https://doi.org/10.1016/j.physletb.2020.135375>. URL <https://www.sciencedirect.com/science/article/pii/S0370269320301799>
- [204] B. I. Abelev, (for STAR Collaboration), Systematic measurements of identified particle spectra in pp , $d + Au$, and $Au + Au$ collisions at the STAR detector, Phys. Rev. C 79 (2009) 034909. doi:10.1103/PhysRevC.79.034909. URL <https://link.aps.org/doi/10.1103/PhysRevC.79.034909>
- [205] G. Agakishiev, (for STAR Collaboration), Evolution of the differential transverse momentum correlation function with centrality in Au+Au collisions at $\sqrt{s_{NN}}=200$ GeV, Physics Letters B 704 (5) (2011) 467–473. doi:<https://doi.org/10.1016/j.physletb.2011.09.075>. URL <https://www.sciencedirect.com/science/article/pii/S0370269311011609>

- [206] S. Gavin, M. Abdel-Aziz, [Measuring shear viscosity using transverse momentum correlations in relativistic nuclear collisions](#), Phys. Rev. Lett. 97 (2006) 162302. doi:10.1103/PhysRevLett.97.162302.
URL <https://link.aps.org/doi/10.1103/PhysRevLett.97.162302>
- [207] M. Sharma, C. A. Pruneau, [Methods for the study of transverse momentum differential correlations](#), Phys. Rev. C 79 (2009) 024905. doi:10.1103/PhysRevC.79.024905.
URL <https://link.aps.org/doi/10.1103/PhysRevC.79.024905>
- [208] F. Becattini, [The Quark Gluon Plasma and relativistic heavy ion collisions in the LHC era](#), Journal of Physics: Conference Series 527 (1) (2014) 012012. doi:10.1088/1742-6596/527/1/012012.
URL <https://dx.doi.org/10.1088/1742-6596/527/1/012012>
- [209] K. Aamodt, (for ALICE Collaboration), [Two-pion Bose–Einstein correlations in central Pb+Pb collisions at \$\sqrt{s_{NN}}=2.76\$ TeV](#), Physics Letters B 696 (4) (2011) 328–337. doi:<https://doi.org/10.1016/j.physletb.2010.12.053>.
URL <https://www.sciencedirect.com/science/article/pii/S0370269310014565>
- [210] V. V. Skokov, A. Y. Illarionov, V. D. Toneev, [Estimate of the magnetic field strength in heavy-ion collisions](#), International Journal of Modern Physics A 24 (31) (2009) 5925–5932. arXiv:<https://doi.org/10.1142/S0217751X09047570>, doi:10.1142/S0217751X09047570.
URL <https://doi.org/10.1142/S0217751X09047570>
- [211] M. Asakawa, A. Majumder, B. Müller, [Electric charge separation in strong transient magnetic fields](#), Phys. Rev. C 81 (2010) 064912. doi:10.1103/PhysRevC.81.064912.
URL <https://link.aps.org/doi/10.1103/PhysRevC.81.064912>
- [212] A. Bzdak, V. Skokov, [Event-by-event fluctuations of magnetic and electric fields in heavy ion collisions](#), Physics Letters B 710 (1) (2012) 171–174. doi:<https://doi.org/10.1016/j.physletb.2012.02.065>.
URL <https://www.sciencedirect.com/science/article/pii/S037026931200216X>
- [213] W.-T. Deng, X.-G. Huang, [Event-by-event generation of electromagnetic fields in heavy-ion collisions](#), Phys. Rev. C 85 (2012) 044907. doi:10.1103/PhysRevC.85.044907.
URL <https://link.aps.org/doi/10.1103/PhysRevC.85.044907>

- [214] K. Dmitri, L. Karl, S. Andreas, Y. Ho-Ung, [Strongly Interacting Matter in Magnetic Fields](#), 1st Edition, no. 0075-8450 in *Lecture Notes in Physics*, Springer Berlin, Heidelberg, 2013.
URL <https://doi.org/10.1007/978-3-642-37305-3>
- [215] X.-G. Huang, [Electromagnetic fields and anomalous transports in heavy-ion collisions—a pedagogical review](#), *Reports on Progress in Physics* 79 (7) (2016) 076302. doi:10.1088/0034-4885/79/7/076302.
URL <https://dx.doi.org/10.1088/0034-4885/79/7/076302>
- [216] K. Fukushima, D. E. Kharzeev, H. J. Warringa, [Chiral magnetic effect](#), *Phys. Rev. D* 78 (2008) 074033. doi:10.1103/PhysRevD.78.074033.
URL <https://link.aps.org/doi/10.1103/PhysRevD.78.074033>
- [217] B. Abelev *et al.* (The ALICE Collaboration), [Charge separation relative to the reaction plane in Pb-Pb collisions at \$\sqrt{s_{NN}}=2.76\$ TeV](#), *Phys. Rev. Lett.* 110 (2013) 012301. doi:10.1103/PhysRevLett.110.012301.
URL <https://link.aps.org/doi/10.1103/PhysRevLett.110.012301>
- [218] D. T. Son, A. R. Zhitnitsky, [Quantum anomalies in dense matter](#), *Phys. Rev. D* 70 (2004) 074018. doi:10.1103/PhysRevD.70.074018.
URL <https://link.aps.org/doi/10.1103/PhysRevD.70.074018>
- [219] X.-G. Huang, J. Liao, [Axial current generation from electric field: Chiral electric separation effect](#), *Phys. Rev. Lett.* 110 (2013) 232302. doi:10.1103/PhysRevLett.110.232302.
URL <https://link.aps.org/doi/10.1103/PhysRevLett.110.232302>
- [220] D. E. Kharzeev, H.-U. Yee, [Chiral magnetic wave](#), *Phys. Rev. D* 83 (2011) 085007. doi:10.1103/PhysRevD.83.085007.
URL <https://link.aps.org/doi/10.1103/PhysRevD.83.085007>
- [221] D. E. Kharzeev, D. T. Son, [Testing the chiral magnetic and chiral vortical effects in heavy ion collisions](#), *Phys. Rev. Lett.* 106 (2011) 062301. doi:10.1103/PhysRevLett.106.062301.
URL <https://link.aps.org/doi/10.1103/PhysRevLett.106.062301>
- [222] L. Adamczyk *et al.* (The STAR Collaboration), [Global \$\lambda\$ hyperon polarization in nuclear collisions](#), *Nature* 548 (7665) (2017) 62–65. doi:10.1038/nature23004.
URL <https://doi.org/10.1038/nature23004>

- [223] K. Tuchin, [On viscous flow and azimuthal anisotropy of the quark–gluon plasma in a strong magnetic field](#), *Journal of Physics G: Nuclear and Particle Physics* 39 (2) (2012) 025010, publisher: IOP Publishing. doi:[10.1088/0954-3899/39/2/025010](https://doi.org/10.1088/0954-3899/39/2/025010).
URL <https://dx.doi.org/10.1088/0954-3899/39/2/025010>
- [224] M. Kurian, S. K. Das, V. Chandra, [Heavy quark dynamics in a hot magnetized QCD medium](#), *Phys. Rev. D* 100 (2019) 074003. doi:[10.1103/PhysRevD.100.074003](https://doi.org/10.1103/PhysRevD.100.074003).
URL <https://link.aps.org/doi/10.1103/PhysRevD.100.074003>
- [225] J. O. Andersen, W. R. Naylor, A. Tranberg, [Phase diagram of QCD in a magnetic field](#), *Reviews of Modern Physics* 88 (2) (2016) 025001, publisher: American Physical Society. doi:[10.1103/RevModPhys.88.025001](https://doi.org/10.1103/RevModPhys.88.025001).
URL <https://link.aps.org/doi/10.1103/RevModPhys.88.025001>
- [226] X. Zhu, S.-Q. Feng, [Shear viscosity coefficient of magnetized qcd medium near chiral phase transition](#), *Phys. Rev. D* 107 (2023) 016018. doi:[10.1103/PhysRevD.107.016018](https://doi.org/10.1103/PhysRevD.107.016018).
URL <https://link.aps.org/doi/10.1103/PhysRevD.107.016018>
- [227] S. Ghosh, P. Mohanty, B. Chatterjee, A. Mukharjee, H. Mishra, [Impact of magnetic field on shear viscosity of quark matter in Nambu-Jona-Lasinio model](#), *Phys. Rev. D* 100 (2019) 034024. doi:[10.1103/PhysRevD.100.034024](https://doi.org/10.1103/PhysRevD.100.034024).
URL <https://link.aps.org/doi/10.1103/PhysRevD.100.034024>
- [228] S. Rath, B. K. Patra, [Viscous properties of hot and dense QCD matter in the presence of a magnetic field](#), *The European Physical Journal C* 81 (2) (2021) 139. doi:[10.1140/epjc/s10052-021-08931-1](https://doi.org/10.1140/epjc/s10052-021-08931-1).
URL <https://doi.org/10.1140/epjc/s10052-021-08931-1>
- [229] A. Shaikh, M. Kurian, S. K. Das, V. Chandra, S. Dash, B. K. Nandi, [Heavy quark transport coefficients in a viscous QCD medium with collisional and radiative processes](#), *Phys. Rev. D* 104 (2021) 034017. doi:[10.1103/PhysRevD.104.034017](https://doi.org/10.1103/PhysRevD.104.034017).
URL <https://link.aps.org/doi/10.1103/PhysRevD.104.034017>
- [230] J. E. Bernhard, J. S. Moreland, S. A. Bass, [Bayesian estimation of the specific shear and bulk viscosity of quark–gluon plasma](#), *Nature Physics* 15 (11) (2019) 1113–1117, number: 11 Publisher: Nature Publishing Group. doi:[10.1038/s41567-019-0611-8](https://doi.org/10.1038/s41567-019-0611-8).
URL <https://www.nature.com/articles/s41567-019-0611-8>

- [231] E. W. Lemmon, M. O. McLinden, D. G. Friend, [Thermophysical properties of fluid systems](#), National Institute of Standards and Technology, 2018.
URL <https://webbook.nist.gov/chemistry/fluid>
- [232] D. Everett, W. Ke, J.-F. Paquet, G. Vujanovic, S. A. Bass, L. Du, C. Gale, M. Heffernan, U. Heinz, D. Liyanage, M. Luzum, A. Majumder, M. McNelis, C. Shen, Y. Xu, A. Angerami, S. Cao, Y. Chen, J. Coleman, L. Cunqueiro, T. Dai, R. Ehlers, H. Elfner, W. Fan, R. J. Fries, F. Garza, Y. He, B. V. Jacak, P. M. Jacobs, S. Jeon, B. Kim, M. Kordell, A. Kumar, S. Mak, J. Mulligan, C. Nattrass, D. Oliinychenko, C. Park, J. H. Putschke, G. Roland, B. Schenke, L. Schwiebert, A. Silva, C. Sirimanna, R. A. Soltz, Y. Tachibana, X.-N. Wang, R. L. Wolpert, [Multisystem bayesian constraints on the transport coefficients of QCD matter](#), Phys. Rev. C 103 (2021) 054904. doi:10.1103/PhysRevC.103.054904.
URL <https://link.aps.org/doi/10.1103/PhysRevC.103.054904>
- [233] D. Everett, W. Ke, J.-F. Paquet, G. Vujanovic, S. A. Bass, L. Du, C. Gale, M. Heffernan, U. Heinz, D. Liyanage, M. Luzum, A. Majumder, M. McNelis, C. Shen, Y. Xu, A. Angerami, S. Cao, Y. Chen, J. Coleman, L. Cunqueiro, T. Dai, R. Ehlers, H. Elfner, W. Fan, R. J. Fries, F. Garza, Y. He, B. V. Jacak, P. M. Jacobs, S. Jeon, B. Kim, M. Kordell, A. Kumar, S. Mak, J. Mulligan, C. Nattrass, D. Oliinychenko, C. Park, J. H. Putschke, G. Roland, B. Schenke, L. Schwiebert, A. Silva, C. Sirimanna, R. A. Soltz, Y. Tachibana, X.-N. Wang, R. L. Wolpert, [Phenomenological constraints on the transport properties of qcd matter with data-driven model averaging](#), Phys. Rev. Lett. 126 (2021) 242301. doi:10.1103/PhysRevLett.126.242301.
URL <https://link.aps.org/doi/10.1103/PhysRevLett.126.242301>
- [234] E. Alhassan, D. Rochman, A. Vasiliev, M. Hursin, A. J. Koning, H. Ferroukhi, [Iterative bayesian monte carlo for nuclear data evaluation](#), Nuclear Science and Techniques 33 (4) (2022) 50. doi:10.1007/s41365-022-01034-w.
URL <https://doi.org/10.1007/s41365-022-01034-w>
- [235] W.-B. He, Y.-G. Ma, L.-G. Pang, H.-C. Song, K. Zhou, [High-energy nuclear physics meets machine learning](#), Nuclear Science and Techniques 34 (6) (2023) 88. doi:10.1007/s41365-023-01233-z.
URL <https://doi.org/10.1007/s41365-023-01233-z>
- [236] W.-B. He, Q.-F. Li, Y.-G. Ma, Z.-M. Niu, J.-C. Pei, Y.-X. Zhang, [Machine learning in nuclear physics at low and intermediate energies](#), SCIENCE CHINA Physics, Mechanics and Astronomy 66 (2023) 282001. doi:10.1007/s11433-023-2116-0.

- [237] J. E. Parkkila, A. Onnerstad, D. J. Kim, Bayesian estimation of the specific shear and bulk viscosity of the quark-gluon plasma with additional flow harmonic observables, Phys. Rev. C 104 (2021) 054904. doi:10.1103/PhysRevC.104.054904.
URL <https://link.aps.org/doi/10.1103/PhysRevC.104.054904>
- [238] J. Auvinen, K. J. Eskola, P. Huovinen, H. Niemi, R. Paatelainen, P. Petreczky, Temperature dependence of η/s of strongly interacting matter: Effects of the equation of state and the parametric form of $\eta/s(T)$, Phys. Rev. C 102 (2020) 044911. doi:10.1103/PhysRevC.102.044911.
URL <https://link.aps.org/doi/10.1103/PhysRevC.102.044911>

A. Appendices, if necessary